ABSTRACT

Title of Dissertation: INTERACTIONS BETWEEN APPETITIVE AND AVERSIVE PROCESSING DURING PERCEPTION AND ATTENTION

Srikanth Padmala,
Doctor of Philosophy, 2017

Dissertation directed by: Professor Luiz Pessoa,
Department of Psychology

Although understanding brain mechanisms of appetitive-aversive interactions is relevant to our daily lives and has potential clinical relevance, our knowledge about these brain mechanisms is rudimentary. To address this gap in the literature, we conducted two functional MRI studies that investigated appetitive-aversive interactions during perception and attention in healthy adult human brain.

In the first study, we probed how potential reward signaled by advance cues altered aversive distractor processing during a subsequent visual task. Behaviorally, the deleterious influence of aversive stimuli on task performance was reduced during the reward compared to no-reward condition. In the brain, at the task phase, paralleling the observed behavioral pattern, significant interactions were observed in the anterior insula and dorsal anterior cingulate cortex, such that responses during the negative (vs. neutral) condition were reduced during the reward compared to no-

reward condition. Notably, negative distractor processing in the amygdala appeared to be independent of the reward manipulation. During the initial cue phase, we observed increased reward-related responses in the ventral striatum, which were correlated with behavioral interference scores at the subsequent task phase, revealing that participants with increased reward-related responses exhibited a greater behavioral benefit of reward in reducing the adverse effect of negative images. Furthermore, the ventral striatum exhibited stronger functional connectivity with fronto-parietal regions important for attentional control. These findings contribute to the understanding of how potential reward influences attentional control and reduces negative distractor processing in the human brain.

In the second study, we investigated brain mechanisms underlying the joint processing of positive and negative emotional information during a passive viewing task. Specifically we focused on probing the pattern of appetitive-aversive interactions in brain regions sensitive to the valence and salience of emotional stimuli. In a subset of regions that were sensitive to stimulus valence, *competitive* interaction patterns were observed. Notably, in other valence-coding regions such as the ventro-medial prefrontal cortex no evidence for competitive interactions was detected. Conversely, in regions sensitive to salience, *cooperative* interaction patterns were observed. The findings of competitive and cooperative type interactions supported contextual modulation of emotional processing in the human brain.

INTERACTIONS BETWEEN APPETITIVE AND AVERSIVE PROCESSING DURING PERCEPTION AND ATTENTION

by

Srikanth Padmala

Dissertation submitted to the Faculty of the Graduate School of the
University of Maryland, College Park, in partial fulfillment
of the requirements for the degree of
Doctor of Philosophy
2017

Advisory Committee:
Professor Luiz Pessoa, Chair
Professor Matthew Roesch
Professor Lea Dougherty
Professor Elizabeth Redcay
Professor Donald Bolger, Dean's Representative

Dedication

To my wonderful parents.

Acknowledgements

I would like to thank my advisor and mentor, Professor Luiz Pessoa, for his excellent guidance and support over past many years. I could never imagine thinking about mechanisms underlying complex functioning of a human brain without Luiz and I will always be grateful for his mentorship and training that allowed me to transform from a Bio-medical engineer to a Cognitive Neuroscientist.

I would like to express my sincere appreciation and gratitude to Dr. Matthew Roesch, Dr. Lea Dougherty, Dr. Elizabeth Redcay and Dr. Donald Bolger for serving on my dissertation committee.

I would like to thank Dr. Jens Herberholz and Pam Komarek for providing constant guidance throughout my graduate studies and also Katie Sacksteder who has greatly helped with my NSF GRFP submission that eventually got funded.

I greatly appreciate the help from some excellent research assistants in Dr. Pessoa's lab, Mihai Sirbu, Daniel Levitas and Heirangi Torrico who did bulk of the data collection for the two functional MRI studies reported in this dissertation work. I would like to thank Jason Smith and Joshua Kinnison for help with processing scripts, Brenton McMenamin and Nicola Sambuco for many useful discussions, Mirtes Pereira for sharing stimuli, Nicola Friedman and Jessica Berman for help with subject recruitment, and Kelly Morrow for patiently proofreading and editing some of my dissertation chapters.

Support for this dissertation work was provided in part by the National Institute of Mental Health (R01 MH071589 to Dr. Pessoa) and a National Science Foundation Graduate Research Fellowship to Srikanth Padmala. I also acknowledge

the Behavioral and Social Sciences College, University of Maryland high performance computing resources (http://bsos.umd.edu/oacs/bsos-highperformance) made available for conducting the research reported in this dissertation.

Finally but most importantly, I would like to thank my family members especially my parents for their constant encouragement and support, without whom none of this would have been possible.

Table of Contents

List of Tables

List of Figures

Chapter 1 General Introduction and Background

Many of our daily decisions and behaviors are shaped by the influence of both positive and negative information. For instance, a thirsty animal that walks in an unfamiliar territory and comes across a lake would probably consider both the rewarding value of water along with the risk of any nearby predators before making a decision about stepping into the lake. In some other instances one might have to process a mixture of appetitive and aversive information. For example, the parents of two children serving in the army hear news that one child has escaped a fierce enemy attack in combat, whereas the other unfortunately did not; how would the parents react to this incoming ambivalent emotional information? Thus, there is a clear need to understand how the brain integrates both positive and negative information (Barberini et al., 2012; Hayes et al., 2014). Furthermore, from a clinical standpoint, anxiety and depression which are frequently associated with biases in negative and positive processing respectively are highly co-morbid (Gorman, 1996; Calkins et al., 2015). Therefore a deeper understanding of how the brain integrates positive and negative processing is highly relevant to these mental disorders and could potentially aid in developing better treatment strategies (Dillon et al., 2014; Pizzagalli, 2014).

Some prominent behavioral researchers have stressed the importance of investigating appetitive-aversive interactions for several decades now (Dickinson and Dearing, 1979). However, somewhat surprisingly, we still have a limited understanding of how the brain integrates positive and negative information (Bissonette et al., 2014; Hayes et al., 2014). A few recent studies have investigated interactions between appetitive and aversive processing mainly focusing on decision

making (Talmi et al., 2009; Amemori and Graybiel, 2012) and stress-reward type paradigms (Ossewaarde et al., 2011; Porcelli et al., 2012). Hence, our knowledge about how the brain integrates appetitive and aversive information especially during perception and attention is incomplete. *Therefore, the objective of this dissertation work is to advance our understanding of appetitive-aversive interactions in the healthy adult human brain during perception and attention.*

Models of appetitive-aversive interactions

It is well known that behavior under different situations are mainly influenced by two motivational systems – appetitive and aversive. The appetitive motivation system plays a key role in approach and reward type behaviors, whereas the aversive system plays an important role in avoidance and defensive type behaviors (Lang et al., 1997a). Based on behavioral findings from learning paradigms, some researchers proposed that appetitive and aversive motivational systems are mutually inhibitory (Konorski, 1967; Dickinson and Dearing, 1979). Additionally, other proposals advocate for competitive interactions between appetitive and aversive processing such as reward-induced analgesia and pain-reduced pleasure (Leknes and Tracey, 2008). Taken together, these models consistently point to the idea of *opponency* between appetitive and aversive systems, mainly focusing on value/valence aspect of the information. On the other hand, both appetitive and aversive information are more salient than the neutral information, which might lead to increased attention, motivation, or arousal. Based on the concept of salience, some recent studies have also proposed *cooperative* type interactions between appetitive and aversive

processing (Barberini et al., 2012). *Some of the studies in this dissertation work systematically investigated joint processing of appetitive-aversive information based on the concepts of valence and salience to better understand the nature of the interactions (i.e., competitive vs. cooperative).*

Review of literature on brain mechanisms of appetitive and aversive processing

Evidence for and against localized view of appetitive and aversive processing

Early work in rodent models mainly centered on classical fear conditioning paradigms have frequently tied the amygdala to aversive processing (Davis, 1992; LeDoux, 2000). Similarly, many initial human brain imaging studies that have exclusively focused on different aspects of aversive processing (e.g., fear conditioning and processing of emotional stimuli such as fearful faces) have frequently reported the involvement of the amygdala (LaBar et al., 1998; Adolphs and Tranel, 2000). When studying reward processing, an appetitive domain, many early studies frequently implicated regions including the dopaminergic midbrain and ventral striatum (Schultz, 2000; Knutson et al., 2001). For instance, Schultz and colleagues reported selective involvement of dopaminergic midbrain neurons in processing of reward information in monkeys, especially in coding of prediction errors (Schultz et al., 1997). Similar findings have been reported in a human fMRI study where participants were cued in advance about the potential for performance-based reward/punishment during the subsequent task phase. In this monetary incentive delay task, the ventral striatum was reported to be selectively involved during processing of reward cues (Knutson et al., 2001). Other studies employing

tasks specifically focused on reward outcome processing (e.g. card guessing task), have also reported the involvement of striatal regions during more *hedonic* aspects of reward processing (Tricomi et al., 2004; Delgado, 2007). In line with these findings, ventral striatal activation has been reported selectively during processing of erotic stimuli (Sabatinelli et al., 2007) and beautiful faces (Aharon et al., 2001). Together, these separate findings from aversive and appetitive processing literature initially supported the notion of a *one-to-one mapping between structure and function*, for instance linking the amygdala and ventral striatum to aversive and appetitive processing respectively.

While some earlier work reported evidence inconsistent with one-to-one mapping, it received less attention (Rolls, 1972; Thierry et al., 1976). Later studies strongly challenged the simplistic notion of localized mapping of appetitive and aversive processing, arguing that the amygdala is also involved in reward processing (Baxter and Murray, 2002; Everitt et al., 2003), and involvement of the ventral striatum during processing of aversive information such as noxious thermal stimuli (Becerra et al., 2001) and anticipation of aversive shock (Jensen et al., 2003). Though I have mainly focused on the amygdala and ventral striatum to demonstrate the evidence against simple one-to-one mapping, similar findings have been reported in many other brain regions previously linked to appetitive or aversive processing exclusively. For instance, processing of aversive information has been reported in midbrain dopaminergic neurons (Brischoux et al., 2009) and processing of appetitive information has been reported in the anterior insula (Liu et al., 2011; Mizuhiki et al.,

2012) and bed nucleus of the stria terminalis (McGinty et al., 2011; Jennings et al., 2013), both of which were previously linked to aversive processing.

Evidence for and against one-to-one mapping at the level of neurotransmitters

Initial ideas of one-to-one mapping between structure and function were not confined to the level of brain regions: several researchers suggested this type of modular mapping even at the neurotransmitter level, frequently linking dopamine to appetitive and serotonin to aversive processing (Daw et al., 2002). Supporting this theory, although some studies reported selective effects of dopamine medications on reward related processing (Palminteri et al., 2009), many recent studies have provided evidence inconsistent with simple one-to-one mapping. For instance, some studies have reported dopamine involvement in aversive processing (Pezze and Feldon, 2004; Zweifel et al., 2011) and others reported involvement of serotonin in appetitive processing (Kranz et al., 2010; Seymour et al., 2012; Cohen et al., 2015). These studies counter the simplistic idea of one-to-one mapping even at the level of neurotransmitters and are consistent with proposals of dopamine playing a role in both appetitive and aversive motivation (Salamone, 1994; Salamone and Correa, 2012).

Value and salience coding in brain regions

Building on the initial evidence against one-to-one mapping, later studies that have employed both positive and negative stimuli (along with a neutral condition) reported evidence for *value*/*valence* and/or *salience*/*intensity* type signals in multiple brain regions. In a region that codes valence/value, one would expect signals to

increase monotonically from aversive to appetitive dimension (i.e., appetitive > neutral > aversive in the case of positive valence coding) or from appetitive to aversive dimension (i.e., aversive > neutral > appetitive in the case of negative valence coding). This type of valence signal would be important for approach and defensive behaviors as learning to approach positive stimuli (rewards) and avoiding negative stimuli (threats) is crucial for survival. Additionally, in regions that represent salience type signals both aversive and appetitive conditions would exhibit stronger activation compared to a neutral condition (i.e., both appetitive and aversive > neutral). Salience signals would be important for increased attention, arousal, and general motivation, all of which are common for appetitive and aversive stimuli.

Many human and animal studies have reported processing of both types of information (i.e., both positive & negative > neutral) in the amygdala, suggesting this region encodes *salience/intensity*. For instance, the amygdala has been reported to play an important role during both aversive and appetitive classical conditioning in non-human primates (Paton et al., 2006; Shabel and Janak, 2009). In one influential study (Belova et al., 2007), Salzman and colleagues modulated expectancy of appetitive/aversive reinforcements in a paradigm that combined trace-conditioning with reversal learning. The authors reported convergence of both appetitive and aversive reinforcement information on the same neurons in the primate basolateral amygdala, supporting the idea of salience processing at the level of individual neurons (Belova et al., 2007). Consistent with animal literature, human imaging studies have also reported amygdala activation during processing of both appetitive and aversive stimuli during olfaction and gustation (Anderson et al., 2003; Small et

al., 2003). Subsequently, Dolan and colleagues reported interactions between valence and intensity in the amygdala during an fMRI study investigating human olfaction. The authors observed effects of intensity only for pleasant and unpleasant odors but not neutral odors, suggesting the amygdala codes a combination of valence and intensity (Winston et al., 2005).

Although the majority of human fMRI studies report coding of salience-related signals in the amygdala, the coarse spatial resolution of typical fMRI data makes it difficult to rule out the possibility of the observed fMRI signal arising from separate neuronal populations sensitive to appetitive and aversive stimuli (Bissonette et al., 2014). Interestingly, in one of the studies from Salzman and colleagues discussed above (Belova et al., 2007), separate neuronal populations that were sensitive to positive or negative stimuli were also reported. Additionally, recent studies have also reported positive and negative valence sensitive neurons in the mouse basolateral amygdala (Namburi et al., 2015; Kim et al., 2016). Moreover, Tonegawa and colleagues not only reported separate neuronal populations sensitive to positive and negative stimuli, but also provided evidence suggesting these neuronal populations are antagonistic (Kim et al., 2016).

Analogously, the midbrain and ventral striatum regions have been reported to be involved during processing of both appetitive and aversive information (Bromberg-Martin et al., 2010; Bissonette et al., 2014). In a seminal work with non-human primates using classical conditioning paradigms, Hikosaka and colleagues found two different groups of dopaminergic midbrain neurons involved in the processing of motivational information (Matsumoto and Hikosaka, 2009). Using

aversive and appetitive conditioning paradigms, the authors examined spiking activity in dopaminergic neurons during processing of conditioned cues that predicted appetitive (liquid reward) and aversive (air puff) outcomes as well as during the processing of actual outcomes. During processing of cues and outcomes, the authors identified dopaminergic neurons in dorsolateral locations sensitive to value type signals (i.e., appetitive > neutral > aversive), whereas neurons in ventromedial locations were involved in processing of both appetitive and aversive information (relative to neutral), supporting the idea of salience processing (Matsumoto and Hikosaka, 2009). Similar findings of two distinct population of neurons coding for valence and salience were also reported in the rat ventral striatum (Bissonette et al., 2013). Nevertheless, researchers have recently argued for selective processing of reward information in dopaminergic midbrain neurons (Fiorillo, 2013), though there are potential issues with exact recording location (Morrens, 2014). Additionally, many human imaging studies have supported the idea of salience processing in the midbrain and ventral striatum during processing of reward/punishment cues (Cooper and Knutson, 2008; Carter et al., 2009), pleasant/unpleasant auditory stimuli (Levita et al., 2009), prediction error type signals (Jensen et al., 2007; Delgado et al., 2008) and anticipation of reward/shock (Choi et al., 2014). Interestingly, in a decision-making study involving ratings of food items, Rangel and colleagues reported coding of both value and salience type signals in the ventral striatum (Litt et al., 2010).

Conversely, a pattern consistent with *value or valence* related signals (i.e., positive > neutral > negative) was consistently reported in the ventromedial prefrontal cortex (vmPFC)/orbito-frontal cortex (OFC) (Bissonette et al., 2014; Clithero and

Rangel, 2014). In an ingenious study, Roesch and colleagues investigated value related signals in OFC neurons while monkeys performed an incentive cue-guided saccade task to maximize rewards and minimize penalty (Roesch, 2004). The study was cleverly designed such that *value* related signals could be dissociated from general motivation related signals. The authors observed evidence for positive value coding in OFC neurons where the strongest responses were observed during processing of cues that signaled large reward, and the weakest responses during cues that signaled large penalty (with an intermediate firing rate during processing of neutral cues). In contrast, general motivation-related activity was observed in premotor neurons where the strongest responses were observed during large reward and large penalty conditions relative to the neutral condition (Roesch, 2004). In a subsequent monkey study, Salzman and colleagues used a classical trace-conditioning task and found evidence for both positive and negative value coding neurons in the OFC (Morrison and Salzman, 2009). Interestingly, during processing of reinforcements both positive and negative outcomes activated the same neurons, suggesting some OFC neurons can integrate appetitive and aversive information (Morrison and Salzman, 2009). In addition to the vmPFC/OFC, a recent monkey study reported evidence for a similar type of value coding in the ventral striatum (Strait et al., 2015). Additionally, human brain imaging studies also reported value/valence type signals in the OFC during olfaction (Anderson et al., 2003), gustation (Small et al., 2003) and decision-making (Litt et al., 2010). Finally, a recent fMRI study investigated processing of conditioned stimuli that were previously paired with rewards or punishments and reported evidence for value coding in the lateral

OFC, whereas salience coding was observed in the medial OFC (Rothkirch et al., 2012).

To summarize, many regions were initially thought to be exclusively linked to appetitive or aversive processing, and later studies have provided evidence against this by reporting processing of both types of information in the same regions. Furthermore, by employing both positive and negative stimuli in a single experiment, some studies were able to probe neurons or regions that encode *value/valence* and/or *salience/intensity*. However, these studies manipulated positive and negative stimuli *separately* from one another and hence were not able to investigate any potential interactions between appetitive and aversive processing.

Review of literature on appetitive-aversive interactions

Based on the evidence supporting processing of both appetitive and aversive information in many brain regions, investigations have recently begun to probe interactions between appetitive and aversive information processing in the brain. Below, I reviewed this literature separately in the domains of learning, decision-making, stress manipulations, and during perception and attention.

Appetitive-aversive interactions during learning

Previously, studies in humans have reported competitive interactions between appetitive and aversive motivational systems based on behavioral learning paradigms (Dickinson and Pearce, 1977). Based on these findings in humans, recent studies have investigated appetitive-aversive interactions in brain and behavior using classical

conditioning paradigms in rodents (Nasser and McNally, 2012, 2013). These studies focused specifically on mechanisms involved in the transfer of appetitive-to-aversive value associated with a conditioned stimulus. The authors reported inhibitory-type interactions between appetitive and aversive learning systems where fear learning was retarded for a conditioned stimulus previously associated with food reward (Nasser and McNally, 2012). Regarding brain mechanisms, the authors reported altered levels of protein kinase activity in several regions including the amygdala and ventral striatum, suggesting changes in the fear prediction error circuit (Nasser and McNally, 2013). Although these rodent studies provided important insights regarding appetitive-aversive interactions at a cellular level, these inhibitory interactions are tied to specific contexts where appetitive and aversive manipulations are sequential in nature (i.e., appetitive followed by aversive learning).

Recently, Matsumoto and colleagues investigated the integration of appetitive and aversive outcomes in midbrain dopaminergic neurons of the mouse lateral ventral tegmental area (Matsumoto et al., 2016). In a classical conditioning paradigm, the authors used four cues that signaled different outcomes: one cue ($CS_{Appetitive}$) signaled appetitive reward outcome, second cue ($CS_{Aversive}$) signaled aversive air puff outcome, third cue ($CS_{Nothing}$) signaled no outcome and the novel fourth cue ($CS_{App\text{-}Aver}$) signaled both reward *or* air puff outcomes. The first experiment involved low-reward context (reward outcome probability of 25%), where researchers observed a positive value coding pattern in spiking activity during processing of cues where responses during appetitive cues increased and responses during aversive cues decreased relative to cues signaling nothing (i.e., $CS_{Aversive} > CS_{Nothing} > CS_{Appetitive}$). Notably,

responses to cues signaling appetitive or aversive outcomes ($CS_{App\text{-}Aver}$) were between $CS_{Appetitive}$ and $CS_{Aversive}$ cues, suggesting these dopaminergic neurons signaled integrated value of appetitive and aversive outcomes (Matsumoto et al., 2016; but see Fiorillo., 2013). Intriguingly, in a second experiment involving high-reward context (reward outcome probability of 90%), the authors observed a short latency excitation followed by a weaker inhibition during processing of aversive cues which nullified the positive value coding pattern observed during low-reward contexts. These novel results indicate contexts (low or high reward probability) influence the processing of aversive cues in midbrain dopaminergic neurons. On a broader level, these findings signify the need for studies to probe the joint processing of appetitive and aversive information in the brain.

In a recent rodent study (Burgos-Robles et al., 2017), Tye and colleagues investigated behavior and underlying neural mechanisms during processing of a cue that signaled both appetitive *and* aversive outcomes. In terms of behavior, both reward and aversive behaviors were intermediate (i.e., reduced) while processing a cue that signaled both appetitive and aversive outcomes relative to cues that signaled only one type of outcome (appetitive or aversive). This behavioral finding provided more evidence for competition between appetitive and aversive information during processing of cues signaling conflicting motivational outcomes. Regarding neural mechanisms, the authors found functional interactions between the amygdala and prefrontal cortex (specifically input from the amygdala to prefrontal cortex) are critical for guiding behaviors during situations involving motivationally conflicting information.

Another fMRI study in humans examined the interaction between negative emotion and reward learning (Watanabe et al., 2013). To do so, the authors presented a fearful or neutral face before visual cues that predicted reward or no-reward outcomes. When presenting a task-*irrelevant* fearful (relative to neutral) face before a reward-predicting cue, there was an increase in the rate of learning that was paralleled by increased reward prediction error signals in the ventral striatum (Watanabe et al., 2013). While these initial human neuroimaging findings are reported under different task context, they contradict the pattern of competitive interactions reported in animal studies discussed above. Hence, conducting parallel work in human and animal models employing similar task paradigms might help us better understand the behavior and underlying brain mechanisms of appetitive-aversive interactions.

Appetitive-aversive interactions during decision-making

Additionally, other studies have investigated the processing of *simultaneous* positive and negative information, focusing on decision making tasks involving instrumental behaviors in humans and animals (Talmi et al., 2009; Park et al., 2011; Amemori and Graybiel, 2012). For instance, Talmi et al conducted a human fMRI study that investigated integration of reward and pain signals during a decision making task. On each trial, participants were asked to make a choice between two options: one with a higher probability and the other with a lower probability of outcome, where an outcome consisted of a combination of different values of reward and a highly aversive pain stimulus. The results showed an interaction between pain and reward such that at low values of reward, participants avoided the high probability option to minimize the chance of pain. Conversely, at higher values of

reward they chose the high probability outcome more frequently, thus enduring pain. These behavioral results indicate subjective value of reward was modified in the presence of highly aversive pain. A signature of this behavioral appetitive-aversive interaction pattern was observed during the decision-making stage in the ventral striatum (and anterior cingulate cortex), where pain *reduced* the reward prediction error-related activation. A similar pattern of opponent interactions in the ventral striatum has been reported in a recent decision-making study that used anticipatory anxiety via threat of shock as aversive manipulation (Engelmann et al., 2015), though somewhat surprisingly, this study did not observe any effects at the behavioral level. One key difference that may explain the lack of behavioral findings in Engelmann et al is that the threat of shock was task-irrelevant, while in the Talmi et al study both pain and reward were task-relevant.

In another human fMRI study, Tobler and colleagues sought to understand how salience related activity integrates positive and negative information during decision making (Kahnt and Tobler, 2013). To investigate this, the authors tested two different concepts of salience, global and elemental, during choice options simultaneously associated with both positive and negative outcomes. Global salience is based on the salience of the integrated sum of positive and negative outcomes (i.e., |Pos + Neg|) and elemental salience is defined as the sum of the saliences of positive and negative outcomes (i.e., |Pos| + |Neg|). The results showed elemental, but not global salience influenced behavior by speeding up behavioral choices, and a correlated brain activity consistent with the elemental salience pattern was found in the right temporoparietal junction.

Taken together, the decision making studies discussed so far have reported two different patterns of appetitive-aversive interactions; consistent *competitive* interactions between reward and threat processing in value-related brain signals, and *cooperative* interactions in salience-related brain signals.

Appetitive-aversive interactions during stress manipulations

Interactions of stress manipulations and aspects of reward processing have also been investigated by different research groups. One study reported acute stress manipulated via threat of shock reduced reward responsiveness in a behavioral setting (Bogdan and Pizzagalli, 2006). Additionally, human fMRI studies have reported reduced reward cue processing under stress using a monetary incentive delay task (Ossewaarde et al., 2011) and reward-outcome processing in the striatum during a card guessing task (Porcelli et al., 2012). We have recently reported competitive interactions between reward and threat of shock during anticipatory stages between cue and task phases (Choi et al., 2014). More recently, Pizzagalli and colleagues investigated the effect of stress on anticipatory and consummatory stages of reward processing using negative performance feedback. In line with the findings of Porcelli and colleagues, results showed reduced outcome-related processing under stress, whereas, somewhat surprisingly, stress enhanced anticipatory reward processing (Kumar et al., 2014). Lastly, an fMRI study using an expectation type paradigm involving emotional (happy/fearful) facial stimuli reported no effects of threat of shock manipulation on appetitive prediction error signal related activation in the ventral striatum, though the authors reported increased aversive prediction errors under threat of shock (Robinson et al., 2013). When considered together, these

findings suggest that stress has an opponent influence on reward processing in most cases, but some evidence for facilitative or null effects also exists. Notably, most of these studies investigated influence of aversive stress on reward-related processing but not the converse i.e., effect of rewards on stress-related processing (Ulrich-Lai et al., 2010).

Appetitive-aversive interactions during perception and attention

Using behavioral and brain imaging techniques, we and others have investigated interactions between positive and negative processing during basic perceptual and attentional tasks, primarily the effects of reward on negative emotion (Hu et al., 2013; Padmala and Pessoa, 2014; Wei and Kang, 2014). In a behavioral setting, participants performed a visual bar orientation task on peripheral stimuli in the presence of a central neutral/negative emotional distractor stimulus (Padmala and Pessoa, 2014). On each trial, participants were cued in advance about the potential of a performance-based monetary reward on the subsequent discrimination task. Reaction time (RT) data revealed during reward (relative to no-reward) trials, the impact of negative (relative to neutral) distractor stimuli on task performance was reduced (Padmala and Pessoa, 2014). Similar behavioral findings have been reported in other recent studies that involved other kind of reward manipulations (Hu et al., 2013; Yokoyama et al., 2015). However, two other behavioral studies reported no interactions between reward and task-irrelevant negative processing during processing of face (Wei and Kang, 2014) and word stimuli (Kaltwasser et al., 2013).

Additionally, two event-related potential (ERP) studies investigated the brain mechanisms underlying the influence of performance-based rewards on negative

processing. (Kaltwasser et al., 2013) investigated the influence of reward on neutral and emotional word stimuli during a semantic categorization task. The authors reported *independence* of reward and negative emotional processing and suggested emotion- related processing was privileged and immune to reward manipulation. In a related ERP study, Wei and colleagues investigated the interaction between performance-based reward and negative emotion during processing of visual word stimuli (Wei et al., 2016). The results of task-irrelevant emotional manipulation (where participants were asked to judge the color of words) showed a *competitive* interaction: negative emotional processing indexed by late positive potential ERP component was *reduced* during reward compared to no-reward condition. Given these mixed results, further investigation is needed to understand the brain mechanisms underlying the influence of reward on negative processing.

Functional interactions during appetitive and aversive processing

Traditional activation-based univariate analysis in fMRI studies provides information about involvement of individual brain regions in appetitive and aversive processing. However, brain regions do not work in isolation and how they interact with other brain regions is critical during many tasks (Bullmore and Sporns, 2009; Turk-Browne, 2013). In fMRI studies, functional interactions between regions are characterized by the idea of functional connectivity which is indexed by the correlation in responses between brain regions. To note, functional connectivity does not provide information about directionality of interactions nor does it imply anatomical connectivity between regions. Finally, in theory, just as correlation

between two signals does not depend on their mean levels, functional interactions between brain regions are independent from the activation strengths typically estimated from standard univariate analysis. In task-based fMRI studies, functional connectivity is typically compared between task conditions to understand how different task contexts uniquely influence functional coupling between brain regions (Friston et al., 1997). In the context of emotional processing, significant task-based functional connectivity implies responses of two regions were strongly correlated during one task condition (e.g., emotional) relative to the other (e.g., neutral). Both human and monkey fMRI studies of emotional processing have reported that functional interactions between the amygdala and visual cortex play an important role during processing of emotional visual stimuli (Vuilleumier et al., 2004; Hadj-Bouziane et al., 2012). Likewise, recent animal studies have reported functional connections between the basolateral amygdala and ventral striatum during processing of positive valence information and between the basolateral amygdala and central amygdala during processing of negative valence information (Namburi et al., 2015). The majority of fMRI functional connectivity literature has focused on aversive processing, hence very little is known about functional interactions during appetitive processing (Kang et al., 2016). Moreover, how valence and salience dimensions of emotional information influence functional interactions between brain regions or how these functional interactions might play a role during joint processing of appetitive and aversive information are still unexplored.

Brain basis of emotion

Based on behavioral findings, researchers have proposed different models of how emotion might be represented in the brain. One model, the bipolarity hypothesis (Barrett and Russell, 1999; Russell and Carroll, 1999), argues emotions are represented along a continuum from negative to positive with a neutral midpoint. One direct consequence of this model is that in a situation where simultaneous positive and negative information are presented, one might experience a neutral emotion due to positive and negative information neutralizing each other (Lindquist et al., 2015). Conversely, bivalent hypothesis argues for separate systems that process positive and negative emotional information (Cacioppo et al., 1999; Larsen et al., 2001). According to this hypothesis, one can experience both positive and negative emotion simultaneously (i.e., mixed emotions) as they may have distinct underlying brain substrates (Lindquist et al., 2015). Using meta-analytic techniques on published fMRI and Positron Emission Tomography (PET) imaging data, a recent study tested predictions from these models to understand how emotional information is represented in the brain (Lindquist et al., 2015). Evidence in support of bipolarity hypothesis in regions such as the vmPFC where activation patterns seem to follow a linear trend (positive > neutral > negative) was found, but no findings supported the bivalent model hypothesis. Instead, the authors observed evidence for valence general coding in many brain regions (Lindquist et al., 2015). It should be noted, however, that the studies included in this meta-analysis did not present positive and negative emotional stimuli *simultaneously* in any condition, which we believe is critical for testing these different models of valence. For instance, in an olfactory fMRI study

(Grabenhorst et al., 2007), the authors investigated perception of odor mixtures that contained both pleasant and unpleasant components. Separate processing of pleasant and unpleasant components of those mixtures was found in different brain regions, providing evidence for the bivalent model. Clearly, more studies with *co-joint* positive and negative stimuli are needed to better understand how emotional information is represented in the brain.

To summarize, our current understanding of how the brain integrates positive and negative information is still incomplete (Bissonette et al., 2014; Hayes et al., 2014). The majority of early studies have employed only one type of stimuli, either positive or negative (along with a neutral baseline) and while later studies have employed both positive and negative stimuli, most have treated them separately. *Using functional MRI, our studies attempted to fill some of the critical gaps in the literature and advance our current understanding of appetitive-aversive interactions in the healthy adult human brain.*

Chapter 2 Specific Aims

Our knowledge about how brain integrates positive and negative information is still incomplete. Therefore the objective of this dissertation work is to advance our understanding of appetitive-aversive interactions in healthy adult human brain during perception and attention using functional MRI combined with multiple data-analytic techniques. To fill in some of the critical gaps noted above, we conducted two fMRI studies in this dissertation: Aim 1 investigated the influence of reward on negative distractor processing, and Aim 2 investigated interactions between positive and negative emotional processing.

Aim 1: Interactions between reward motivation and aversive distractor processing

The objective of this aim was to investigate brain mechanisms underlying the influence of performance-based rewards on negative distractor processing during attention. Our primary hypothesis was reward would improve task performance by *counteracting* the impact of negative distractor processing. Furthermore, we probed the relationship between reward-related brain activity and the behavioral impact of reward on negative processing.

Aim 2: Interactions between positive and negative emotional processing

The objective of this aim was to investigate the interactions between positive and negative emotional processing during perception. In terms of standard univariate analysis, our primary hypothesis was in brain regions that code *valence*, we would observe *competitive* interactions between positive and negative processing. In regions

that code *salience*, we tested two alternative hypotheses regarding the overall intensity. Finally, we examined how functional interactions between brain regions were sensitive to valence and salience aspects of the emotional stimuli.

We sought to investigate how the brain integrates positive and negative information, which is relevant for normal human behaviors. Deeper understanding of how the brain integrates positive and negative information could potentially help develop efficacious treatments for people suffering from mental disorders such as anxiety and depression (Dillon et al., 2014; Pizzagalli, 2014). Furthermore, investigating how the brain integrates both positive and negative information could help refine our understanding of how emotions are represented in the brain (Lindquist et al., 2015).

Chapter 3 Interactions between reward motivation and aversive distractor processing

Introduction

In many real life situations, appetitive and aversive information jointly impact brain and behavior. Understanding potential interactions between them is important given their relevance to disorders such as depression and anxiety, where disturbances in reward and negative processing are well documented (Dillon et al., 2014; Pizzagalli, 2014). Brain imaging studies that have investigated interactions between reward and aversive processing have mainly focused on decision-making mechanisms (Talmi et al., 2009; Park et al., 2011); a few studies have also probed the influence of stress on different aspects of reward processing (Ossewaarde et al., 2011; Porcelli et al., 2012; Kumar et al., 2014). Notably, most investigations have focused on understanding the influence of aversive processing on reward mechanisms, but not vice versa (Wittmann et al., 2008). Thus, it is important to probe the influence of reward on negative processing, in particular during perception and attention tasks.

Recent work suggests that potential reward-driven motivation enhances executive control mechanisms that help with prioritizing goal-relevant information, leading to improved performance across perceptual and cognitive tasks (Pessoa, 2013; Botvinick and Braver, 2015). For instance, using a *proactive* manipulation, where the potential for reward was signaled by advance cues, we reported that enhanced selective attention during the reward condition reduced the influence of neutral distractors resulting in better performance during a Stroop-like interference task (Padmala and Pessoa, 2011). In a similar fashion, potential reward has been

shown to reduce switching costs in task-switching paradigms (Savine et al., 2010), decrease stop-signal reaction times during response inhibition tasks (Boehler et al., 2012), and increase post-conflict control in flanker tasks (Braem et al., 2012). These and other recent findings in the literature highlight the role of reward motivation in fine tuning executive function in a manner that ultimately leads to selective effects in behavior.

However, little is known about how potential reward-driven attentional control mechanisms impact the processing of task-irrelevant negative information. Two event-related potential (ERP) studies investigated this question, but yielded mixed results. One study claimed independence between reward expectancy and negative information and suggested that emotion- related processing was privileged and immune to the reward manipulation (Kaltwasser et al., 2013). In contrast, a second study reported that reward expectation reduced the processing of task-irrelevant negative information (Wei et al., 2016). Overall, our knowledge about the mechanisms underlying the influence of reward expectancy on aversive distractor processing is incomplete.

In the present study, we investigated the influence of performance-based rewards on aversive distractor processing with functional MRI. As in our recent behavioral study (Padmala and Pessoa, 2014), we used a proactive manipulation of reward, where each trial started with an advance cue that signaled the potential for reward. During the task phase, participants discriminated the orientation of peripheral bars while ignoring a centrally presented aversive or neutral picture (Figure 3.1). In our previous behavioral study, we detected a interaction between potential reward and

negative items, where the interference of negative distractors was reduced with reward expectancy (Padmala and Pessoa, 2014). We thus anticipated that, in the present study, reward expectancy would reduce the impact of negative distractors at the behavioral level.

Analogous to behavior, we also anticipated interactions between potential reward-driven goal-directed attentional control and negative distractor processing in the brain during the task phase. We were particularly interested in evaluating responses in the amygdala to test for potential mechanisms of interaction. An interaction pattern revealing reduced differential responses to negative vs. neutral pictures during the reward condition would indicate that potential reward helped in filtering out distractors (and would be consistent with the anticipated behavioral effect). In contrast, the lack of an interaction pattern in the amygdala in the presence of the anticipated behavior (decreased negative distractor interference with reward), would provide evidence that negative stimuli were not filtered out, but that enhanced attentional control still was able to counteract their adverse influence.

Furthermore, we hypothesized that the processing of a reward cue would lead to increased responses in the ventral striatum, as well as fronto-parietal regions important for attention (Botvinick and Braver, 2015). We evaluated two (not mutually exclusive) forms of brain-behavior links. If ventral striatum activity reflected a "reward signal," cue-related responses would be associated with a general energizing effect of reward expectancy on behavior (reward main-effect scores across participants); in contrast, if ventral striatum activity reflected more specific processes allowing improved behavior during challenging situations (see Sarter et al., 2006;

Salamone et al., 2009), cue-related responses would be associated with a selective effect of potential reward on behavior (as indexed via reward by emotion interaction scores).

Methods

Participants

Sixty-one participants (31 males; mean age: 21.7 years, range: 18-33 years) with normal or correct-to-normal vision volunteered to participate in the study. Based on self-report, all participants were right-handed and were free from any past history of neurological or psychiatric disease. The study was approved by the Institutional Review Board of the University of Maryland, College Park. All participants provided informed consent prior to participating in the study. Out of 61 participants, two female participants voluntarily quit the study before completion and two other participants (one male and one female) exhibited poor behavioral performance (less than chance performance in one or more conditions). Data from these individuals were excluded from the analysis, resulting in a final dataset with 57 participants.

Stimuli and behavioral paradigm

The task was based on modified versions of the monetary incentive delay task (Knutson et al., 2001) and the bar-orientation discrimination task (Erthal et al., 2005), and was similar to the one we employed in our recent behavioral study (Padmala and Pessoa, 2014) with a few minor changes to fit with the scanner environment. Each trial (Figure 3.1) started with the presentation (1 sec) of a cue stimulus indicating the

Reward condition ("##": no-reward; "$$": reward). The cue was followed by a 2-6 sec variable delay period during which a white fixation cross was shown at the center of the screen. Then, a centrally positioned image (neutral or negative; 4° x 4°) was shown (0.2 sec) together with two oriented bars positioned peripherally (3.5° degrees to the left and right). The participant's task was to indicate whether the two bars were of same or different orientation and were given 1500 msec to respond via button press. The central images were task irrelevant. Forty-eight neutral and 48 negative images were employed from the International Affective Picture System (Lang et al., 1997b, 2005) and a database of mutilation images developed by the Laboratory of Neurophysiology of Behavior at the Federal Fluminense University, Brazil (Mocaiber et al., 2011). We attempted to match for picture complexity by carefully choosing images with a clear counterpart (e.g., a mutilated arm/hand and an intact arm/hand). The trial ended with a 2-6 sec variable blank screen. Participants performed a total of 6 runs of 32 trials each with random trial order, totaling 48 trials per condition for the entire experiment; due to a technical error, for the first 5 participants, one trial of the no-reward/neutral condition in the fifth run was not presented. Each run ended with a 10-sec blank screen to capture the hemodynamic response of the last trial. Across the experiment, neutral and negative images were repeated once; they were shown once during the reward condition and once during the no-reward condition. Responses were made on MR-compatible buttons using index and middle fingers of the right hand and were counterbalanced across participants in terms of "same" and "different" responses. For the presentation of visual stimuli and recording of participant's

responses, Presentation software (https://www.neurobs.com/; Neurobehavioral Systems, Albany, CA, USA) was used.

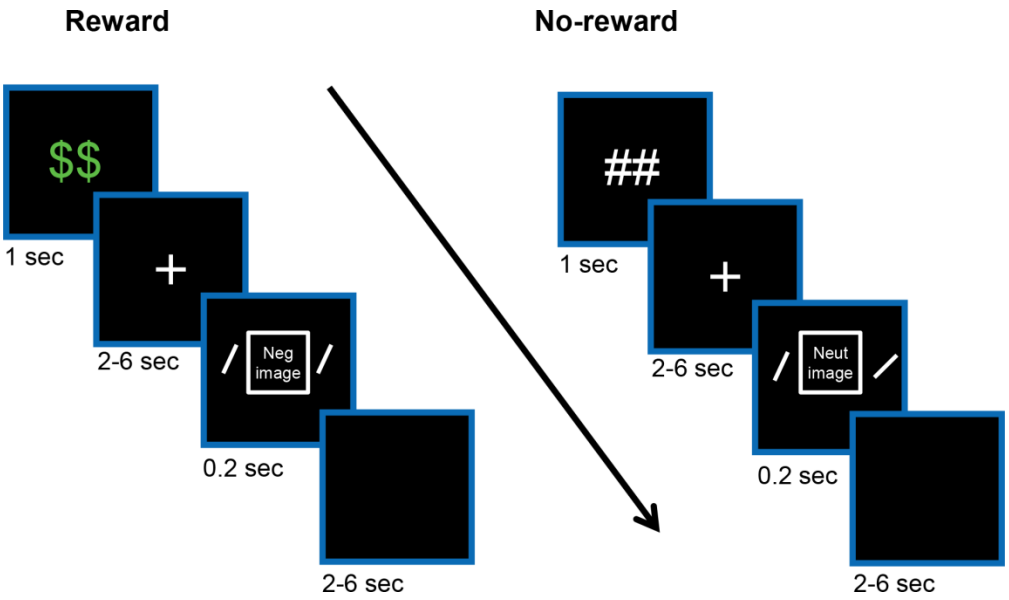

Figure 3.1 Experimental design. On each trial, an initial cue indicated potential for reward followed by a variable delay period during which a white fixation cross was shown. Then a negative or neutral task-irrelevant picture (not shown here) was presented centrally and two bars were presented peripherally (not drawn to scale). The participant's task was to indicate whether the bars are of same or different orientation while ignoring the central picture. Finally, each trial ended with a variable inter-trial interval. During the reward condition (left side), participants were rewarded if performance was both fast and accurate.

Before the start of the experimental runs, participants performed a brief training run to familiarize themselves with the bar-orientation task and buttons. This training run involved only neutral pictures (using a separate set of stimuli) and contained a total of 12 trials without a cue phase. Participants performed a second training run during an initial high-resolution anatomical scan (see below). Again, this training run involved only neutral pictures (using a separate set of stimuli) and

contained a total of 32 trials, each starting with a no-reward or reward cue. Participants were provided feedback after each trial and were explicitly informed that no actual reward would be provided during this training run. To calibrate the difficulty of the bar-orientation task to target an overall accuracy of around 80% correct, at the start of first main run, we adjusted the angle between the bars based on the performance during no-reward trials during the second training run. The goal of this "intermediate" task difficulty was to leave spare attentional resources needed for the processing of pictures and thus potentially interfere with task performance depending on picture type; at the same time, this level potentially allowed reward to have an influence on behavior (Padmala and Pessoa, 2014). If needed, task difficulty was calibrated after every two main runs based on the performance during the no-reward/neutral trials of the preceding two runs. Participants were informed that they could earn 25 cents per trial during the reward condition if they were both fast and accurate. The reaction time (RT) cut-off point to determine fast performance was set up at 750 msec for the reward-neutral condition and an additional 20 msec were added to this value for the reward-negative condition. The total dollar amount accrued was shown at the end of each run (not after each trial). Over the entire experiment, participants could earn an extra $24 based on their performance during reward trials. On average, participants won $16.8 of bonus reward (in addition to the base pay of $25/hour).

MRI Data Acquisition

MRI data were collected using a 3 Tesla Siemens TRIO scanner (Siemens Medical Systems, Erlangen, Germany) with a 32-channel head coil (without parallel imaging). The scanning session began with a high-resolution MPRAGE anatomical scan (TR = 1900 ms, TE = 2.32 ms, TI = 900 ms, 0.9 mm isotropic voxels). Subsequently, during each functional run, 126 BOLD EPI volumes were acquired with a TR of 2500 and TE of 25 ms. Each volume consisted of 44 oblique slices with a thickness of 3 mm and an in-plane resolution of 3 mm x 3 mm (192 mm field of view). Slices were positioned approximately 30 degrees clockwise relative to the plane defined by the line connecting the anterior and posterior commissures, helping to decrease susceptibility artifacts at regions such as the orbitofrontal cortex and amygdala.

Behavioral data analysis

As in past studies (Erthal et al., 2005; Padmala and Pessoa, 2014), to investigate negative interference effects, we focused on RT data, but additional analyses on accuracy data were also conducted. For the RT analysis, error trials and trials with an RT exceeding three standard deviations from the condition-specific mean (0.8% of the trials) were excluded in each participant. For each participant, mean RT and accuracy rate data were determined as a function of *Reward* (reward, no-reward) and *Distractor* type (negative, neutral), and repeated-measures ANOVAs were conducted in SPSS software (IBM SPSS Statistics for Windows, Version 23.0, Armonk, New York). To further evaluate observed interaction effects, we performed post-hoc

comparisons using a paired *t*-test. We used an alpha level of 0.05 for all statistical tests.

General fMRI data analysis

Preprocessing of functional and anatomical MRI data was conducted with AFNI software (Cox, 1996; http://afni.nimh.nih.gov/), except as outlined below. The first three volumes of each functional run were discarded to account for equilibration effects. Data from the remaining volumes were slice-time corrected (3dTshift program) using Fourier interpolation to align the onset times of every slice in a volume to the first acquisition slice. Then a six-parameter rigid body motion correction (3dvolreg program) was applied to spatially register all volumes to the first volume, which was closest in time to the high-resolution anatomical image. The high-resolution anatomical image was rotated (3dWarp program) to match the oblique plane of functional data, and the ROBEX package (Iglesias et al., 2011); https://www.nitrc.org/projects/robex) was used to skull strip the anatomical image. The anatomical images in the oblique plane were used by the FSL software (Epi_reg program) to calculate a 12-parameter affine transformation matrix to co-register the first functional volume with the anatomical image using a boundary-based registration technique (Greve and Fischl, 2009). Data were normalized to standard space via a two-step procedure. In the first step, the anatomical image in the oblique plane was normalized to the MNI152 template at 1 mm resolution (from the FSL package) using nonlinear registration via the ANTs software (Avants et al., 2009) (http://stnava.github.io/ANTs/). Functional data were subsequently aligned to anatomical data and normalized to the MNI152 template by applying transformation

matrices from co-registration and normalization in a single step and resampled to 2-mm isotropic voxels. A 6-mm full-width half-maximum (FWHM) Gaussian filter was used to spatially smooth (3dBlurInMask program) all functional volumes (restricted to grey-matter voxels). Finally, to interpret the estimated regression coefficients in terms of percent signal change, the average intensity at each voxel (per run) was scaled to 100.

Voxelwise analysis

Each participant's preprocessed functional MRI data were analyzed using multiple linear regression with AFNI using the 3dDeconvolve program. As noted above, our design included, on each trial, a variable delay between the cue and task phases and a variable inter-trial interval. When cue-phase responses are transient and independent of signals during the cue-to-task delay, this kind of design enables estimation of separate cue and task responses (Serences, 2004). However, in the present experiment, it is conceivable that cue responses would be sustained during the delay period, in particular in regions involved in preparatory attention (Engelmann et al., 2009). In this scenario, because cue-phase responses might be present until the onset of the task phase (Figure 3.2), estimation of unique contributions of the two phases is problematic because of the considerable response overlap (Ruge et al., 2009); note that the overlap would be present for short or long delay periods, that is, it is independent of delay duration.

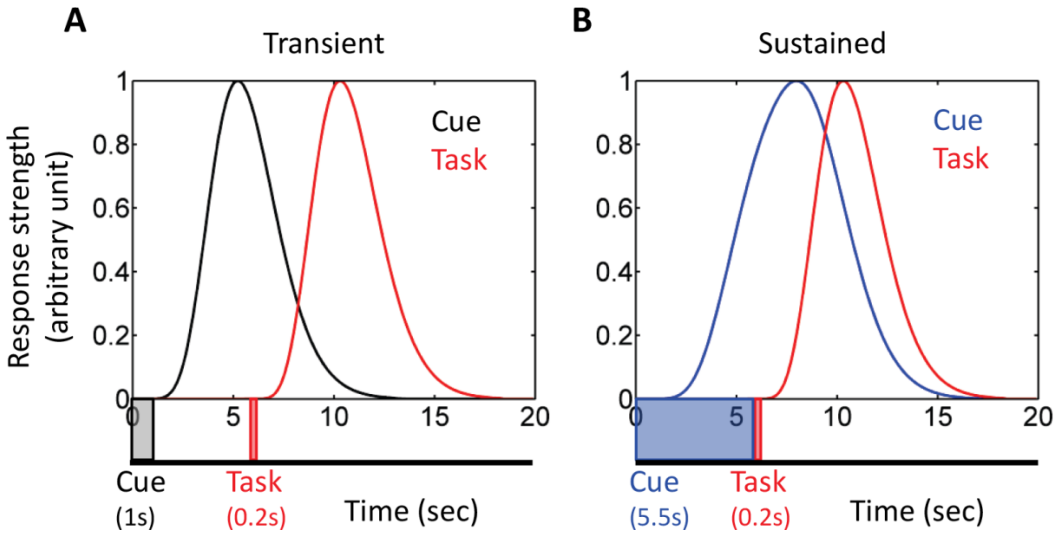

Figure 3.2 Simulated functional MRI responses and potential cue-task overlap. (A) To simulate transient cue responses, the cue was assumed to be presented for 1 sec (as in the experiment), followed by a 4.5-sec delay period (which varied between 2-6 secs in the experiment), and a 0.2-sec task phase (indicated by the timeline). The overlap between cue and task responses is small. (B) To simulate sustained cue responses, the cue was assumed to the presented for 5.5 secs and followed immediately by a 0.2-sec task phase (indicated by the timeline). The overlap between cue and task responses is quite substantial. Simulated responses were generated by employing a canonical gamma variate hemodynamic response function (Cohen, 1997).

To address this issue, we estimated cue and task responses using a two-step procedure, as follows. First, we estimated cue-phase responses after controlling for task-related activity. To do so, we ran multiple regression on the preprocessed functional data including only *task phase* regressors in the model: no-reward and reward events at the task phase separately for the neutral and negative conditions, and a separate regressor of no interest that modeled error trials (pooled over all four conditions) during the task phase. Additionally, to model baseline and drifts of the MR signal, constant, linear, and quadratic terms were included for each run separately as covariates of no interest; six estimated motion parameters and their first derivatives

were also included as regressors in the model. Subsequently, the residual time series from this initial multiple regression model was used as input for a subsequent multiple regression analysis which included only *cue phase* regressors: reward and no-reward events at the cue phase, and error trials (pooled over all four conditions) at the cue phase. In this manner, estimates of *cue phase* responses from the second model were uncontaminated from task-phase responses.

Likewise, task phase responses were estimated after controlling for cue-related activity. To do so, we ran a multiple regression on the preprocessed functional data including only *cue phase* regressors in the model: reward and no-reward events at the cue phase, and error trials (pooled over all four conditions) at the cue phase. Additionally, baseline, drift, and motion-related contributions were handled as above. Subsequently, as above, the residual time series from this initial multiple regression model was used as input for a subsequent multiple regression model which included only *task phase* regressors: no-reward and reward events at the task phase separately for the neutral and negative conditions, and a separate regressor that modeled error trials (pooled over all four conditions) during the task phase. In this manner, estimates of *task phase* responses from the second model were uncontaminated from cue-phase responses.

In the multiple regression analyses above, the following additional steps were performed. (1) To further control for head motion-related artifacts in the data (Siegel et al., 2014), we excluded volumes (on average 0.25%) with a frame-to-frame displacement of more than 1 mm Euclidean distance. (2) To estimate cue-related responses, no assumptions were made about the shape of the hemodynamic response,

because as noted above potential responses could be transient or sustained during the delay period depending on the brain region. Responses were estimated starting from cue onset to 15 secs using cubic spline basis functions. As an index of response strength, we used the average of the estimated responses at 5 and 7.5 sec after cue onset (as determined via the spline-based estimates); (3) To estimate task-phase responses which were expected to be transient, we used a canonical gamma variate hemodynamic response function model that was convolved with a square wave of 0.2 sec stimulus duration (Cohen, 1997). (4) For the first five participants, the last four volumes of the fifth run were censored as the run finished early due to a technical error.

Finally, as a control analysis to confirm that the results were not unduly related to the two-step procedure, we ran a separate multiple regression analysis which included both cue and task phase regressors in the same model: no-reward and reward events at the cue phase, and no-reward and reward events at the task phase separately for the neutral and negative conditions. Error trials (pooled over all four conditions) were modeled separately using two additional regressors of no interest, one for the cue phase and the other for the task phase. Cue-related responses were estimated starting from cue onset to 15 secs post onset using cubic spline basis functions. As an index of response strength, we used the average of the estimated responses at 5 and 7.5 sec after cue onset (as determined via the spline-based estimates). Task-phase responses were estimated using a canonical gamma variate hemodynamic response function model that was convolved with a square wave of 0.2 sec duration. Since cue-related responses were estimated using cubic spline basis

functions for 15 secs from onset, considerable collinearity was present in the model (R^2 values ranged between 0.67-0.78; note that is because multi-collinearity potentially impairs the estimation of regression coefficients (Mumford et al., 2015) that we employed the two-step procedure in the main analyses described above). Finally, to model baseline and drifts of the MR signal, constant, linear, and quadratic terms were included for each run separately (as covariates of no interest), and six estimated motion parameters and their first derivatives were included as nuisance regressors in the model.

Group analysis

Whole-brain voxelwise random-effects analyses were conducted using response estimates from individual-level analyses (restricted to gray-matter voxels) in AFNI. To probe reward processing during the cue phase, we used cue-phase responses (controlling for task-related activity) and ran a paired *t*-test to contrast reward and no-reward conditions using the 3dttest++ program. To probe the interaction between reward and distractor processing during the task phase, we used task-phase responses (controlling for cue-related activity) and ran a 2 *Reward* (reward, no-reward) × 2 *Distractor* (negative, neutral) repeated-measures ANOVA using the 3dANOVA3 program.

The alpha-level for voxelwise statistical analysis was determined by simulations using the 3dClustSim program. For these simulations, the smoothness of the data was estimated using 3dFWHMx program based on the residual time series from the individual-level voxelwise analysis. Taking into account the recent report of

increased false-positive rates linked to the assumption of Gaussian spatial autocorrelation in fMRI data (Eklund et al., 2016), we used the new `-acf` (i.e., auto-correlation function) option recently added to the `3dFWHMx` and `3dClustSim` tools, which models spatial fMRI noise as a mixture of Gaussian plus mono-exponential distributions. This improvement was shown to control false positive rates around desired alpha level, especially with randomized fast event-related designs as employed in this study (Cox et al., 2017). Based on a voxel-level uncorrected p-value of 0.001, simulations indicated a minimum cluster extent of 48 voxels (2.0 x 2.0 x 2.0 mm) for a cluster-level corrected alpha of 0.05.

Relationship between cue-phase brain responses and behavior during the task phase

The only difference between the reward and no-reward conditions in our design was the type of advance cue employed (Figure 3.1). Thus, to investigate the potential link between brain responses at the cue phase and subsequent behavior during the task phase, we focused on the ventral striatum, a region consistently implicated in reward-related processing (Haber and Knutson, 2010; Bissonette et al., 2014). We defined bilateral ventral striatum regions of interest (ROIs) based on the structural atlas provided in the FSL package (http://fsl.fmrib.ox.ac.uk/fsl/fslwiki/Atlases/striatumstruc). This anatomical "ventral striatum" ROI included nucleus accumbens, portions of medial caudate and rostral-ventral putamen. For each participant, and separately for each hemisphere, we averaged the difference of the response estimates (reward minus no-reward) within the ROI. First, we probed the relationship between cue-phase responses and an

energizing effect of reward on behavior, as indexed by reward main effect scores. To do so, for each ROI and across participants, we ran a robust skipped correlation analysis (Rousselet and Pernet, 2012; Wilcox, 2012) between cue-phase differential responses (Reward – No_Reward) and behavioral RT reward scores ([Negative + Neutral]$_{NO\_REWARD}$ – [Negative + Neutral]$_{REWARD}$). Next, we probed the relationship between cue-phase responses and selective effects of reward on behavior, as indexed by a reward by distractor interference scores. To do so, for each ROI and across participants, we ran a robust skipped correlation analysis between cue-phase differential responses (Reward – No_Reward) and behavioral RT interaction scores ([Negative – Neutral]$_{NO\_REWARD}$ – [Negative – Neutral]$_{REWARD}$). The p-values for robust skipped correlation was estimated via bootstrapping based on 100,000 simulations (Wilcox, 2015).

Relationship between task-phase brain responses and behavior during the task phase

To investigate the potential link between brain responses at the task phase (controlling for cue-related activity) and behavior, we ran a voxelwise robust skipped correlation analysis (across participants) between fMRI-based interaction scores at the task phase and RT-based interaction scores. For computational expediency, the p-value for robust skipped correlation was estimated via bootstrapping based on 5000 simulations. To control for multiple comparisons, we used a voxel-level uncorrected p-value of 0.001 with a minimum cluster extent of 48 voxels (cluster-level alpha of 0.05).

Functional connectivity analysis during cue phase

Recent fMRI studies employing a proactive manipulation of reward have reported increased functional connectivity between striatal regions and cortical sites that are important for top-down attention (Harsay et al., 2011; Padmala and Pessoa, 2011). We thus investigated functional interactions between the ventral striatum and the rest of the brain by employing voxelwise functional connectivity analysis based on trial-by-trial responses. Similar to the so-called "beta series correlation method" (Rissman et al., 2004), for each participant, we estimated trial-based responses at the cue phase (controlling for task-related activity) using the 3dLSS command in AFNI, a recently proposed method to improve estimation of trial-based responses in fast-event related designs (Mumford et al., 2012) (we modified 3dLSS to model the trial of interest, two additional "combined" regressors, one for the remaining reward trials, one for the remaining no-reward trials, as well as a regressor for error trials). As in our recent studies (Padmala and Pessoa, 2011; Choi et al., 2012), to estimate trial-based responses at the cue phase, we assumed that responses were transient in nature and used a canonical gamma variate hemodynamic response function model that was convolved with a square wave of 1.0 sec stimulus duration (Cohen, 1997). Although the assumption of transient responses may not be optimal for some brain regions, without assuming a fixed shape the estimation of trial-based responses during fast event-related designs is rather poor and possibly unfeasible. We therefore believe that the assumption is defensible.

To create representative ROI estimates, trial-based responses were averaged across voxels within the anatomically defined left and right ventral striatum ROI,

separately. We then calculated the trial-by-trial robust skipped correlation between ventral striatum responses and the rest of the brain in a voxelwise fashion, separately for the reward and no-reward conditions. Estimated correlations were then initially transformed (via Fisher's *Z*-transform) and contrasted between reward and no-reward conditions at the group level via a paired *t*-test using the 3dttest++ program. We would like to note that the connectivity analysis employed here is conceptually similar to the standard Psycho-physiological interaction (PPI) analysis (Friston et al., 1997) and has shown to have better power to detect functional interactions in event-related designs as employed in this study (Cisler et al., 2014). To control for multiple comparisons, we used a voxel-level uncorrected p-value of 0.001 with a minimum cluster extent of 48 voxels (cluster-level alpha of 0.05).

Results

Behavioral results

Mean RT data were evaluated according to a 2 *Reward* (reward, no-reward) x 2 *Distractor* (negative, neutral) repeated-measures ANOVA (Figure 3.3A). The main effect of *Reward* was significant ($F_{1, 56} = 135.59$, $p = .000$, $\eta^2_p = 0.71$). Mean RT was faster during the reward (686 msec) compared to the no-reward condition (716 msec), demonstrating the effectiveness of the reward manipulation. The main effect of *Distractor* was also significant ($F_{1, 56} = 6.17$, $p = .016$, $\eta^2_p = 0.10$), such that RTs during the negative condition (705 msec) were slower compared to the neutral condition (697 msec), revealing a small but consistent effect of the distractor

stimulus. Critically, the *Reward* x *Distractor* interaction was significant ($F_{1, 56}$ = 4.44, p = .040, η^2_p = 0.07). To further probe the two-way interaction, we ran two additional paired *t*-tests (negative vs. neutral) for the reward and no-reward conditions, separately. We detected a robust negative interference effect during the no-reward condition (13 msec; $t(56)$ = 2.98, p = .004, d = 0.39), but not during the reward condition (2 msec; $t(56)$ = 0.66, p = .51, d = 0.09).

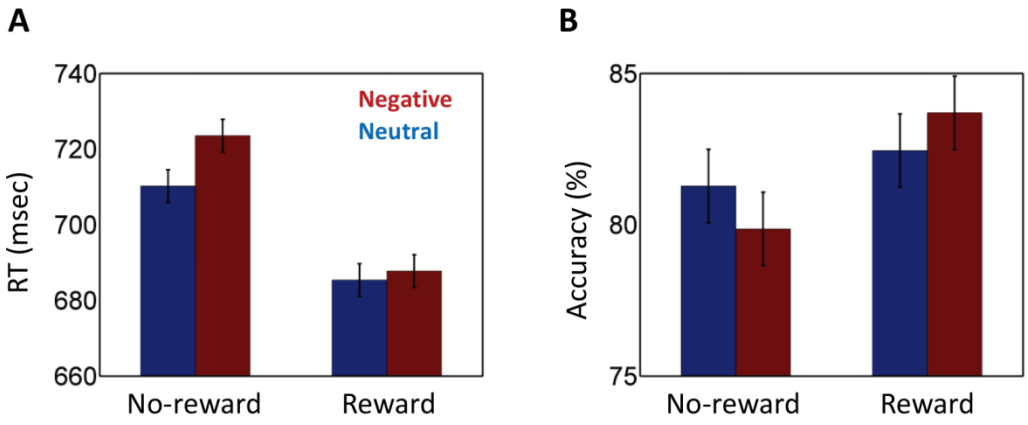

Figure 3.3 Behavioral results. (A) RT data. During no-reward trials, negative images slowed responses relative to neutral ones. This interference effect was reduced during the reward condition. (B) *Accuracy data*. During no-reward trials, negative images reduced accuracy relative to neutral ones. This effect was reduced during the reward condition. Error bars denote standard within-subject error term for interaction effects (Loftus and Masson, 1994)

Because we observed a main effect of *Reward* such that the overall RT was faster during the reward condition, it is conceivable that the reduced negative interference during the reward condition was due to overall faster RTs (faster RTs would leave less room for interference). Therefore, we calculated a ratio-based index of interference (negative/neutral) separately for the reward and no-reward conditions. A comparison of the two via a paired *t*-test revealed a difference that is just outside the critical boundary ($t(56)$ = 1.896, p = .06, d = 0.25), supporting the interpretation

of reduced negative interference during the reward condition. Furthermore, the main effect of *Reward* and interaction scores were not strongly correlated across participants (robust skipped correlation: r = .17, p = 0.32) while the original and ratio-based indices of interaction scores were highly correlated across participants (robust skipped correlation: r = .99, p < 0.001), suggesting that the reduction of negative interference during reward was not simply due to overall faster RTs.

The 2 *Reward* x 2 *Distractor* repeated-measures ANOVA on mean accuracy rate data (Figure 3.3B) also revealed a main effect of *Reward* ($F_{1, 56}$ = 17.71, p < 0.001, η^2_p = 0.24), such that accuracy was higher during reward (83.1%) compared to no-reward (80.6%). The main effect of *Distractor* was not significant ($F_{1, 56}$ = 0.02, p = 0.895, η^2_p = 0.00). Finally, the *Reward* x *Distractor* interaction was just outside the critical decision boundary ($F_{1, 56}$ = 3.62, p = 0.06, η^2_p = 0.06).

The RT and accuracy results taken together rule out the possibility of a speed-accuracy tradeoff, as participants were both more accurate and faster during the reward compared to no-reward condition. Further, faster RTs also rule out the possibility of cautious responding during reward trials, which could help reduce negative-picture interference. Overall, the behavioral results point to a more selective effect of reward on negative distractor processing.

Functional MRI voxelwise analysis results

Cue phase

To investigate the impact of the reward processing, we contrasted cue-related responses (controlling for task-related activity) during reward vs. no-reward conditions. This contrast revealed stronger responses during the reward condition in a large cluster that spanned multiple subcortical and cortical sites (Figure 3.4 and Table 3.1), including dorsal and ventral striatum (the latter including the accumbens), midbrain, thalamus, as well as fronto-parietal regions.

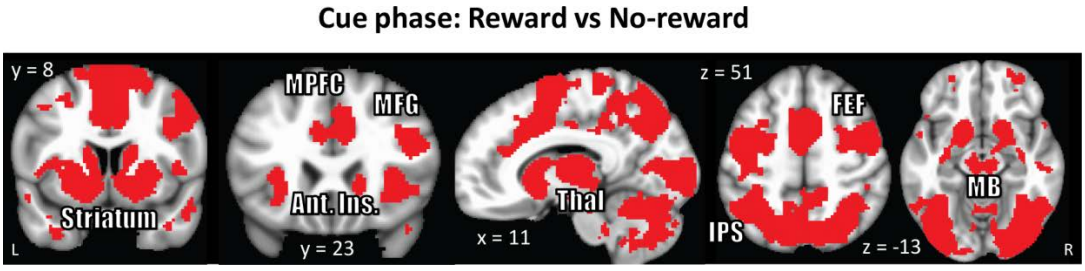

Figure 3.4 Cue phase functional MRI results displayed at an uncorrected p = .001 and 48-voxel cluster extent (cluster-level alpha of 0.05). Because cluster-extent based thresholding was used for multiple comparisons correction, voxels are displayed using a binary threshold. For further rationale about using binary maps in the context of cluster-based thresholding, see Woo et al., 2014. Increased responses were observed during processing of reward (vs. no-reward) cue in subcortical regions and fronto-parietal regions. MPFC: medial prefrontal cortex, MFG: middle frontal gyrus, Ant. Ins: anterior insula, Thal: Thalamus, MB: midbrain, FEF: frontal eye-fields, IPS: intraparietal sulcus

Table 3.1 Clusters that survived multiple comparisons correction in voxelwise analysis at the cue phase (peak MNI coordinates, t(56) values, and cluster size [k]). Peak coordinates are presented for completeness and potential meta-analysis; with cluster-based thresholding, it is not possible to conclude that all the reported peaks were activated [see Woo et al., 2014]

Cluster		*x*	*y*	*z*	*t*	*k*
Cluster 1 (including fronto-parietal cortical regions and subcortical areas)	R/ L	36	-88	-8	10.03	51669
Lateral orbitofrontal cortex	L	-22	46	-16	5.29	96
Frontal cluster (including middle frontal gyrus)	L	-26	46	18	8.06	1910
Inferior temporal gyrus	L	-58	-18	-30	4.46	50
Temporal pole	R	50	18	-20	6.24	155
Temporal pole	L	-42	12	-24	4.61	124

Task phase

The main focus of this study was to investigate the influence of potential reward on negative interference, which was examined via the *Reward* x *Distractor* interaction on task-phase responses (controlling for cue-related activity). We observed significant interaction effects in several activation clusters, including in medial prefrontal cortex (spanning dorsal anterior cingulate cortex and supplementary motor area), posterior cingulate cortex, right anterior/mid-insula, right inferior parietal lobule, left lateral occipital cortex (at inferior and superior locations) and right lateral occipital cortex (at a superior location), as well as a large left fronto-parietal cluster (spanning inferior parietal lobule and anterior/mid-insula) (Figure 3.5 and Table 3.2). Paralleling the behavioral interaction pattern, in the clusters that exhibited an interaction pattern, stronger negative (vs. neutral) responses during the no-reward condition were *reduced* during the reward condition. In the control analysis where cue and task phase

regressors were modeled simultaneously (see METHODS), a similar interaction pattern was observed in the clusters mentioned above except that medial prefrontal cortex (35 voxels), posterior cingulate cortex (35 voxels), and bilateral lateral posterior occipital cortex (left inferior: 36 voxels; left superior: 15 voxels; right superior: 10 voxels) did not survive the multiple comparisons correction.

We observed a main effect of *Distractor* in clusters including the bilateral amygdala, bilateral ventral visual cortex/fusiform gyrus, bilateral lateral orbitofrontal cortex, and left ventral striatum (a similar pattern was seen in right ventral striatum at a slightly lower threshold; Figure 3.6 and Table 3.2). In the amygdala, ventral visual cortex/fusiform gyrus and orbitofrontal cortex, stronger responses were observed during the negative compared to the neutral condition. However, in the ventral striatum we observed the converse pattern, where responses were weaker during the negative compared to the neutral condition.

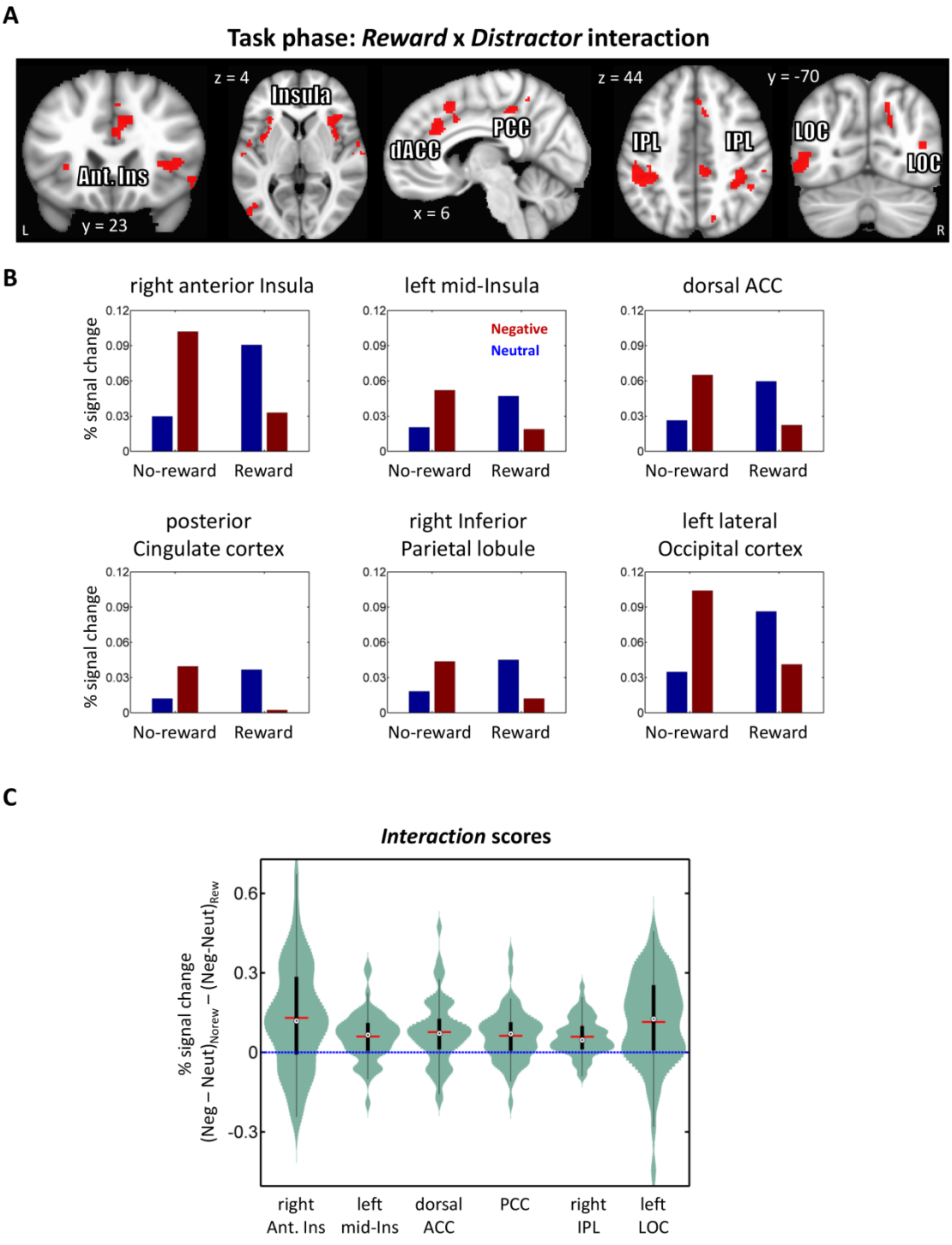

Figure 3.5 Task phase functional MRI results. (A) Clusters exhibiting significant *Reward* (reward, no-reward) x *Distractor* (neutral, negative) interactions displayed at an uncorrected p = .001 and 48-voxel cluster extent (cluster-level alpha of 0.05). Because cluster-extent based thresholding was used for multiple comparisons correction, voxels are displayed using a binary threshold. For further rationale about

using binary maps in the context of cluster-based thresholding, see Woo et al., 2014. (B) Average responses within clusters that exhibited interaction effects. As some clusters spanned large sectors, for illustration purposes, clusters were selected at an uncorrected p = .0005 and 34-voxel cluster extent (cluster-level alpha of 0.05). To avoid circularity, error bars are not plotted. (C) Distributions of within-subject interaction scores in units of % signal change. The box plots within the violins indicate the interquartile range (first quartile to third quartile), red lines show the mean values, and black dots inside white circles show median values. Ant. Ins: anterior insula, IPL: inferior parietal lobule, dACC: dorsal anterior cingulate cortex, PCC: posterior cingulate cortex, LOC: lateral occipital cortex.

Table 3.2 Clusters that survived multiple comparisons correction in voxelwise analysis at the task phase (peak MNI coordinates, F(1,56) values, and cluster size [k]). Peak coordinates are presented for completeness and potential meta-analysis; with cluster-based thresholding, it is not possible to conclude that all the reported peaks were activated [see Woo et al., 2014]

Cluster		x	y	z	*F*	*k*
Reward* x *Distractor						
Medial prefrontal cortex (including dorsal anterior cingulate cortex and supplementary motor area)	R	6	28	36	21.17	258
Inferior parietal lobule	R	34	-34	52	34.67	350
Fronto-parietal cluster (including inferior parietal lobule and anterior/mid insula)	L	-46	-38	44	30.67	1176
anterior/mid insula	R	42	24	6	22.95	360
Posterior cingulate cortex	R	8	-36	46	26.09	88
Lateral occipital cortex (inferior)	L	-52	-70	-6	23.18	224
Lateral occipital cortex (superior)	L	-44	-82	18	23.41	86
Lateral occipital cortex (superior)	R	42	-72	12	24.13	77
Supramarginal gyrus (inferior)	R	62	-24	26	18.55	72
Supramarginal gyrus (superior)	R	62	-34	48	16.86	79
Superior temporal gyrus	R	64	-2	-4	20.81	187

Precuneus	R	18	-68	32	18.29	56
Main effect of *Reward*						
Postcentral gyrus	R	-66	-22	18	20.65	103
Main effect of *Distractor*						
Ventral visual cortex (including fusiform gyrus)	R	38	-68	-12	76.64	1682
Ventral visual cortex (including fusiform gyrus)	L	-36	-80	-10	73.58	1695
Amygdala	R	24	-4	-14	32.99	84
Amygdala	L	-22	-6	-12	26.05	48
lateral orbitofrontal cortex	R	28	32	-12	35.62	97
lateral orbitofrontal cortex	L	-38	34	-12	28.58	166
Anterior insula	L	-40	26	4	24.98	66
Inferior frontal gyrus	R	44	12	26	20.61	86
Superior parietal/occipital cortex	R	26	-60	52	28.89	153
Superior parietal/occipital cortex	L	-22	-66	40	24.96	61
Ventral striatum	R	16	18	-4	17.18	31[U]
Ventral striatum	L	-6	16	-6	21.09	133
Lateral occipital cortex (superior)	R	44	-70	36	28.48	315
Lateral occipital cortex (superior)	L	-42	-60	50	16.81	92
Middle frontal gyrus	R	30	18	46	24.35	402
Middle frontal gyrus	L	-34	16	50	21.36	103
Supramarginal gyrus (posterior)	R	48	-42	40	23.76	118
Occipital cluster (including lingual gyrus)	R	12	-76	-2	32.74	731
Superior parietal lobule	L	-26	-48	70	25.83	276
Precuneus	R	14	-54	8	21.37	69
Precuneus	L	-6	-66	52	18.53	56

[U]Cluster did not survive correction for multiple comparisons.

A

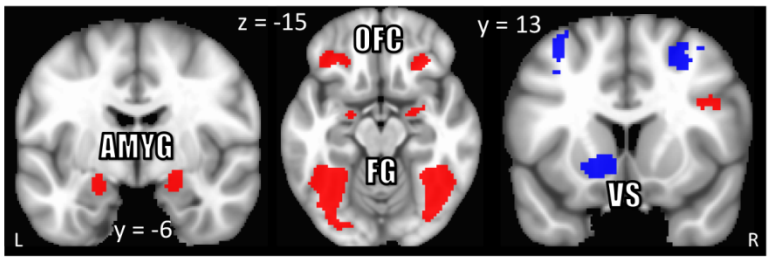
Task phase: Main effect of *Distractor*
z = -15
OFC
y = 13
AMYG
FG
VS
y = -6
L
R
Neg > Neut
Neut > Neg

B

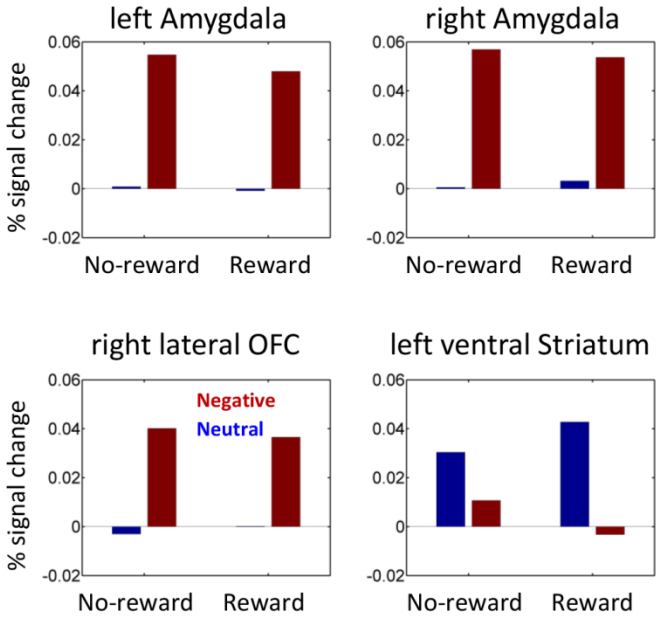
left Amygdala
right Amygdala
% signal change
0.06
0.04
0.02
0
-0.02
No-reward
Reward
right lateral OFC
left ventral Striatum
Negative
Neutral

C

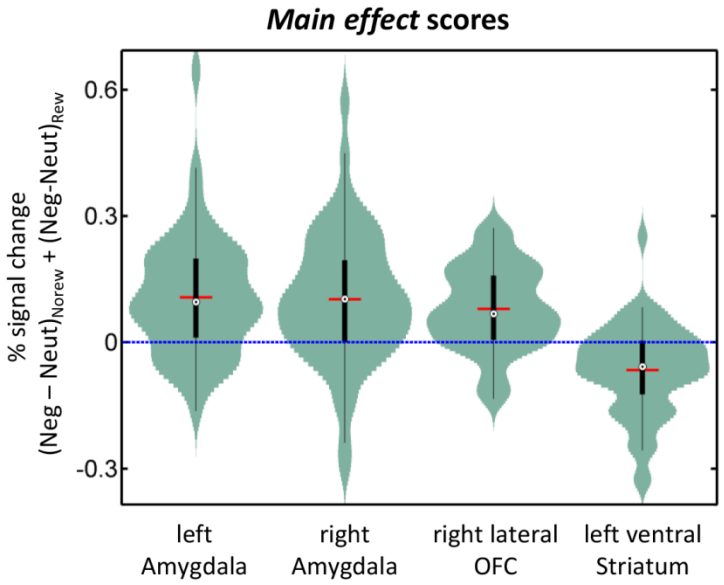
Main effect scores
% signal change
(Neg – Neut)Norew + (Neg-Neut)Rew
0.6
0.3
0
-0.3
left Amygdala
right Amygdala
right lateral OFC
left ventral Striatum

Figure 3.6 Task phase functional MRI results displayed at an uncorrected p = .001 and 48-voxel cluster extent (cluster-level alpha of 0.05). Because cluster-extent based thresholding was used for multiple comparisons correction, voxels are displayed using a binary threshold. For further rationale about using binary maps in the context of cluster-based thresholding, see Woo et al., 2014. (A) Clusters exhibiting significant main effect of *Distractor* type (neutral, negative). (B) Main-effect response pattern from a subset of regions. To avoid circularity, error bars are not plotted. (C) Distributions of within-subject main effect of Distractor scores in units of % signal change. The box plots within the violins indicate the interquartile range (first quartile to third quartile), red lines show the mean values, and black dots inside white circles show median values. Amyg: amygdala, OFC: orbital frontal cortex, VS: ventral striatum, FG: fusiform gyrus

Relationship between cue-related responses and behavior

To probe the link between cue-related responses and subsequent behavior, we focused on the ventral striatum, a region that has been consistently implicated in reward-related processing. We evaluated the relationship between cue-phase responses and behavioral reward main effects, which would reflect an unspecific reward effect. The robust correlation analysis revealed a positive relationship between reward (vs. no-reward) responses to the cue and behavioral RT scores in the right ventral striatum ROI (robust skipped correlation r = -.31, p = .02) and was just outside the critical decision boundary in the left ventral striatum ROI (robust skipped correlation r = -.25, p = .06), indicating that participants with stronger reward-related cue responses were behaviorally faster during the reward condition. We also evaluated the relationship between cue-phase responses and behavioral interaction scores which would reflect a more specific effect of reward on behavior. In both left and right ventral striatum anatomical ROIs, across-subject robust correlation analysis revealed a significant positive relationship between reward (vs. no-reward) responses to the cue and behavioral RT interaction scores (Figure 3.7). This linear relationship indicates that

participants with stronger reward-related responses in the ventral striatum during the cue phase were more successful at reducing the impact of negative images on task performance.

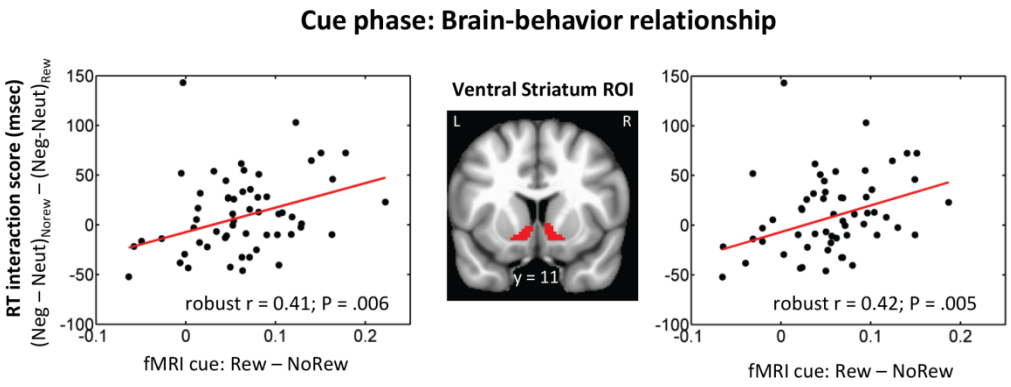

Figure 3.7 Brain-behavior relationship. A positive linear relationship was observed between reward (vs. no-reward) cue responses and behavioral RT interaction scores in the right and left ventral striatum ROIs.

Relationship between task-related responses and behavior

A whole-brain voxelwise robust correlation analysis between task phase-responses and behavior did not detect significant linear relationships.

Functional connectivity during cue phase

In line with previous studies investigating the impact of cues signaling reward (Harsay et al., 2011; Padmala and Pessoa, 2011), we anticipated stronger functional connectivity between the ventral striatum and cortical sites involved in attention and goal-directed processing during reward trials. To probe functional interactions, we determined trial-based functional connectivity of the ventral striatum with voxels

across the brain. This analysis revealed stronger functional coupling during reward (vs. no-reward) with cortical sites, including parietal cortex and sites consistent with the frontal eye-fields (Figure 3.8 and Table 3.3).

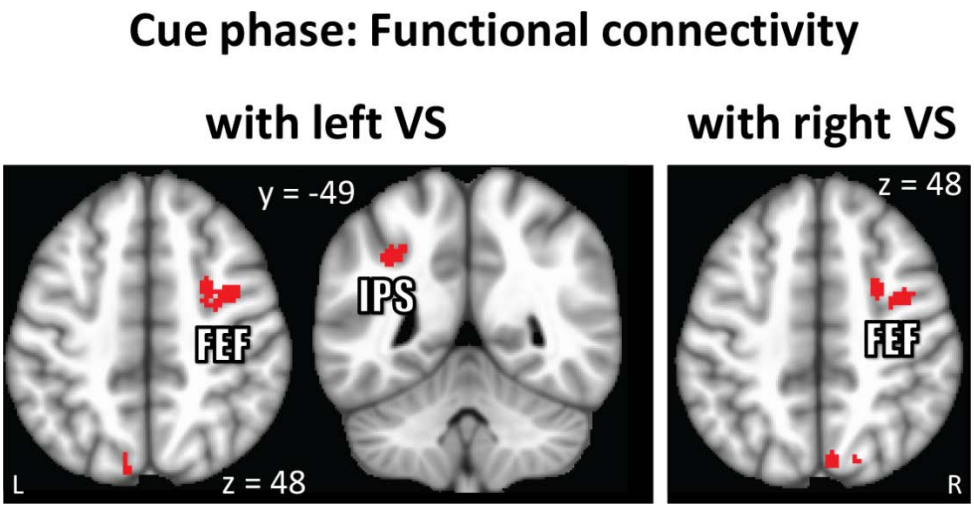

Figure 3.8 Cue phase functional connectivity results displayed at an uncorrected p = .001 and 48-voxel cluster extent (cluster-level alpha of 0.05). Because cluster-extent based thresholding was used for multiple comparisons correction, voxels are displayed using a binary threshold. For further rationale about using binary maps in the context of cluster-based thresholding, see Woo et al., 2014. Stronger functional coupling was observed between ventral striatum and fronto-parietal regions during the processing of reward relative to no-reward cues. VS: ventral striatum, FEF: frontal eye-fields, IPS: intraparietal sulcus.

Table 3.3 Clusters that survived multiple comparisons correction in voxelwise functional connectivity analysis with ventral striatum at cue phase (peak MNI coordinates, t(56) values, and cluster size [k]). Peak coordinates are presented for completeness and potential meta-analysis; with cluster-based thresholding, it is not possible to conclude that all the reported peaks were activated [see Woo et al., 2014]

Peak location		*x*	*y*	*z*	*t*	*k*
With left ventral striatum ROI						
Frontal eye fields	R	38	-2	46	6.27	345
Intraparietal sulcus	L	-32	-48	42	4.79	60
Supplementary motor cortex	R/L	-2	-4	68	5.05	173
Lateral occipital cortex (superior)	L	-8	-80	50	5.50	76
With right ventral striatum ROI						
Frontal eye fields	R	26	2	48	5.16	118
Precuneus	R	6	-72	50	4.74	50

Discussion

We investigated the interaction between potential reward and negative distractor processing in the human brain. Behaviorally, the prospect of reward signaled by an advance cue reduced the influence of negative distractors during a subsequent perceptual discrimination task. In terms of brain responses, interactions paralleling behavior were observed across multiple sites, including the anterior insula and dorsal anterior cingulate cortex. Notably, in some brain regions, including the amygdala and fusiform gyrus, we did not detect the influence of potential reward on distractor processing. Together, our fMRI findings revealed evidence for both interaction and independence between potential reward driven top-down attentional control mechanisms and negative-distractor processing.

Based on observed patterns of behavior, a few studies have proposed that aversive distractor processing is immune to potential reward, at least under certain conditions (Kaltwasser et al., 2013; Wei and Kang, 2014). Kaltwasser et al. (2013) did not detect an interaction between reward expectancy and task-irrelevant valence in a word categorization task, and suggested that the processing of emotionally valenced words is immune to a reward manipulation. Wei and colleagues (2014) did not detect an interaction between the valence of face stimuli and potential reward when faces were task irrelevant like in the present study; they did observe an interaction when the valence of the faces was relevant to the task. The behavioral findings of the present study revealed a potential reward by distractor type interaction that replicated our previous behavior-only study (Padmala and Pessoa, 2014). More broadly, the interaction pattern observed here is consistent with other behavioral findings of enhanced processing of goal-relevant information in the presence of threat-related distractors (Vogt et al., 2013; Vromen et al., 2015).

In terms of brain signals, during the cue phase, consistent with the previous literature from both human and animal studies (Haber and Knutson, 2010; Liu et al., 2011), we observed stronger responses during reward trials in a large cluster that included subcortical regions involved in reward-related processing, including the striatum and midbrain, as well as parietal and frontal cortical sites important for attention and executive function (Padmala and Pessoa, 2011; Krebs et al., 2012). In addition, we detected increased functional connectivity between the ventral striatum and a subset of the fronto-parietal regions (Harsay et al., 2011; Padmala and Pessoa, 2011). As the only difference between the reward and no-reward conditions was the

type of cue employed, these results suggest that the processing of the reward relative to the no-reward cue led to the enhancement of proactive executive control mechanisms (Chiew and Braver, 2013) that enabled participants to better handle the impact of the negative distractors.

Consistent with this notion, across participants, we observed a significant link between cue-related response strength in the ventral striatum/accumbens and behavioral interaction scores during the subsequent task phase. Participants with stronger responses to reward cues in the ventral striatum exhibited a greater benefit of reward in reducing negative-picture interference. This brain-behavior relationship is in line with proposals that ascribe a role for the ventral striatum in driving the redistribution of processing resources (Sarter et al., 2006; Salamone et al., 2009), which can lead to more selective effects of reward on behavioral performance (see also Pessoa, 2013). In this context, cue-related activity in the ventral striatum might have reflected processes engaged to handle challenging situations (in this case, handling aversive distractors). As observed here, these processes might have involved the up-regulation of attentional control regions in frontal and parietal cortex, as reflected in the enhanced functional connectivity observed during reward cues (see also Harsay et al., 2011; Padmala and Pessoa, 2011). But note that an association between cue responses and an unspecific effect of reward on behavior was also detected, consistent with the idea that reward cues also served an energizing function.

During the task phase, we detected significant interaction effects in frontal and parietal brain regions, including the anterior and mid-insula, medial prefrontal cortex, and inferior parietal lobule. Paralleling the behavioral data, in all these sites,

differential responses (negative minus neutral) were *reduced* during the reward condition. The finding in the anterior insula is noteworthy given its involvement in negative processing (Phillips et al., 2003; Craig, 2009), including the processing of mutilation images (Wright et al., 2004; Sarinopoulos et al., 2010). Another noteworthy site of interaction was in a medial prefrontal cortex cluster that included the dorsal anterior cingulate cortex. Based on the review of human and animal literatures, Etkin and colleagues (2011) suggested that dorsal aspects of the anterior cingulate cortex are involved in emotional appraisal/expression. Our findings mesh well with this proposal as, in line with behavior, the differential response (negative minus neutral) to distractors was positive during the control condition (no-reward), but flipped sign during the reward condition. Thus, in the context of our task, the dorsal anterior cingulate exhibited a profile consistent with emotional reactivity (see also Etkin et al., 2015) that was influenced by motivational processing.

We also observed a significant interaction effect during the task phase in the lateral occipital cortex where negative (vs. neutral) responses were decreased during the reward condition. Intriguingly, in a meta-analysis of emotional perception studies (Sabatinelli et al., 2011), the lateral occipital cortex was found to be engaged during the processing of complex emotional images such as mutilated bodies. If, in our study, the lateral occipital cortex activation reflected engagement by aversive pictures, the interaction pattern would be consistent with the idea that potential reward decreased the impact of such stimuli.

An important question concerns the pattern of responses in the amygdala. Given that negative-distractor interference was essentially eliminated behaviorally,

one could have anticipated that differential responses (negative greater than neutral) observed during no-reward would be eliminated (or at least reduced) during the reward condition. However, only a main effect of distractor type in the anticipated direction (negative greater than neutral) was observed, not an interaction. Thus, in our task, the prospect of reward did not appreciably influence how the amygdala responded to aversive images. This overall pattern of response should be contrasted to the one observed during demanding attentional manipulations; when attention is robustly consumed elsewhere, the impact of unattended emotional stimuli is largely decreased or even eliminated (Pessoa, 2002; Mitchell et al., 2007). Such findings have been interpreted as indicating that the processing of emotional stimuli is not automatic, and that they can be filtered out during strong attentional manipulations. In the present study, we observed interaction effects across several regions, including the anterior insula, dorsal anterior cingulate, and inferior parietal lobule, but not in the amygdala. Thus, advance reward did not appear to lead to the filtering out of emotional distractors (see Vuilleumier, 2005). However, the deleterious impact of negative images was eliminated behaviorally. It is thus likely that the regions exhibiting the reward by emotion interaction play a role in reducing the impact of negative distractors. It is worth pointing out that the pattern of responses observed in the amygdala was similar to the one we saw when reward was manipulated in a *reactive* fashion, that is, where certain stimuli were linked to reward and no advance reward cues were used (Hu et al., 2013; see also Wittmann et al., 2008); in such cases, the impact of negative stimuli in the amygdala was not counteracted by reward.

Previous studies have shown that motivation enhances attention when participants are explicitly informed of the possibility of reward (Engelmann et al., 2009; Hubner and Schlosser, 2010; Krebs et al., 2012). In a previous study (Padmala and Pessoa, 2011), participants were informed of the possibility of reward by a cue stimulus that preceded the target phase during which a Stroop-like interference stimulus was displayed. Behaviorally, participants exhibited reduced conflict during the reward versus no-reward condition. Brain imaging results revealed that a group of subcortical and frontoparietal regions was robustly influenced by reward at cue processing and, importantly, that increased cue-related responses in fronto-parietal regions important for attention were correlated with reduced conflict-related signals during the upcoming target phase. Together, our findings were consistent with a model in which motivationally salient cues are employed to upregulate top-down control processes that bias the selection of visual information, thereby leading to more efficient stimulus processing during conflict conditions.

In the current study, we observed a similar behavioral pattern of reduced interference (here with negative distractors) as in our previous study (Padmala and Pessoa, 2011). However, the absence of an interaction effect in the amygdala and fusiform gyrus suggests a modified interpretation of our results. Given the intermediate attentional demands of the bar task, negative images were registered by the amygdala (and lateral orbitofrontal cortex; see Fig. 6), impacting processing along visual cortex (Vuilleumier et al., 2004; Hadj-Bouziane et al., 2012). However, enhanced attentional control mechanisms during the reward condition enabled participants to reduce the deleterious impact of negative images. Enhanced attentional

control appeared to be linked to interactions between the ventral striatum and fronto-parietal regions important for executive control (in and around the frontal eye fields, and posterior intraparietal sulcus). Furthermore, as previously stated, it is likely that the regions exhibiting the reward by emotion interaction play a more direct role than regions possibly involved in registering the stimulus itself (for instance, amygdala and fusiform gyrus). We note, however, that in regions exhibiting the reward by emotion interaction, evidence for a brain-behavior relationship was not detected in the present study.

In conclusion, our study demonstrated the influence of performance-based monetary rewards on aversive processing. In terms of behavior, negative interference scores were reduced during the reward condition and a parallel interaction pattern was observed in several brain regions, including the anterior insula, dorsal anterior cingulate, and inferior parietal lobule. During reward cue processing, stronger responses were observed in subcortical regions important for reward processing, as well as fronto-parietal regions important for cognitive control. Notably, stronger reward-cue responses in the ventral striatum were associated with reduced behavioral negative interference during the subsequent task phase. Together, our study refines our understanding of the brain mechanisms underlying the influence of potential reward on the processing of negative distractors in the human brain.

Chapter 4 Interactions between positive and negative emotional processing

Introduction

Over the course of evolution, human beings developed strategies to detect, recognize, and rapidly react to significant stimuli in the environment. The perceptual system, particularly the visual modality, identifies and evaluates potential threats and rewards, both important for well-being and continued survival. While research has sought to understand how appetitive and aversive stimuli separately influence brain responses, it remains unclear how pleasant and unpleasant stimuli *potentially interact* in the brain. In many real world situations, both types of stimuli are present: for example, in nature, a prey animal may see a food reward (an appetitive stimulus) while a predator lurks around the area (aversive stimulus). So, it is important to study these two types of stimuli together to better understand how the brain processes appetitive and aversive stimuli in real world settings.

According to the dimensional models of affect (Lang et al., 1990; Russell and Barrett, 1999), two major dimensions underlie our emotional experience: valence and arousal or salience. The valence dimension ranges from unpleasant to pleasant with a neutral midpoint, and the arousal dimension varies from low to high intensity with medium in between. Previously, neuroimaging studies have used both positive and negative stimuli (along with a neutral baseline) to investigate the sensitivity of responses to valence and salience dimensions (Figure 4.1). Many of these studies consistently reported responses in the ventro-medial prefrontal cortex (vmPFC) were sensitive to valence, whereas responses in the amygdala were sensitive to salience

(Anderson et al., 2003; Small et al., 2003), suggesting that the valence and salience dimensions of emotional stimuli are largely encoded in distinct brain regions (but see Winston et al., 2005; Jin et al., 2015).

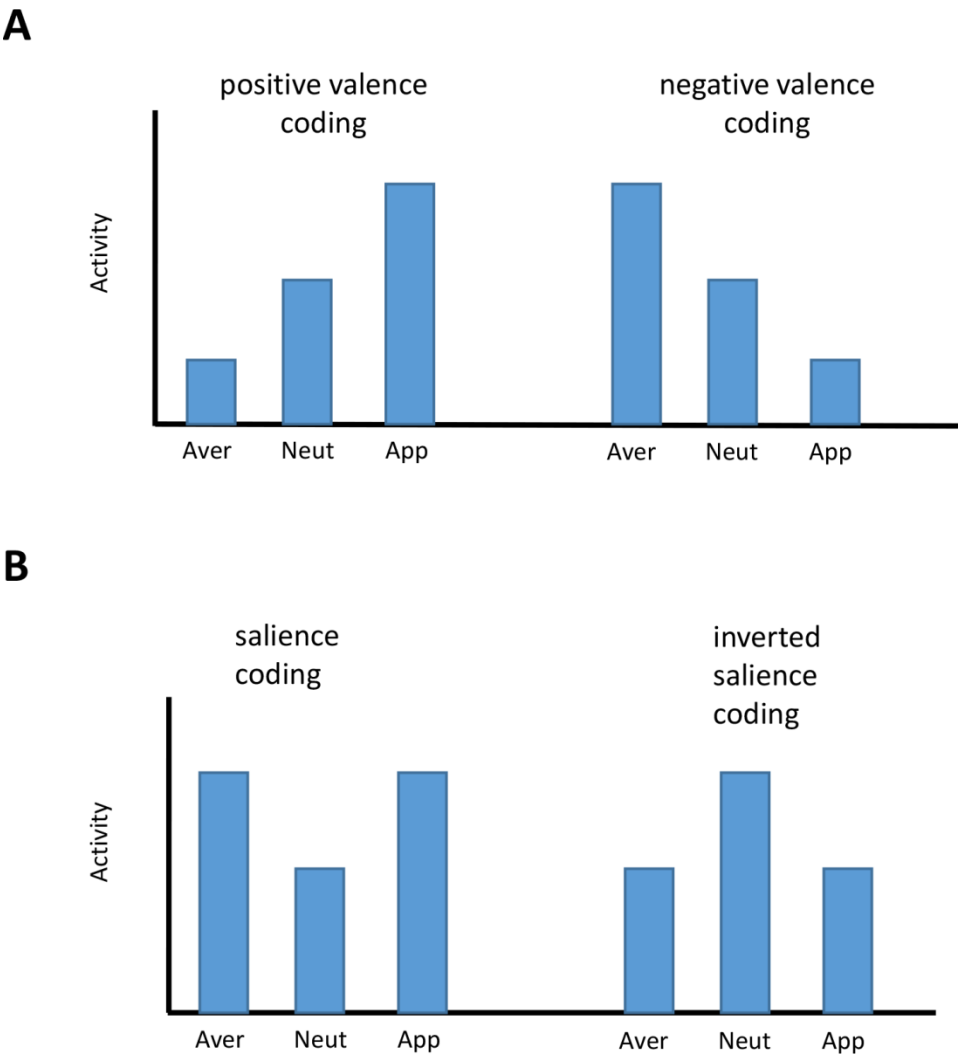

Figure 4.1 Valence and salience coding schemes. (A) Responses consistent with positive ("Aver" > "Neut" > "App") and negative ("App" > "Neut" > "Aver") valence coding. (B) Responses consistent with salience ("Aver" & "App" > "Neut") or inverted salience ("Aver" & "App" < "Neut") coding. Aver: aversive, Neut: neutral, App: appetitive.

While previous research has studied brain responses to pleasant and unpleasant stimuli, the majority have focused on how these responses were influenced by each individually (but see Grabenhorst et al., 2007). Therefore, our knowledge of the joint influence of pleasant and unpleasant stimuli on brain responses is rudimentary. In particular, very little is known about how regions that code valence or arousal information *integrate* positive and negative information. For instance, in salience coding regions, when both pleasant and unpleasant stimuli are presented, the overall intensity may be represented in two distinct ways: one solely dependent on the intensity of items, and alternatively, another dependent on valence (Kahnt and Tobler, 2013). Furthermore, some recent frameworks argue against the localized view of emotional processing and propose that the *integration* of information between multiple brain regions is central during emotional processing (Hamann, 2012; Pessoa, 2017). Nevertheless, very little is known about how valence and salience dimensions influence functional interactions during emotional processing.

To fill in these gaps, the current fMRI study investigated how the joint processing of pleasant (pictures of heterosexual erotica) and unpleasant (pictures of mutilation) stimuli influenced univariate brain responses and functional interactions during a passive viewing task (Figure 4.2). Specifically, the study aimed to investigate how regions that code valence and salience integrate positive and negative information. Because of mutually opponent interactions between appetitive and aversive motivational systems (Konorski, 1967; Dickinson and Dearing, 1979), in valence coding regions, we hypothesized *competitive* interactions during the joint processing of pleasant and unpleasant stimuli. Additionally, in salience coding

regions, two alternative hypotheses of overall intensity were tested: if the overall intensity can be considered equal to the sum of individual intensities of the oppositely valenced stimuli (i.e., |Pleasant| + |Unpleasant|, where |x| indicates the absolute value of x), then responses during the processing of pleasant-plus-unpleasant stimuli would be greater compared to responses during the processing of one pleasant or unpleasant stimulus. Conversely, if the overall intensity can be considered to be equal to the combined intensity of the valence of the stimuli (i.e., |Pleasant + Unpleasant|), then responses during processing of pleasant-plus-unpleasant stimuli would be weaker than responses to pleasant or unpleasant stimulus. The latter hypothesis is supported by evidence of antagonistic interactions between positive and negative coding neurons recently reported in the amygdala (Kim et al., 2016), and by findings of valence dependence in structures sensitive to both positive and negative stimuli, such as the amygdala (Winston et al., 2005).

While previous work focused on activation based responses has consistently implicated the vmPFC in valence-related processing (Anderson et al., 2003; Small et al., 2003), very little is known about how the vmPFC potentially integrates information with other brain regions during emotional perception. To address this, we conducted functional connectivity analysis to specifically investigate how valence and salience dimensions influence the integration of information between the vmPFC and rest of the brain. Additionally, we explored functional interactions between the vmPFC and other brain regions during joint processing of pleasant and unpleasant stimuli. By investigating these unexplored questions in terms of univariate responses

and functional connectivity, the current study sought to enhance our understanding of the brain mechanisms of appetitive-aversive interactions during emotional perception.

Methods

Participants

Fifty-six male participants (age range: 18-30 years; average: 20.61 years) with normal or corrected-to-normal vision and no self-reported neurological or psychiatric disease were recruited from the University of Maryland community. Based on self-report, all participants were right-handed. The study was approved by the University of Maryland College Park Institutional Review Board and all participants provided written informed consent before participation. Out of 56 participants, two participants voluntarily quit the study before completion. The task paradigm was presented incorrectly to another participant due to programming error. Data from these three individuals were excluded from the analysis, resulting in a final dataset of 53 participants.

As noted in the Introduction, this study used erotic pictures of heterosexual couples to manipulate positive emotional processing. Based on previously reported gender differences in processing erotic images (Hamann et al., 2004; Sabatinelli et al., 2004; Rupp and Wallen, 2008), we only included male participants in this study. Further, participants' sexual orientations were screened using a behavioral sexual attraction questionnaire (Appendix A) and all were heterosexual based on self-report.

Procedure and Stimuli

In this study we employed a fast event-related fMRI design: each trial started with presentation of a 200 msec central white fixation, followed by a centrally-positioned image (pleasant, neutral, or unpleasant; 4° x 4°) for 1000-ms, followed immediately by another centrally-positioned image (pleasant, neutral, or unpleasant; 4° x 4°) for the same duration (Figure 4.2). Finally, each trial ended with a variable inter-stimulus interval (2-6 sec) where a blank screen was shown. Participants were instructed to passively view and pay attention to the images shown on the screen. A passive viewing task was used (i.e., no button press responses) to avoid any potential contamination from motor related activity and allow for better interpretation of responses in structures such as the striatum (Hayes et al., 2014). To ensure participants attention to the images, prior to the task, participants were told of a subsequent task (outside the scanner) involving images from the current task that could result in a bonus reward (up to $20) based on performance.

Because of the sluggish nature of the BOLD response measured by fMRI, responses to two successive images shown on each trial would substantially overlap; therefore we focused on estimating *pooled* responses to the pair of images presented during each trial (Figure 4.2). Six main experimental conditions based on combinations of the different emotional images were used: Neutral-Neutral ("N-N"); Pleasant-Pleasant ("P-P"); Unpleasant-Unpleasant ("U-U"); Pleasant-Neutral/Neutral-Pleasant ("N-P"); Unpleasant-Neutral/Neutral-Unpleasant ("N-U"); and Pleasant-Unpleasant/Unpleasant-Pleasant ("P-U"). Each of the six experimental conditions included 54 trials for a total of 324 trials. The main experiment session was divided

into 6 runs of 54 trials each (9 trials per each condition) and each run lasted ~5.5 minutes in duration. Trials were presented in a pseudorandom order with a constraint that no more than 2 trials of same condition would be presented in sequence.

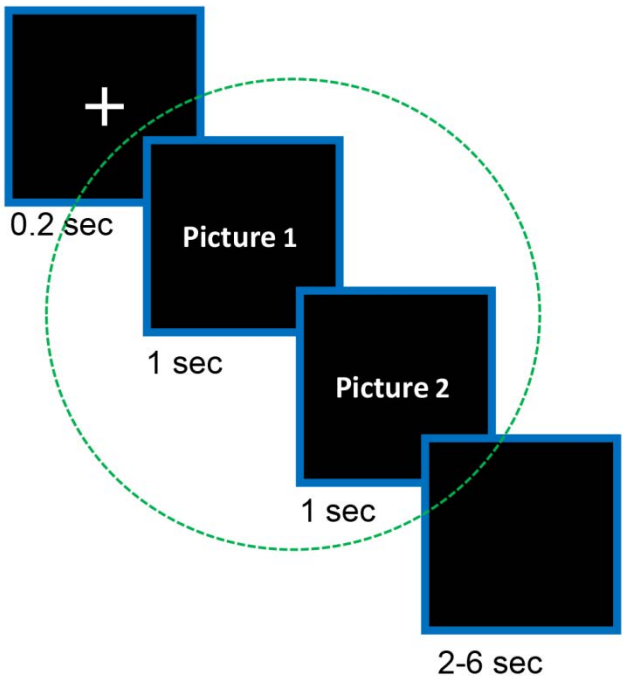

Figure 4.2 Experimental paradigm. On each trial participants passively viewed two emotional pictures (each for 1 sec; not shown here) in quick succession. Six experimental conditions were used based on different types of emotional image pairings: Neutral-Neutral ("N-N"), Pleasant-Pleasant ("P-P"), Unpleasant-Unpleasant ("U-U"), Pleasant-Neutral/Neutral-Pleasant ("N-P"), Unpleasant-Neutral/Neutral-Unpleasant ("N-U"), and Pleasant-Unpleasant/Unpleasant-Pleasant ("P-U"). Because of sluggish nature of the fMRI BOLD response, pooled response to both images on each trial (indicated by green dotted line) was estimated.

To reduce potential confounds linked to low-level stimulus properties, a relatively large picture set (216 stimuli in each emotional category) was used with eight different trial order sequences that were randomly assigned to participants, each

of which with random pairings of pictures. Each image was presented only once to minimize any potential habituation effects (Ishai et al., 2004; Codispoti et al., 2016). Images were employed from the International Affective Picture System (Lang et al., 1997a; Lang et al., 2005), a database of mutilation images developed by the Laboratory of Neurophysiology of Behavior at the Federal Fluminense University, Brazil (Mocaiber et al., 2011), and from online websites. Images of bodily injury and mutilation were used as unpleasant stimuli, neutral images consisted of people in a neutral context, and images of erotic heterosexual couples were used as pleasant stimuli. Pictures of mutilation and erotica were chosen based on previous reports showing both categories have similar intensity levels based on self-reported arousal ratings (Appendix A) and also physiological skin conductance responses (Bradley et al., 2001; Schupp et al., 2004).

Prior to the experimental runs, participants viewed two sample trials of each of the six experimental conditions (total of 12 trials) with separate set of images during a short practice run presented during anatomical scan. As a measure of physiological arousal, skin conductance response (SCR) was collected during the scanning session using MP-150 system from BioPac systems at a sampling rate of 250 Hz using MRI-compatible electrodes attached to the index and middle fingers of the non-dominant left hand. However, when we analyzed SCR responses, they appeared to be very weak (about an order of magnitude less than those observed in our previous studies). Since more detailed investigation is needed to explore the SCR data, SCR results were not included in this dissertation.

As informed, after the scan session participants performed a “old”/”new” recognition memory task using a subset of images presented during the scan session along with new images. In addition to their base pay for participation in the fMRI session ($25/hour), participants received an additional bonus (average: $12.7) based on their memory task performance.

MRI data acquisition

Functional and structural MRI data were acquired using a 3T Siemens TRIO scanner with a 32-channel head coil. First, a high-resolution T1-weighted MPRAGE anatomical scan (0.9 mm isotropic) was collected. Subsequently, we collected six functional runs of 149 EPI volumes each (3 out of 53 participants had only 5 runs) using a multiband scanning sequence (Feinberg et al., 2010) with TR = 2.2 sec, TE = 58 ms, FOV = 192 mm, and multiband factor = 6. Each volume contained 84 non-overlapping oblique slices oriented approximately 20°-30° clockwise relative to the AC-PC axis (1.5 mm isotropic) helping to decrease susceptibility artifacts at regions such as the orbitofrontal cortex and amygdala. Additionally, in each session spin-echo field maps with opposite phase encoding direction were acquired with acquisition parameters matched to the functional scans.

Functional MRI preprocessing

A combination of packages and in-house scripts were used to preprocess both the functional and anatomical MRI data. The first three volumes of each functional run

were discarded to account for equilibration effects. Slice-timing correction (with AFNI's 3dTshift) used Fourier interpolation to align the onset times of every slice in a volume to the first acquisition slice, and then a six-parameter rigid body transformation (with AFNI's 3dvolreg) corrected head motion within and between runs by spatially registering each volume to the first volume.

Skull stripping determines which voxels are to be considered part of the brain and, although conceptually simple, plays a very important role in successful subsequent co-registration and normalization steps. Currently, available packages perform sub-optimally in specific cases, and mistakes in the brain-to-skull segmentation can be easily identified. Accordingly, to skull strip the T1 high-resolution anatomical image (which was rotated to match the oblique plane of the functional data with AFNI's 3dWarp), six different packages were used: ANTs (Avants et al., 2009; http://stnava.github.io/ANTs/), AFNI (Cox, 1996; http://afni.nimh.nih.gov/), ROBEX (Iglesias et al., 2011; https://www.nitrc.org/projects/robex), FSL (Smith et al., 2004; http://fsl.fmrib.ox.ac.uk/fsl/fslwiki/), SPM (http://www.fil.ion.ucl.ac.uk/spm/), and BrainSuite (Shattuck and Leahy, 2002; http://brainsuite.org/). Then, a "voting scheme" was employed: based on T1 data, a voxel was considered to be part of the brain if four-out-of-six packages estimated it to be a brain voxel; otherwise the voxel was not considered to be brain tissue.

Subsequently, FSL was used to process field map images and create a phase-distortion map for each participant ("top-up" command). Then, FSL's epi_reg was used to apply boundary-based co-registration in order to align the first EPI volume

image with the skull-stripped T1 anatomical image along with simultaneous EPI distortion-correction (Greve and Fischl, 2009).

Next, ANTS was used to learn a nonlinear transformation that mapped the skull-stripped anatomical image to the skull-stripped MNI152 template (interpolated to 1-mm isotropic voxels). Finally, ANTS combined the transformations from co-registration (from mapping first functional EPI volume to the anatomical T1) and normalization (from mapping T1 to the MNI template) into a single transformation that was applied to map volume registered functional volumes to standard space (interpolated to 2-mm isotropic voxels). The resulting spatially normalized functional data was blurred using a 4mm full-width half-maximum (FWHM) Gaussian filter. Spatial smoothing was restricted to grey-matter mask voxels (3dBlurInMask program). Finally, to interpret the estimated regression coefficients in terms of percent signal change, the average intensity at each voxel (per run) was scaled to 100.

Voxelwise analysis

Each participant's preprocessed functional data were analyzed using multiple linear regression (restricted to gray-matter voxels) using AFNI's 3dDeconvolve program. The six main event types in the design matrix reflected the six experimental conditions: "N-N", "P-P", "U-U", "N-P", "N-U", and "P-U". To estimate responses for these six conditions, a canonical gamma variate hemodynamic response function model convolved with a square wave of 2 sec stimulus duration was used (Cohen, 1997). Other regressors included in the model comprised 6 motion parameters (3 linear displacements and 3 angular rotations), and their discrete temporal derivatives.

To further control for head motion-related artifacts in the data (Siegel et al., 2014), volumes (on average 0.2%) with a frame-to-frame translational displacement of more than 1 mm Euclidean distance were excluded. Additionally, to model baseline and drifts of the MR signal, regressors corresponding to polynomial terms up to third orders were included (for each run separately).

To investigate valence and salience coding patterns, two general linear contrast tests were used in the voxelwise analysis. A linear trend analysis with "U-U', "N-N" and "P-P" conditions (using contrast weights of [-1 0 +1] respectively) was employed to identify voxels that coded valence type signals. In this general linear contrast, voxels with positive linear trend indicate positive valence coding (i.e., "P-P" > "U-U") whereas voxels with negative linear trend are indicative of negative valence coding ("U-U" > "P-P"). Similarly, a quadratic trend analysis using "U-U', "N-N" and "P-P" conditions (using contrast weights of [+1 -2 +1] respectively) identified voxels that coded salience type signals. Further, three additional general linear tests were used to separately contrast "P-U" vs. "N-P", "P-U" vs "N-U" and "P-U" vs. average of "N-P" and "N-U" conditions. These additional contrasts probed interactions between positive and negative processing in voxels that coded valence and salience type response patterns (see the conjunction analysis below for further details)

Group analysis

Whole-brain voxelwise random-effects analyses were conducted using response estimates from individual-level analyses (restricted to gray-matter voxels) in AFNI.

The alpha-level for voxelwise statistical analysis (except for voxelwise conjunction analyses described below) was determined by 3dClustSim simulations (restricted to gray-matter voxels). For these simulations, smoothness of the data was estimated using 3dFWHMx program (restricted to gray-matter voxels) based on the residual time series from the individual-level voxelwise analysis. In response to the recent report of increased false-positive rates linked to the assumption of Gaussian spatial autocorrelation in fMRI data (Eklund et al., 2016), the new -acf (i.e., auto-correlation function) option was implemented. This recently added function models spatial fMRI noise as a mixture of Gaussian plus mono-exponential distributions in the 3dFWHMx and 3dClustSim tools. The new auto-correlation function was shown to control false positive rates around desired alpha level, especially in randomized fast event-related designs with stringent voxel-level uncorrected *p* values (Cox et al., 2017). Based on a voxel-level uncorrected *p* value of 0.001, simulations indicated a minimum cluster extent of 10 voxels (2.0 x 2.0 x 2.0 mm) for a cluster-level corrected alpha of 0.05.

Valence and Salience coding

At the group level, to probe regions that code valence, a one-sample *t*-test (against zero) was performed on linear trend coefficients from individual-level analysis using the AFNI's 3dttest++ program. Similarly, to probe for regions that code salience, we ran a one-sample *t*-test (against zero) on quadratic trend coefficients from individual-level analysis. Because the "N-N" condition was assigned a zero weight in the linear trend analysis contrast, regions that code salience type signals (i.e., where responses during both "P-P" and "U-U" conditions are

greater than responses during “N-N” condition) might also be picked up if one emotion results in a larger activation over another i.e., if a difference exists between “P-P” and “U-U” conditions (Figure 4.3). Indeed, this is a possibility—a meta-analysis recently reported that regions including left amygdala exhibited salience-type coding along with preference for negative over positive valence (Lindquist et al., 2015). Thus, to identify voxels that exhibited clear linear trend (i.e., “P-P” > “N-N” > “U-U” or “U-U” > “N-N” > “P-P”), we masked voxels that exhibited salience coding (at a liberal uncorrected *p* value of .05) from valence coding group map (see (Lindquist et al., 2015) for similar strategy in the context of meta-analysis).

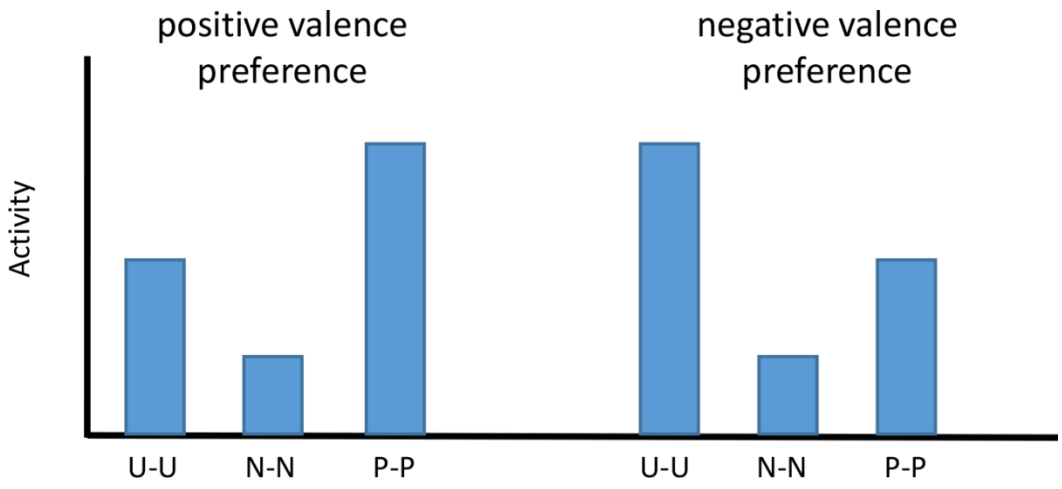

Figure 4.3 Salience coding with preference for valence. Regions that code salience type signals and that have preference for one valence over the other (positive or negative valence preference) could be picked by linear trend contrast because “N-N” condition was assigned a zero weight in that contrast which effectively “P-P” vs “U-U” conditions.

Interactions between pleasant and unpleasant emotional processing

One of our main goals in this study was to investigate how regions that code valence- and salience-type signals integrated pleasant and unpleasant emotional information. To test the hypothesis of competitive interactions in positive valence coding regions, a voxelwise conjunction analysis (Friston et al., 2005; Nichols et al., 2005) was ran with voxels that exhibited positive valence coding and voxels that exhibited differences between "P-U" vs. "N-P" conditions. The logic behind this conjunction analysis is that positive valence coding voxels that exhibit evidence for competitive interactions, should show reduced response during pleasant-plus-unpleasant stimuli ("P-U") compared to responses during pleasant-plus-neutral stimuli ("N-P"; Figure 4.4A). Similarly, to test for competitive interactions in negative valence coding regions, a voxelwise conjunction analysis was ran with voxels that exhibited negative valence coding and voxels that exhibited differences between "P-U" vs. "N-U" conditions. The logic behind this conjunction analysis is that in voxels that code negative valence and exhibit evidence for competitive interactions, response during pleasant-plus-unpleasant stimuli ("P-U") should be reduced in comparison to unpleasant-plus-neutral stimuli ("N-U"; Figure 4.4B). Moreover, because the linear trend estimation was based only on "P-P", "N-N" and "U-U" conditions, the contrasts of "P-U" vs. "N-P" and "P-U" vs. "N-U" conditions are independent of the contrast used to define positive and negative valence coding voxels (Figure 4.4A-B).

To test competing hypotheses about the overall intensity in salience coding regions, a voxelwise conjunction analysis was performed with voxels that exhibited

salience coding and voxels that exhibited differences between “P-U” vs. average of “N-P” and “N-U” conditions. If overall intensity was determined by the intensity of individual items (i.e., |Pleasant| + |Unpleasant|), then responses during processing of two salient stimuli of opposite valence (i.e., “P-U”) would be greater than the average response to one salient stimuli (Figure 4.4C). On the other hand, if overall intensity is based on the combined valence of the stimuli (i.e., |Pleasant + Unpleasant|), then responses during processing of two salient stimuli of opposite valence (i.e., “P-U”) would be weaker than the average response to one salient stimuli (Figure 4.4C). Moreover, as the quadratic trend estimation was based on only “P-P”, “N-N” and “U-U” conditions, the contrast of “P-U” vs. average of “N-P” and “N-U” conditions is independent of the contrast used to define salience coding voxels (Figure 4.4C).

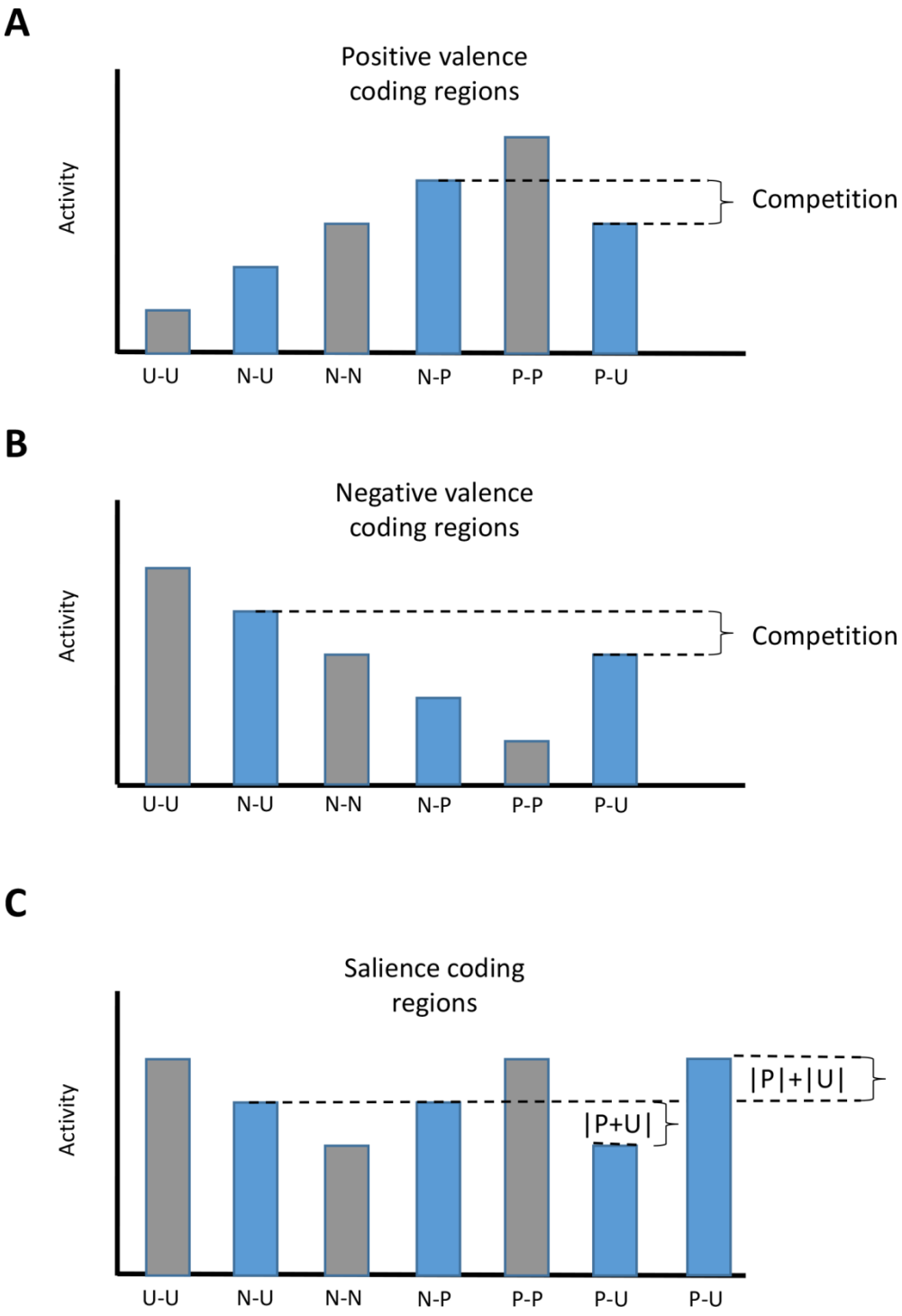

Figure 4.4 Contrasts used for testing interactions in valence and salience coding regions. (A) in positive valence coding regions, contrast between responses during "P-U" and "N-P" conditions would allow to test the hypothesized competitive interaction; (B) in negative valence coding regions, contrast between responses during "P-U" and "N-U" conditions would allow to test the hypothesized competitive

interaction; and (C) in salience coding regions, contrast between response during "P-U" and average response during "N-P" and "N-U" conditions would allow to test two competing hypothesis about the overall intensity. All these contrasts used to test interactions are independent of the contrasts used to define valence and salience coding regions which were only based on "P-P", "N-N" and "U-U" conditions that were marked in gray.

Although the cluster level multiple comparison correction techniques have better sensitivity in detecting the effects in voxelwise analysis, they do not allow inferences to be drawn at the level of individual voxels (Woo et al., 2014a). Therefore, it has been suggested that voxel level correction methods such as false discovery rate (FDR) correction are more appropriate for voxelwise conjunction analysis (Woo et al., 2014a). To run each conjunction analysis described above, for each contrast separately, we first created a mask based on voxels that survived the FDR correction at $p = .05$ level. Then, an intersection map of the two masks was created, revealing voxels with common significant activation. To control for isolated voxels, only clusters with a minimum cluster extent of 5 voxels (an arbitrary cut-off) in the intersection mask were reported.

vmPFC functional connectivity analysis

To investigate how different task contexts influenced functional interactions between vmPFC and rest of the brain, a voxelwise functional connectivity analysis based on trial-by-trial responses was employed. Similar to the so-called "beta series correlation method" (Rissman et al., 2004), trial-based responses were estimated for each participant using the `3dLSS` command in AFNI, a recently proposed method to improve estimation of trial-based responses in fast-event related designs (Mumford et

al., 2012). The 3dLSS was used to model the trial of interest and modified to include six additional "combined" regressors for each task condition: “N-N”, “P-P”, “U-U”, “N-P”, “N-U” and “P-U”. As in the standard activation analysis described above, to estimate trial-based responses a canonical gamma variate hemodynamic response function model that was convolved with a square wave of 2.0 sec stimulus duration was used (Cohen, 1997).

To create representative ROI estimates, trial-based responses were averaged across voxels within a functionally defined vmPFC ROI. For this analysis, the vmPFC cluster that exhibited valence coding in the activation based analysis was used. To note, because correlations between two signals are independent of their mean levels, selection of vmPFC cluster based on activation analysis does not lead to circularity issues. Then, a trial-by-trial robust correlation between responses of vmPFC and the rest of the brain in a voxelwise fashion was calculated separately for each of the six task conditions. Initially we probed how the functional interactions between vmPFC and rest of the brain were shaped by valence and salience type coding. To identify voxels that exhibited valence type connectivity pattern with the vmPFC, a linear trend analysis was performed with estimated correlations (initially transformed via Fisher’s *Z*-transform) based on “U-U”, “N-N” and “P-P” conditions using contrast weights of [-1 0 +1] respectively. In this analysis, voxels with positive linear trend are indicative of positive valence coding type connectivity pattern (i.e., “P-P” > “U-U”) whereas voxels with negative linear trend are indicative of negative valence coding type connectivity pattern (“U-U” > “P-P”). In a similar fashion, a quadratic trend analysis using estimated correlations (initially transformed via

Fisher's *Z*-transform) of "U-U", "N-N" and "P-P" conditions (contrast weights of [+1 -2 +1] respectively) was used to identify voxels that exhibited salience type connectivity pattern with the vmPFC.

vmPFC functional connectivity: Valence and Salience coding

At the group level, to probe for regions that exhibited valence type connectivity patterns with vmPFC, a one-sample *t*-test (against zero) was ran on linear trend coefficients from individual-level analysis using AFNI's 3dttest++ program. Similarly, to probe for regions that exhibited salience type connectivity patterns with vmPFC, a one-sample *t*-test (against zero) was ran on quadratic trend coefficients from individual-level analysis using the AFNI's 3dttest++ program. Based on the same logic used in activation based group analysis, in order to identify voxels that exhibited a clear linear trend pattern of functional connectivity (i.e., "P-P" > "N-N" > "U-U" or "U-U" > "N-N" > "P-P"), voxels that exhibited salience type connectivity coding (at a liberal uncorrected *p* value of .05) were masked from valence coding group connectivity map. To control for multiple comparisons, functional connectivity group statistical maps were thresholded at voxel-level uncorrected *p*-value of 0.001 with a minimum cluster extent of 10 voxels for a cluster-level corrected alpha of 0.05.

vmPFC functional connectivity: Interactions between pleasant and unpleasant emotional processing

We investigated the joint influence of pleasant-plus-unpleasant stimuli on vmPFC functional connectivity with rest of the brain. Specifically, to probe for competitive interactions, a conjunction analysis (Friston et al., 2005; Nichols et al., 2005) was conducted with voxels with exhibited connectivity to vmPFC in a positive valence coding pattern and voxels that exhibited differential vmPFC connectivity between "P-U" vs. "N-P" conditions. In the case of competitive interactions, the conjunction analysis would reveal reduced functional connectivity during the pleasant-plus-unpleasant stimulus ("P-U") in comparison to connectivity during the pleasant-plus-neutral stimulus ("N-P"). Moreover, the linear trend estimation used to identify valence coding connectivity voxels was based only on "P-P", "N-N" and "U-U" conditions, therefore the contrast of "P-U" vs. "N-P" is independent of the contrast used to define positive valence coding connectivity voxels.

Additionally, functional connectivity of the vmPFC during pleasant-unpleasant ("P-U") condition was probed with regions that exhibited salience type connectivity patterns. In order to do so, a voxelwise conjunction analysis was conducted between voxels that exhibited connectivity with vmPFC in a salience coding pattern and voxels that exhibited differential vmPFC connectivity between "P-U" vs. average of "N-P" and "N-U" conditions. If cooperative interactions exist, functional connectivity during processing of two salient stimuli of opposite valence (i.e., "P-U") would be greater than connectivity during processing of one neutral and one salient stimulus as presented in neutral-pleasant ("N-P") and neutral-unpleasant

("N-U") conditions. Moreover, as the quadratic trend estimation was based on only "P-P", "N-N", and "U-U" conditions, the contrast of "P-U" vs. average of "N-P" and "N-U" conditions is therefore independent of the contrast used to define salience coding connectivity voxels.

Similar to the activation based analysis, for each conjunction analysis described above, for each contrast separately, a mask based on voxels that survived the FDR correction at $p = .05$ level was created. Based on intersection map of the two masks, voxels with significant common connectivity were revealed.

Results

Valence and salience coding brain regions

In a whole-brain voxelwise analysis, regions whose responses were consistent with positive or negative valence coding patterns were probed (Figure 4.1A). Responses consistent with positive valence coding were observed in multiple regions including the ventro-medial prefrontal cortex (vmPFC), bilateral striatum, bilateral superior temporal gyrus and precuneus (Figure 4.5 and Table 4.1), where responses linearly increased from unpleasant to pleasant conditions (i.e., "P-P" > "N-N" > "U-U"). Conversely, responses consistent with negative valence coding were observed in regions including the bilateral fusiform gyrus (Figure 4.5 and Table 4.1), where responses linearly increased from pleasant to unpleasant conditions (i.e., "U-U" > "N-N" > "P-P").

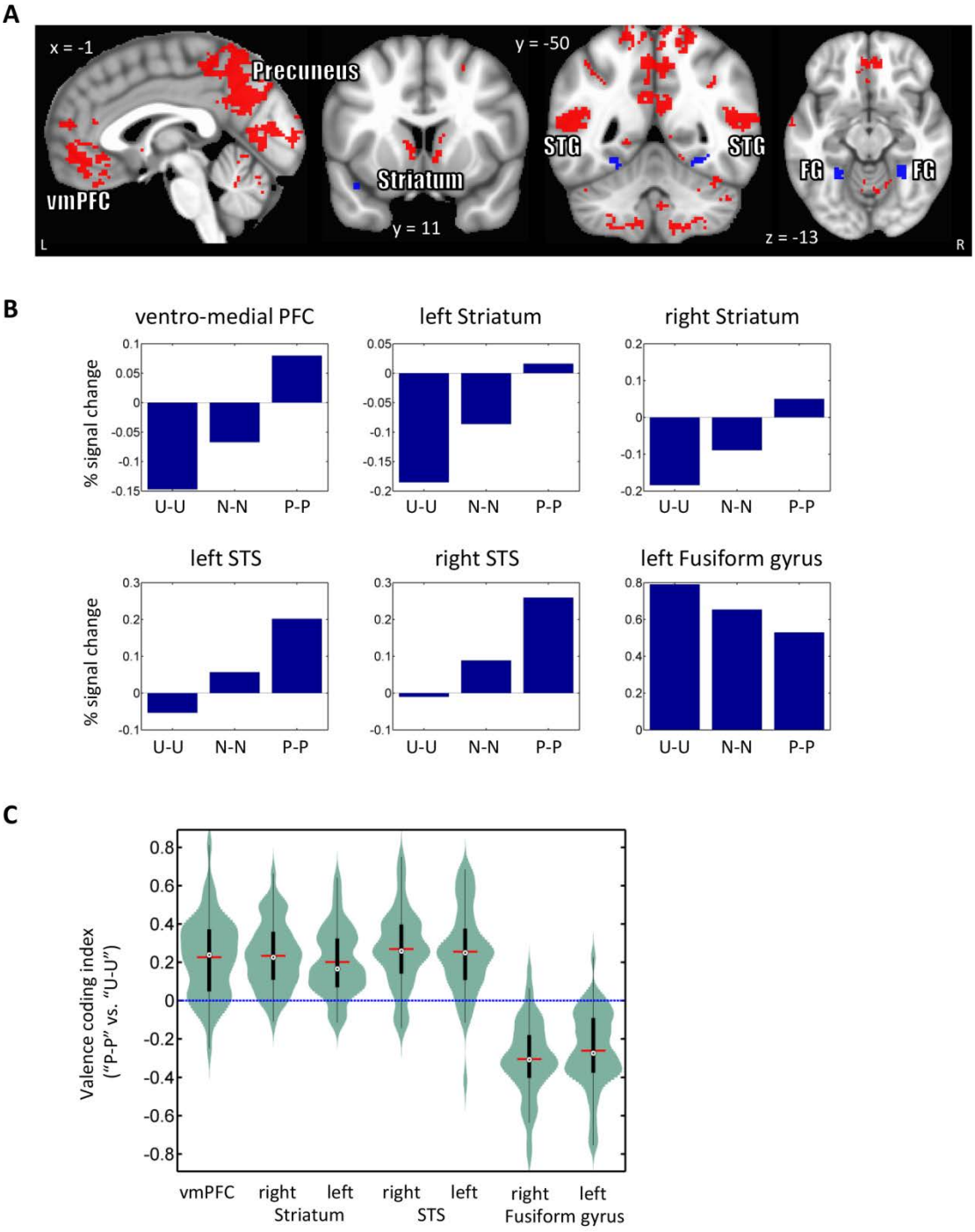

Figure 4.5 Valence coding fMRI results. (A) Clusters exhibiting positive (red) and negative (blue) valence coding (based on "P-P", "N-N" and "U-U" conditions) displayed at an uncorrected p = .001 and 10-voxel cluster extent (cluster-level alpha of 0.05). Because cluster-extent based thresholding was used for multiple comparisons correction, voxels are displayed using a binary threshold. For further rationale about using binary maps in the context of cluster-based thresholding, see Woo et al., 2014. (B) Average responses within clusters that exhibited valence

coding. To avoid circularity, error bars are not plotted. (C) Distributions of within-subject valence coding index in units of % signal change. The box plots within the violins indicate the interquartile range (first quartile to third quartile), red lines show the mean values, and black dots inside white circles show median values. vmPFC: ventro-medial prefrontal cortex, STG: superior temporal gyrus, FG: fusiform gyrus.

Table 4.1 Clusters that survived multiple comparisons correction in voxelwise valence coding analysis (peak MNI coordinates, t(52) values, and cluster size [k]). Peak coordinates are presented for completeness and potential meta-analysis; with cluster-based thresholding, it is not possible to conclude that all the reported peaks were activated [see Woo et al., 2014]

Cluster		*x*	*y*	*z*	*t*	*k*
Positive valence coding						
Precuneus/posterior cingulate cortex	R/L	18	-62	26	9.41	3581
Lingual gyrus/striate area	R/L	-2	-74	4	8.19	801
Angular gyrus	R	46	-68	22	7.58	647
Ventro-medial prefrontal cortex	R/L	6	54	-6	6.73	542
Angular gyrus	L	-44	-66	20	9.08	503
Cerebellum	L	-8	-78	-38	6.97	345
Superior frontal sulcus	R	28	0	54	6.62	263
Middle frontal gyrus	L	-38	-2	56	5.69	211
Cerebellum/fusiform gyrus	R	40	-48	-22	6.71	167
Cerebellum	L	-26	-56	-50	6.94	137
Cerebellum	R	10	-52	-52	7.28	136
Transverse temporal gyrus	L	-60	-36	24	5.99	126
Supramarginal gyrus	R	52	-32	28	6.54	92
Striatum	L	-6	6	-6	4.72	87
Angular gyrus	R	38	-70	44	5.01	82
Superior frontal gyrus	L	-26	42	40	5.31	78
Lingual gyrus	L	-14	-58	4	5.45	69
Lingual gyrus	R	16	-62	8	5.21	58
Superior frontopolar gyrus	L	-8	58	14	5.46	50
Angular gyrus	L	-32	-52	42	4.88	48
Cerebellum	L	-42	-46	-34	6.63	45
Middle frontal gyrus	R	54	26	30	5.64	41
Striatum	R	8	14	0	5.15	40
Superior frontal gyrus	R	20	40	48	4.85	38
Cerebellum	L	-36	-62	-26	4.72	34
Cerebellum	R	40	-62	-40	4.73	33
Cerebellum	R/L	4	-50	-42	4.84	32

Cerebellum	R	44	-66	-28	4.49	32
Cuneus	L	-28	-78	42	5.16	28
Cerebellum	R	28	-58	-30	6.07	27
Inferior/middle frontopolar gyrus	L	-26	52	10	5.16	27
Middle frontal gyrus	L	-44	48	10	5.57	26
Postcentral gyrus	L	-32	-38	50	4.94	23
Cerebellum	L	-28	-28	-34	5.04	22
Cerebellum	L	-40	-54	-32	5.25	22
Middle frontal gyrus	L	-38	44	22	5.19	22
Angular gyrus	R	44	-76	32	4.31	22
Occipital gyrus	L	-22	-52	4	6.01	20
Middle temporal gyrus	L	-64	-4	-12	5.17	19
Cerebellum	L	-32	-62	-48	5.92	18
Posterior cingulate cortex	R	6	-38	34	4.69	17
Middle temporal gyrus	R	62	-4	-22	4.11	15
Anterior cingulate cortex	L	-8	34	16	5.22	15
Superior frontal gyrus	L	-10	50	44	4.31	15
Cerebellum	R	34	-72	-28	4.5	13
Postcentral gyrus	L	-46	-34	54	4.84	13
Precentral gyrus	R	10	-30	70	4.87	13
Precentral gyrus	L	-58	4	36	4.21	12
Rostral gyrus	R/L	-2	34	-24	4.21	11
Cerebellum	R	18	-76	-20	4.77	11
Cerebellum	R	10	-40	-20	4.24	11
Cerebellum	L	-6	-56	-16	4.39	11
Medial orbital gyrus	L	-26	46	-16	4.97	11
Superior temporal gyrus	R	42	-62	8	7.09	11
Thalamus	R	16	-30	12	5.64	11
Anterior cingulate cortex	L	-8	26	30	5.06	11
Striatum (dorsal)	R	12	6	14	3.87	10
Middle frontal gyrus	L	-42	34	24	4.72	10
Negative valence coding						
Fusiform gyrus	R	28	-54	-10	-9.02	117
Fusiform gyrus	L	-26	-58	-10	-6.88	103
Fusiform gyrus (anterior)	R	34	-20	-22	-5.54	19
Planum polare	L	-40	12	-18	-4.73	10

We then probed for regions whose responses were consistent with salience coding (Figure 4.1B). We observed this type of response pattern in multiple cortical and sub-cortical brain regions including the dorsal portions of the bilateral amygdala, bilateral thalamus, bilateral anterior insula, bilateral lateral orbito-frontal cortex and mid-cingulate cortex (Figure 4.6 and Table 4.2), where responses during both pleasant and unpleasant were greater than responses during the neutral condition (i.e., both “P-P” and “U-U” > “N-N”). On the other hand, we observed response patterns consistent with inverted salience pattern in regions including the bilateral parahippocampal gyrus, bilateral lateral parietal cortex and bilateral superior frontal gyrus (Figure 4.6 and Table 4.2), where responses during both positive and negative emotional conditions were smaller than those during the neutral condition (i.e., both “P-P” and “U-U” < “N-N”).

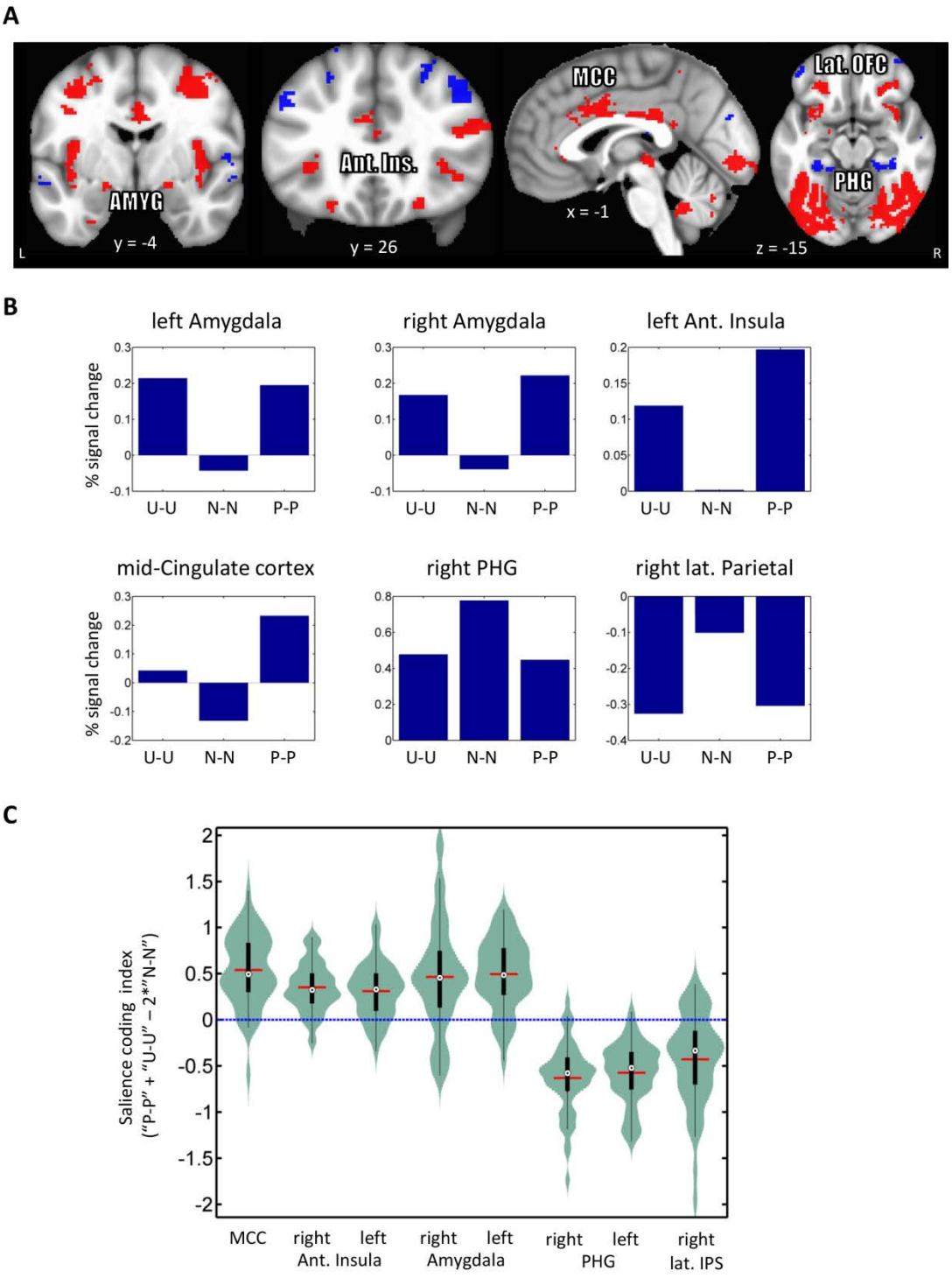

Figure 4.6 Salience coding fMRI results. (A) Clusters exhibiting salience (red) and inverted salience (blue) coding (based on "P-P", "N-N" and "U-U" conditions) displayed at an uncorrected p = .001 and 10-voxel cluster extent (cluster-level alpha of 0.05). Because cluster-extent based thresholding was used for multiple comparisons correction, voxels are displayed using a binary threshold. For further

rationale about using binary maps in the context of cluster-based thresholding, see Woo et al., 2014. (B) Average responses within clusters that exhibited salience coding. To avoid circularity, error bars are not plotted. (C) Distributions of within-subject salience coding index in units of % signal change. The box plots within the violins indicate the interquartile range (first quartile to third quartile), red lines show the mean values, and black dots inside white circles show median values. AMYG: amygdala, Ant. Ins.: anterior insula, MCC: mid-cingulate cortex, Lat. OFC: lateral orbito-frontal cortex, PHG: parahippocampal gyrus.

Table 4.2 Clusters that survived multiple comparisons correction in voxelwise salience coding analysis (peak MNI coordinates, t(52) values, and cluster size [k]). Peak coordinates are presented for completeness and potential meta-analysis; with cluster-based thresholding, it is not possible to conclude that all the reported peaks were activated [see Woo et al., 2014]

Cluster		*x*	*y*	*z*	*t*	*k*
Salience coding						
Occipital/temporal cortex	R/L	-50	-70	-10	11.12	17687
Precentral/middle frontal gyrus	R	46	10	28	10.39	1365
Precentral gyrus	L	-48	4	34	8.28	519
Mid-cingulate cortex	R/L	-2	6	30	8.29	519
Posterior insula	L	-40	-4	10	10.34	383
Insular gyrus	R	38	10	-12	7.37	243
Frontal-eye fields	L	-30	-8	52	6.35	205
Posterior insula	R	38	-4	12	8.66	180
Midbrain/periacqueductal gray	R/L	4	-28	-2	10.09	155
Lateral orbito-frontal cortex	R	30	34	-14	7.48	141
Lateral orbito-frontal cortex	L	-24	28	-16	7.94	127
Cerebellum	R/L	-2	-50	-36	6.72	82
Middle frontal gyrus	L	-46	34	-12	4.97	77
Thalamus	L	-8	-16	8	6.85	63
Anterior insula	L	-34	28	2	7.06	56
Thalamus	R	8	-16	10	7.08	46
Anterior/mid cingulate cortex	R/L	2	20	18	4.68	46
Anterior cingulate cortex	R/L	0	32	4	6.46	44
Thalamus	R	14	-24	10	5.87	26
Paracentral lobule	L	-8	-46	60	5.08	22
Temporal cortex	L	-28	-4	-34	4.72	21
Cerebellum	L	-20	-34	-42	5.34	19
Amygdala (dorsal)	L	-18	-6	-12	7.17	19
Superior frontal gyrus (medial)	R	8	10	56	5.64	19
Cerebellum	R	20	-36	-44	6.78	18
Hippocampus (anterior)	R	28	-36	-2	4.67	18

Cerebellum	L	-16	-44	-46	4.47	17
Supramarignal gyrus	R	48	-36	12	4.56	15
Cerebellum	R	8	-64	-20	5.28	13
Rostral gyrus	R/L	0	32	-20	4.51	13
Amygdala (dorsal)	R	20	-6	-10	5.37	13
Cerebellum	L	-42	-62	-26	4.58	10
Paracentral fissure	L	-34	-28	-22	4.8	10
Amygdala (lateral)	R	26	0	-18	5.59	10
Postcentral/insular cortex	R	32	-12	-6	5.44	10
Inverted salience coding						
Lateral parietal cortex	L	-52	-56	48	-6.37	516
Lateral parietal cortex	R	52	-48	38	-6.75	416
Superior frontal gyrus	R	42	22	40	-6.22	281
Superior frontal gyrus	L	-38	20	54	-5.45	275
Parahippocampal gyrus	L	-26	-44	-6	-10.78	250
Parahippocampal gyrus	R	30	-44	-6	-9.19	244
Occipital gyrus	R	16	-52	8	-7.23	237
Superior temporal gyrus (anterior)	L	-66	-26	-4	-5.57	212
Occipital gyrus	L	-18	-58	8	-7.16	170
Superior temporal gyrus (anterior)	R	64	-22	-2	-5.01	143
Superior frontal gyrus	R	28	20	52	-4.96	130
Transverse temporal gyrus	R	50	-30	18	-5.45	105
Superior frontal gyrus	L	-24	28	46	-4.71	69
Inferior frontal gyrus (orbital part)	L	-50	42	-12	-4.67	58
Middle frontopolar gyrus	R	28	62	6	-5.49	58
Inferior frontal gyrus (opercular part)	R	58	0	8	-5.02	50
Middle frontal gyrus	L	-40	54	0	-4.95	43
Angular gyrus	R	46	-72	36	-4.65	36
Middle temporal gyrus	L	-60	-6	-10	-4.82	35
Transverse temporal gyrus	L	-42	-36	18	-4.93	32
Inferior frontal gyrus (orbital part)	R	42	54	-12	-6.59	28
Parieto-occipitalis	R	10	-84	30	-4.78	21
Angular gyrus	L	-38	-78	36	-4.87	21
Parieto-occipitalis	R/L	0	-84	28	-4.69	17
Thalamus (posterior)	R	6	-30	14	-5.81	14
Anterior central operculum	L	-44	-16	16	-4.97	13
Superior frontal gyrus	R	24	62	22	-3.85	11
Hippocampus	L	-18	-14	-22	-5.75	10

Integration of positive and negative emotion in valence and salience coding regions

This study primarily focused on probing interactions between positive and negative emotional processing in regions that exhibited valence and salience coding. To test our hypothesis of competitive interactions in valence coding regions, we contrasted responses during "P-U" condition with those during "N-P" or "N-U" condition (see Methods for logic behind this comparison). Responses in positive valence coding regions including precuneus, bilateral superior temporal gyrus demonstrated competitive interactions where responses during "P-U" condition were reduced compared to "N-P" condition (Figure 4.7 and Table 4.3). Somewhat surprisingly and contrary to our predictions, in other positive valence coding regions such as vmPFC and bilateral striatum, no differences were detected between "P-U" and "N-P" conditions (Figure 4.8). On the other hand, negative valence coding regions including the bilateral fusiform gyrus exhibited responses supporting competitive interactions where responses during "P-U" condition were reduced compared to "N-U" condition (Figure 4.7 and Table 4.3).

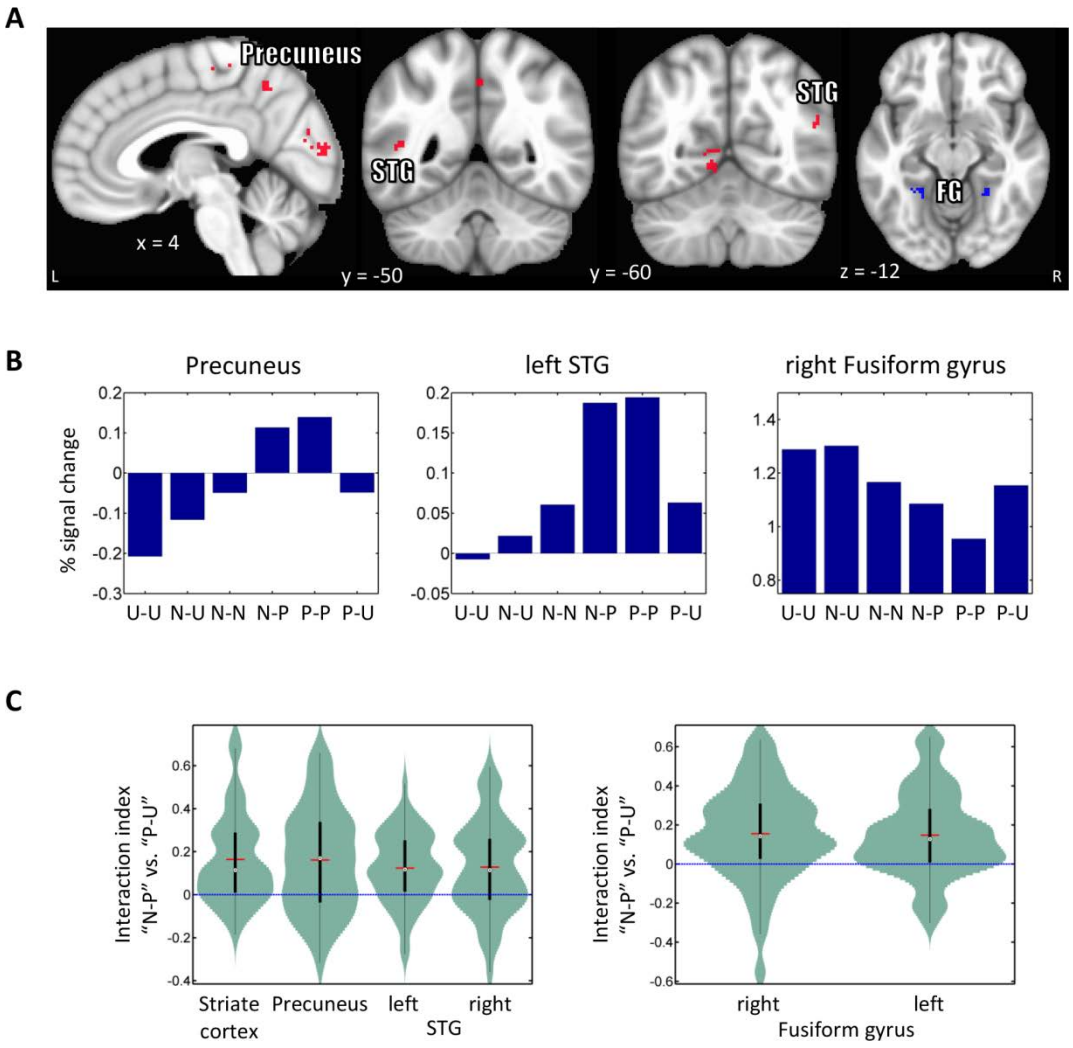

Figure 4.7 Competitive interactions in valence coding regions. (A) Clusters exhibiting competitive interactions during processing of oppositely valenced stimuli displayed at 5-voxel cluster extent. (B) Average responses within clusters that exhibited competitive interactions. To avoid circularity, error bars are not plotted. (C) Distributions of within-subject competitive interaction index in units of % signal change. The box plots within the violins indicate the interquartile range (first quartile to third quartile), red lines show the mean values, and black dots inside white circles show median values. STG: superior temporal gyrus, FG: fusiform gyrus.

Table 4.3 Clusters that exhibited *competitive* interactions in voxelwise conjunction analysis (peak MNI coordinates, t(52) values, and cluster size [k]).

Cluster		*x*	*y*	*z*	*t*	*k*
Positive valence coding						
Superior Occipital gyrus	R/L	2	-86	14	-5.08	43
Precuneus	R/L	-2	-56	46	-4.25	37
Occipital gyrus	L	-16	-62	6	-4.77	23
Lingual gyrus (superior)	L	-10	-60	-2	-4.98	19
Precuneus	L	-4	-74	14	-4.19	13
Lingual/occipital gyrus	L	-22	-52	4	-4.05	9
Lingual gyrus (inferior)	R/L	-2	-76	8	-3.89	9
Superior temporal gyrus	L	-46	-50	10	-4.46	9
Angular gyrus	R	44	-68	26	-3.78	9
Superior temporal gyrus	R	48	-58	22	-4.19	8
Paracentral lobule	R/L	-2	-32	64	-4.21	8
Occipital gyrus	R	8	-56	10	-3.75	7
Parieto-occipitalis/precuneus	R	6	-78	20	-3.83	7
Occipital gyrus	R	18	-64	20	-4.78	7
Parieto-occipitalis	L	-12	-92	30	-3.68	7
Middle temporal gyrus	L	-64	-12	-12	-4.47	6
Occipital gyrus	R	20	-56	6	-3.92	6
Paracentral lobule	L	-4	-46	48	-3.89	6
Paracentral lobule	R/L	2	-16	60	-3.83	6
Superior parietal lobule	R	8	-78	38	-3.52	5
Negative valence coding						
right Fusiform gyrus	R	26	-44	-12	-3.99	23
left Fusiform gyrus	L	-22	-46	-12	-3.68	13
right Planum polare	R	42	8	-16	-3.91	9
right Fusiform gyrus (anterior)	R	30	-38	-14	-3.89	8
right fusiform gyrus (anterior)	R	32	-28	-18	-3.51	6
right Fusiform gyrus (anterior)	R	28	-30	-18	-4.28	5
right Planum polare	R	46	14	-16	-3.83	5

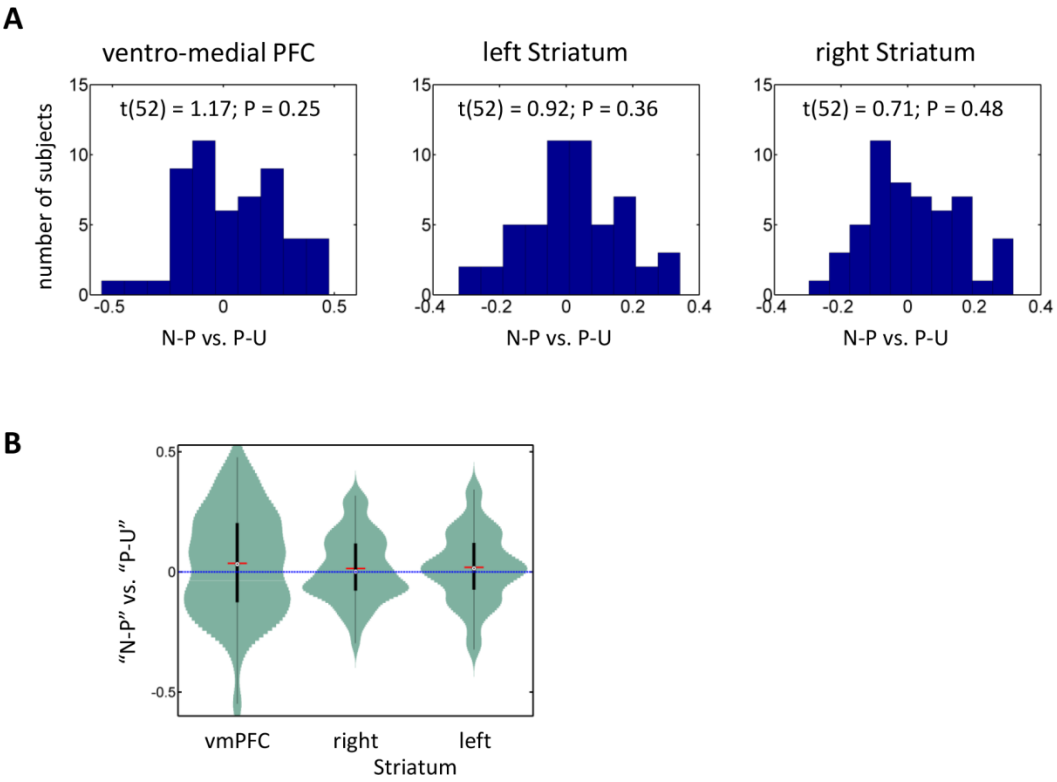

Figure 4.8 Null-findings of competitive interactions in ventro-medial prefrontal cortex and bilateral striatum. (A) Histogram of competitive interaction index in units of % signal change. (B) Distributions of within-subject competitive interaction index in units of % signal change. The box plots within the violins indicate the interquartile range (first quartile to third quartile), red lines show the mean values, and black dots inside white circles show median values. vmPFC: ventro-medial prefrontal cortex.

To evaluate competing hypotheses about the overall intensity in salience coding regions, responses were compared during "P-U" condition to average response during "N-P" and "N-U" conditions (see Methods for logic behind this comparison). Stronger responses were observed during "P-U" condition in multiple regions including the dorsal portions of the bilateral amygdala, bilateral anterior insula, and mid-cingulate cortex (Figure 4.9 and Table 4.4). On the other hand, in regions that exhibited inverted salience coding, including bilateral parahippocampal gyrus,

responses to “P-U” condition were weaker than the average response during “N-P” and “N-U” conditions (Figure 4.9 and Table 4.4).

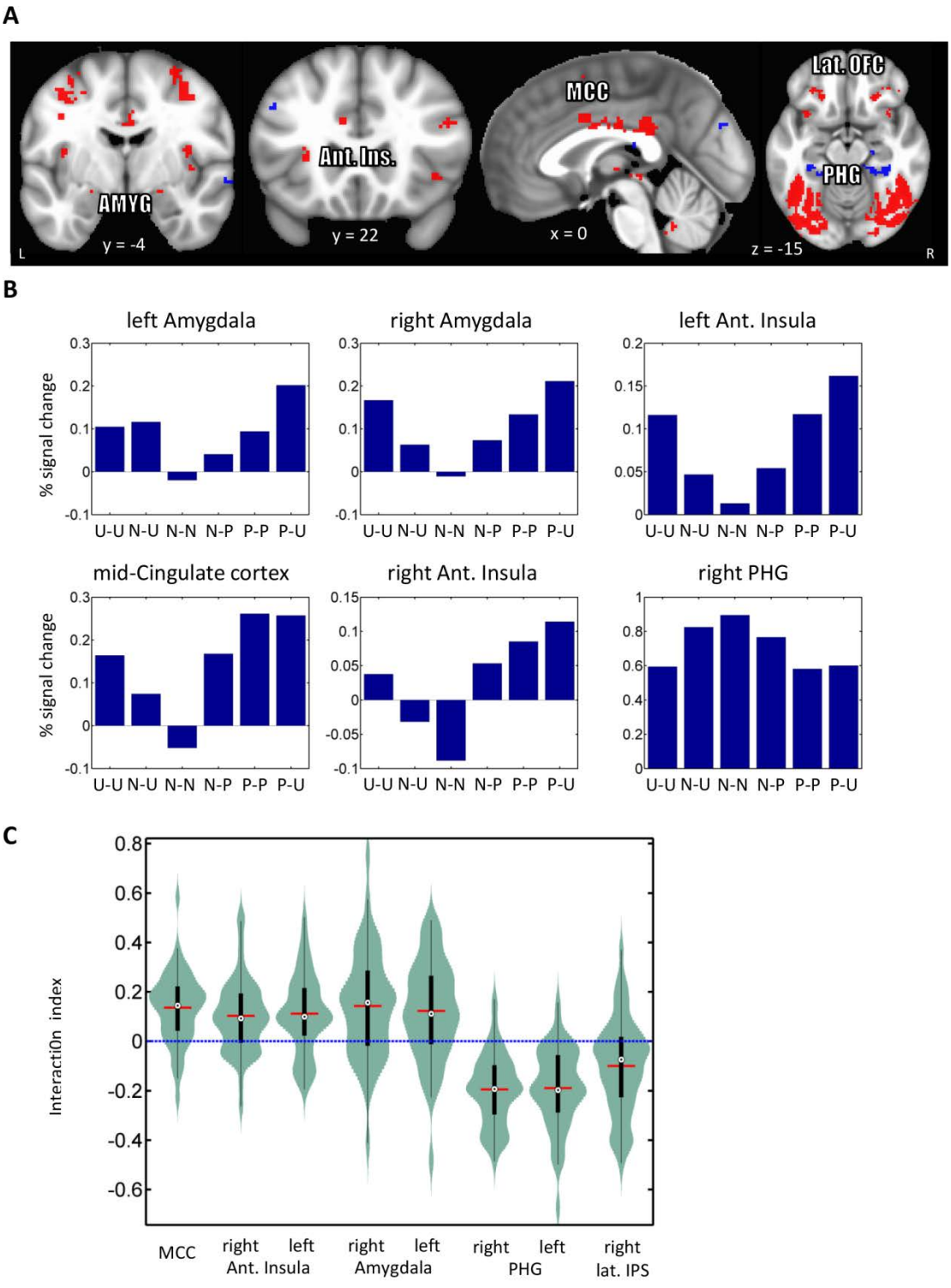

Figure 4.9 Co-operative interactions in salience coding regions. (A) Clusters exhibiting co-operative interactions during processing of oppositely valenced stimuli displayed at 5-voxel cluster extent. (B) Average responses within clusters that exhibited competitive interactions. To avoid circularity, error bars are not plotted. (C) Distributions of within-subject co-operative interaction index in units of % signal change. The box plots within the violins indicate the interquartile range (first quartile to third quartile), red lines show the mean values, and black dots inside white circles show median values. AMYG: amygdala, Ant. Ins.: anterior insula, MCC: mid-cingulate cortex, Lat. OFC: lateral orbito-frontal cortex, PHG: parahippocampal gyrus.

In an additional functional ROI analysis, responses were compared during high-arousing stimuli of opposite valence (i.e., "P-U") condition to average response during high-arousing stimuli of same valence (i.e., "P-P"and "U-U") conditions. Stronger responses were observed during "P-U" condition in dorsal portions of the bilateral amygdala (right: $t(52) = 2.5$; $p = .016$; left: $t(52) = 3.12$; $p = .003$), bilateral anterior insula (right: $t(52) = 2.51$; $p = .015$; left: $t(52) = 2.07$; $p = .043$) and mid-cingulate cortex ($t(52) = 2.27$; $p = .027$).

Table 4.4 Clusters that exhibited *cooperative* interactions in voxelwise conjunction analysis (peak MNI coordinates, t(52) values, and cluster size [k]).

Cluster		*x*	*y*	*z*	*t*	*k*
Salience coding						
Temporal/parietal cortex	R	46	-68	-8	11.65	6689
Temporal/parietal cortex	L	-38	-76	-12	12.85	6312
Precentral gyrus	R	48	6	-24	7.85	749
Precentral gyrus	L	-50	6	28	6.99	365
Posterior cingulate cortex	R/L	-2	-36	26	7.02	170
Middle frontal gyrus	R	46	34	18	4.87	167
Cerebellum	L	-24	-62	-46	5.33	138
Frontal eye-fields	L	-26	-10	50	4.79	84
Cerebellum	R	18	-72	-46	5.00	72
Mid-cingulate cortex	R/L	2	2	32	4.46	68
Cerebellum	L	-8	-70	-18	4.59	60
Midbrain/peri acqueductal gray	R/L	8	-30	-2	4.42	50
Posterior occipital cortex	L	-4	-102	-4	4.28	43
Lateral orbito-frontal cortex	R	26	30	-14	4.72	42
Lateral orbito-frontal cortex	L	-30	34	-14	4.82	42
Anterior insula	R	40	26	2	3.97	40
Precentral gyrus	L	-40	-4	50	4.02	32
Insular gyrus	R	36	12	-8	5.35	31
Cerebellum	R/L	-2	-50	-32	4.09	25
Superior medial frontal cortex	R/L	2	6	60	3.99	25
Middle frontal gyrus	L	-48	34	16	3.95	22
Insular gyrus	L	-34	8	-12	4.51	20
Mid/posterior insula	R	42	-2	6	4.59	20
Mid/posterior insula	L	-40	-4	12	4.53	20
Mid-cingulate cortex	L	-10	24	26	6.67	20
Insular gyrus	L	-22	10	-18	4.81	19
Mid/posterior insula	R	38	-4	12	4.48	17
Cerebellum	R	8	-62	-16	4.19	14
Occipital gyrus	R	16	-80	6	3.88	14
Lateral orbito-frontal cortex	R	36	36	-16	4.01	12
Occipital gyrus	R	12	-74	12	4.59	10
Anterior insula	L	-28	22	8	4.23	9
Amygdala (dorsal)	R	24	-8	-10	3.77	8
Lingual gyrus (inferior)	R	8	-82	-10	4.11	8
Thalamus	R/L	-2	-12	0	3.77	8
Supramarginal gyrus	L	-56	-36	26	3.47	8
Cerebellum	R/L	-2	-46	-38	3.48	7
Mid-insula	L	-34	16	2	4.55	7

Cerebellum	L	-6	-72	-36	3.97	7
Insular gyrus	L	-40	16	-6	3.26	6
Paracentral lobule	L	-8	-50	60	3.54	6
Cerebellum	R	8	-66	-24	4.25	6
Amygdala (dorsal)	L	-22	-6	-12	3.69	5
Anterior cingulate cortex	L	-4	36	6	4.21	5
Middle frontal gyrus	L	-38	32	14	4.02	5

Inverted salience coding

Parahippocampal gyrus	R	30	-44	-6	-8.34	211
Occipital gyrus	R	18	-52	6	-7.07	189
Parahippocampal gyrus	L	-24	-46	-6	-6.5	162
Occipital gyrus	L	-16	-60	8	-5.56	118
Lateral parietal cortex	R	52	-52	42	-3.78	26
Supramarginal gyrus	R	50	-44	38	-3.42	18
Hippocampus	R	20	-22	-16	-3.87	15
Parahippocampal gyrus (anterior)	L	-32	-32	-14	-4.33	15
Middle temporal gyrus	R	62	-2	-4	-3.91	12
Superior frontal gyrus	L	-26	14	46	-3.66	11
Parasubiculum	L	-14	-32	-10	-4.63	10
Subcentral sulcus (anterior)	R	60	4	4	-3.46	9
Parieto-occipitalis	R/L	-2	-84	30	-3.23	9
Middle temporal gyrus	R	66	-20	-6	-3.56	8
Thalamus (posterior)	L	-4	-32	10	-4.29	8
Parietal operculum	R	46	-26	18	-3.31	8
Lateral parietal cortex	L	-52	-50	42	-3.73	8
Superior temporal sulcus	L	-60	-26	0	-3.49	7
Central operculum	L	-48	-12	12	-4.26	7
Central operculum	R	42	-14	14	-4.09	7
Central operculum	R	50	-12	12	-3.26	6
Thalamus (posterior)	R/L	0	-26	16	-3.69	6
Precentral gyrus	L	-62	4	20	-3.65	6
Middle frontal gyrus	L	-46	22	34	-4.37	6
Hippocampus	L	-18	-16	-22	-3.89	5
Parieto-occipitalis	L	-4	-84	20	-3.35	5
Angular gyrus	R	44	-74	34	-3.4	5

Functional interactions with vmPFC: Valence and Salience coding

Using beta series correlation approach, we investigated functional connectivity between vmPFC and rest of the brain in a voxelwise analysis. Our first focus was how valence of the stimuli shaped functional connectivity between vmPFC and other brain regions. Functional connectivity of vmPFC and left precentral gyrus (similar pattern with two right precentral gyrus clusters at $p < .001$ and 4 voxel cluster extent) was observed in a positive valence coding pattern (Figure 4.10 and Table 4.5), where the connectivity strength increased from unpleasant to pleasant conditions (i.e., "P-P" > "N-N" > "U-U"). No regions exhibited negative valence type pattern of functional connectivity with vmPFC (i.e., "U-U" > "N-N" > "P-P").

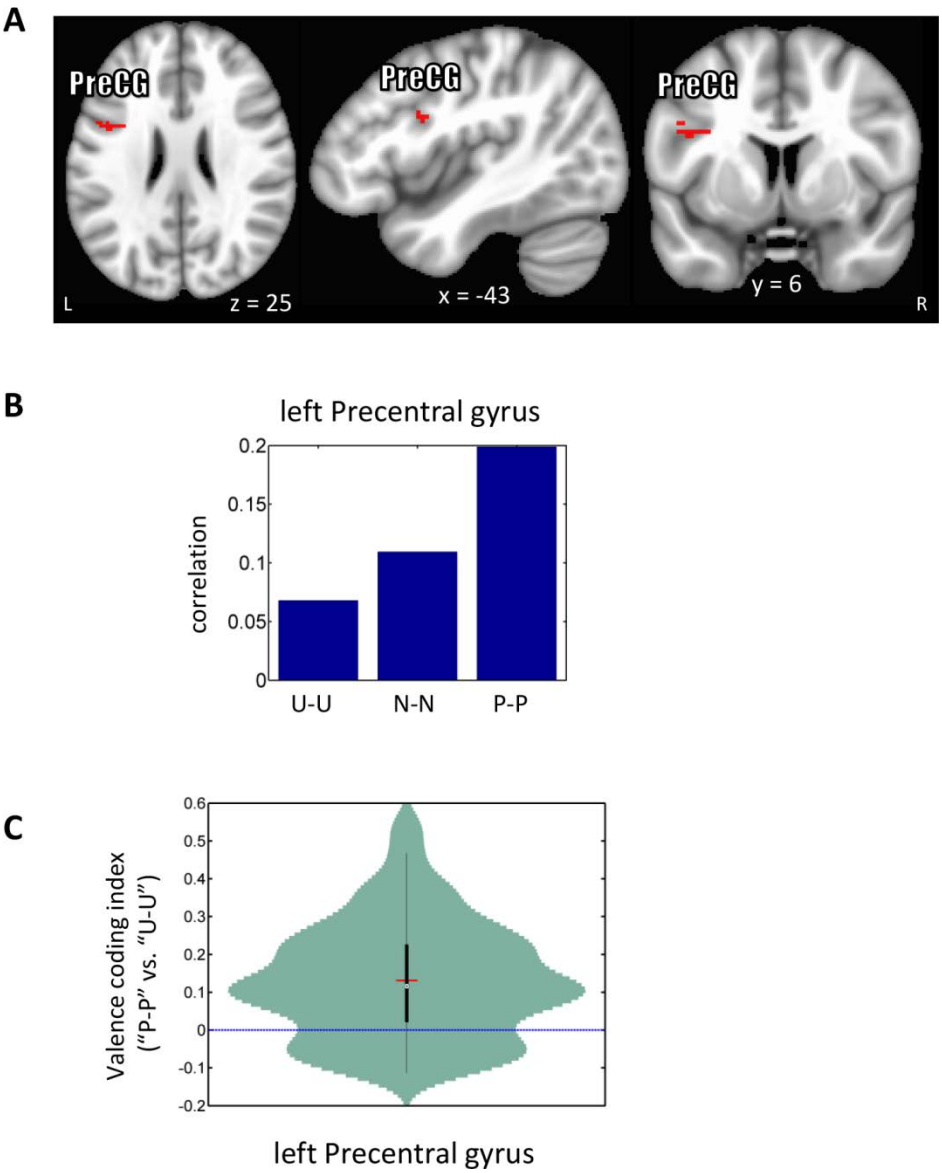

Figure 4.10 Valence coding in vmPFC functional connectivity. (A) Clusters exhibiting positive (red) valence coding (based on functional connectivity with vmPFC during "P-P", "N-N" and "U-U" conditions) displayed at an uncorrected p = .001 and 10-voxel cluster extent (cluster-level alpha of 0.05). Because cluster-extent based thresholding was used for multiple comparisons correction, voxels are displayed using a binary threshold. For further rationale about using binary maps in the context of cluster-based thresholding, see Woo et al., 2014. (B) Average connectivity within left precentral gyrus cluster that exhibited functional connectivity with vmPFC in a valence coding pattern. To avoid circularity, error bars are not plotted. (C) Distributions of within-subject valence coding connectivity index. The box plots within the violins indicate the interquartile range (first quartile to third quartile), red lines show the mean values, and black dots inside white circles show median values. PreCG: precentral gyrus.

Table 4.5 Clusters that survived multiple comparisons correction in voxelwise valence coding connectivity analysis with vmPFC (peak MNI coordinates, t(52) values, and cluster size [k]). Peak coordinates are presented for completeness and potential meta-analysis; with cluster-based thresholding, it is not possible to conclude that all the reported peaks were activated [see Woo et al., 2014]

Cluster		*x*	*y*	*z*	*t*	*k*
vmPFC functional connectivity: Positive valence coding						
Precentral gyrus	L	-48	10	28	4.66	30
Precentral gyrus	R	52	8	26	4.51^{U}	4
Precentral gyrus	R	50	6	22	3.94^{U}	4

^{U}Cluster did not survive correction for multiple comparisons.

Next, we explored how stimulus intensity influenced functional connectivity between vmPFC and other brain regions. Functional connectivity consistent with salience coding was observed in multiple regions including the bilateral anterior insula, mid-cingulate cortex, supplementary motor area and bilateral intraparietal sulcus (Figure 4.11 and Table 4.6), where greater connectivity strength was exhibited during both pleasant and unpleasant conditions than that of the neutral condition (i.e., both “P-P” and “U-U” > “N-N”).

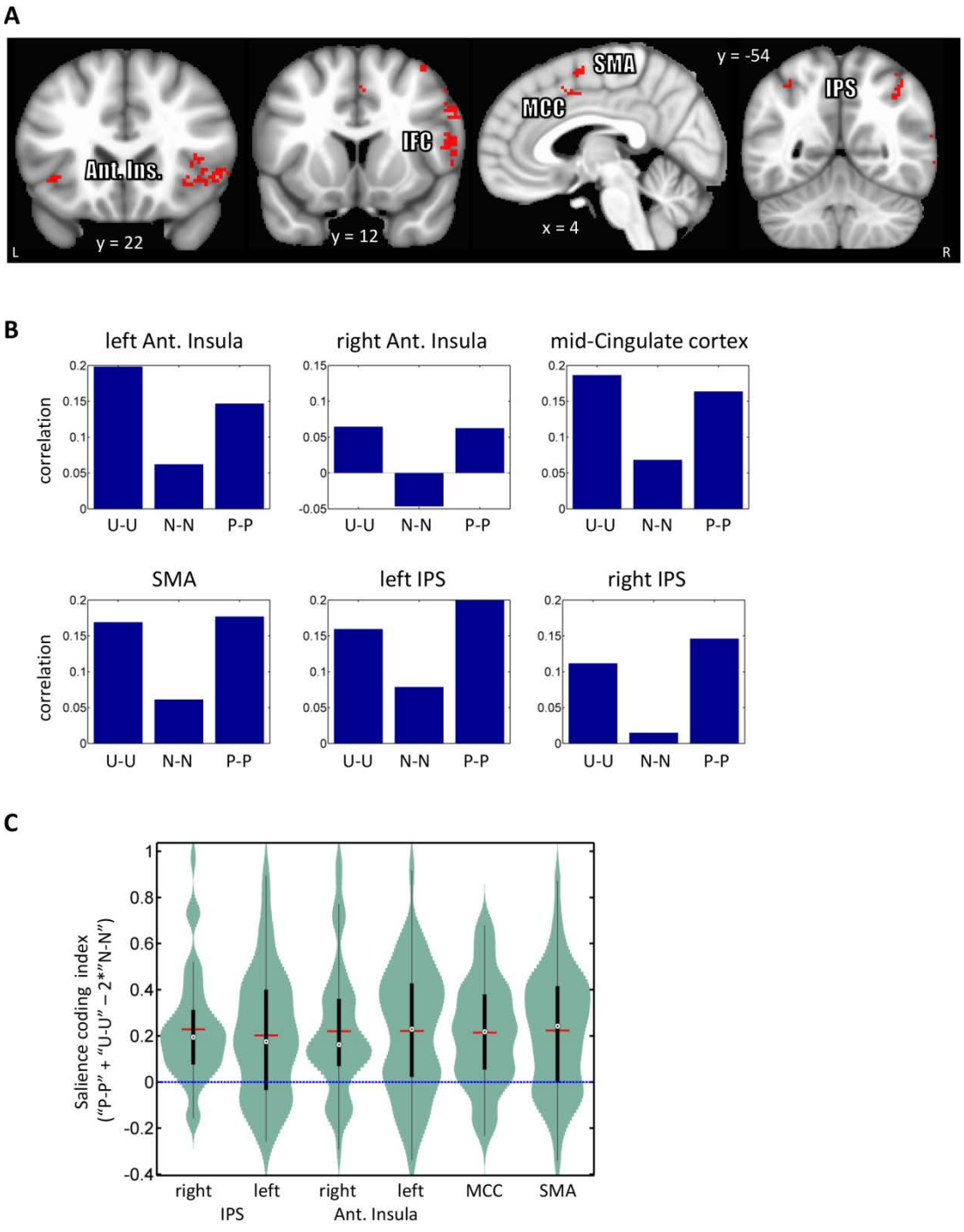

Figure 4.11 Salience coding in vmPFC functional connectivity. (A) Clusters exhibiting salience coding (based on functional connectivity with vmPFC during "P-P", "N-N" and "U-U" conditions) displayed at an uncorrected p = .001 and 10-voxel cluster extent (cluster-level alpha of 0.05). Because cluster-extent based thresholding was used for multiple comparisons correction, voxels are displayed using a binary threshold. For further rationale about using binary maps in the context of cluster-

based thresholding, see Woo et al., 2014. (B) Average connectivity within clusters that exhibited functional connectivity with vmPFC in a salience coding pattern. To avoid circularity, error bars are not plotted. (C) Distributions of within-subject salience coding connectivity index. The box plots within the violins indicate the interquartile range (first quartile to third quartile), red lines show the mean values, and black dots inside white circles show median values. Ant. Ins.: anterior insula, MCC: mid-cingulate cortex; SMA: supplementary motor area; IPS: intra-parietal sulcus; IFC: inferior frontal cortex.

Table 4.6 Clusters that survived multiple comparisons correction in voxelwise salience coding connectivity analysis with vmPFC (peak MNI coordinates, t(52) values, and cluster size [k]). Peak coordinates are presented for completeness and potential meta-analysis; with cluster-based thresholding, it is not possible to conclude that all the reported peaks were activated [see Woo et al., 2014]

Cluster		*x*	*y*	*z*	*t*	*k*
vmPFC functional connectivity: Salience coding						
Intraparietal sulcus	R	42	-48	54	5.85	181
Inferior frontal gyrus/anterior insula	R	58	12	14	5.46	135
Middle frontal gyrus	R	36	-2	62	5.96	117
Supramarginal gyrus	R	64	-18	26	5.53	80
Postcentral gyrus	R	60	-28	42	5.07	60
Inferior frontal gyrus	R	58	12	34	5.06	51
Supplementary motor area	R/L	2	0	62	5.11	33
Superior frontal gyrus	R	26	-10	68	4.55	26
Middle temporal gyrus	R	46	-62	4	5.63	25
Superior temporal gyrus	R	48	-42	18	4.72	25
Mid-cingulate cortex	R	8	4	44	5.00	25
Anterior insula	L	-40	22	-4	4.75	20
Middle temporal gyrus	R	66	-40	10	4.65	20
Angular gyrus	R	46	-68	22	4.66	20
Intraparietal sulcus	L	-34	-54	50	4.19	20
Postcentral gyrus	R	52	-22	46	4.73	19
Supramarginal gyrus	L	-52	-42	28	4.78	17
Superior frontal gyrus	R	40	42	36	4.70	14
Middle temporal gyrus	R	60	-56	-2	5.02	13
Middle frontal gyrus	L	-44	-6	58	4.84	13
Anterior insula	R	40	22	8	4.74	12
Planum temporale	L	-62	-34	20	5.34	12
Superior parietal lobule	R	18	-76	58	4.35	12
Superior temporal gyrus	L	-60	-48	8	5.42	11
Superior parietal lobule	R	20	-62	64	4.88	10

Functional interactions with vmPFC: Integration of positive and negative emotion

Using voxelwise conjunction analysis, we probed for competitive interactions in connectivity during processing of overlapping pleasant and unpleasant emotion in positive valence coding connectivity voxels. We did not detect any evidence supporting competitive interactions in this analysis.

In a separate conjunction analysis, we probed for interactions in connectivity during processing of overlapping pleasant and unpleasant emotion in salience coding connectivity voxels. Again, no evidence supporting interactions were detected in this analysis.

Discussion

Despite the relevance of joint processing of pleasant and unpleasant emotional information to our daily lives, past work has mainly investigated the processing of oppositely-valenced emotional information separately (but see Grabenhorst et al., 2007). In the present fMRI investigation, interactions between pleasant and unpleasant emotional stimuli were probed specifically in regions that were sensitive to valence and salience dimensions of the stimuli. Using standard activation based analysis, competitive interaction patterns were observed in a subset of regions sensitive to valence of the stimuli. Notably, in other valence-related brain regions, including the vmPFC, no evidence for competitive interactions was detected. Conversely, other regions sensitive to stimulus salience exhibited cooperative interaction patterns. Overall, distinct patterns of appetitive-aversive interactions revealed contextual modulation of emotional processing in the human brain.

The primary focus of this study was to investigate the patterns of appetitive-aversive interactions in regions that were sensitive to valence and salience. So, we first probed for brain regions whose responses were sensitive to valence and salience dimensions. We observed responses in multiple regions that varied as a function of valence of emotional stimuli: responses in the vmPFC, striatum, precuneus and superior temporal gyrus exhibited positive valence coding with responses that monotonically increased from unpleasant to pleasant with neutral in between. On the other hand, a salience-related pattern was observed in the dorsal portions of the amygdala, anterior insula, lateral OFC and mid-cingulate cortex with increased responses during unpleasant and pleasant compared to neutral. These results correspond with previous findings (Anderson et al., 2003; Small et al., 2003; Kensinger and Schacter, 2006). However, these past studies did not investigate how these regions that are sensitive to valence or salience integrate positive and negative information.

By employing a novel pleasant-plus-unpleasant stimulus condition, our design allowed us to probe interactions in regions that were sensitive to valence and salience. To note, the contrasts used to probe these interactions were independent of the contrasts used to define valence and salience coding regions. We observed *competitive* interactions between pleasant and unpleasant stimuli in a subset of valence-related regions including the precuneus and bilateral superior temporal gyrus. The precuneus is a node in the distributed network involved in attribution of emotion to the self and others (Ochsner et al., 2004). Additionally, the precuneus has been reported to be valence-sensitive during processing of diverse sets of emotional stimuli

including music, pictures, words and videos (Kensinger and Schacter, 2006; Kim et al., 2017). Likewise, the superior temporal gyrus has been implicated in the processing of emotional stimuli such as fearful faces (Narumoto et al., 2001; Adolphs, 2002). These competitive interactions extend previous findings in an important direction by revealing contextual dependence of emotional information processing in these regions, and are consistent with the opponency between appetitive and aversive motivational systems (Konorski, 1967; Dickinson and Dearing, 1979).

The observed competitive interaction patterns are in line with some behavioral findings reported based on subjective emotional experience (Schimmack and Colcombe, 2007; Fujimura et al., 2013). For instance, to study interactions between positive and negative emotional experience, Schimmack and Colcombe used subjective reports while presenting oppositely-valenced emotional images in a sequential order (as in the present study) or simultaneously (Schimmack and Colcombe, 2007). The authors observed reduced pleasantness ratings of pleasant pictures in the presence of unpleasant pictures and similarly, displeasure ratings of unpleasant pictures were reduced in the presence of pleasant pictures which suggests an antagonistic interaction during joint processing of pleasant and unpleasant stimuli.

However, contrary to our hypothesis, a competitive interaction pattern during joint processing of oppositely-valenced stimuli was not observed in the vmPFC. No difference was detected between responses to pleasant-plus-unpleasant stimuli and pleasant-plus-neutral stimuli. Though caution should be taken due to reliance on null findings, the observed response pattern suggests that in non-threatening conditions (e.g., in an MR machine), processing of erotic content may be resistant to antagonistic

influence of mutilated content in the vmPFC, at least in young male adults. Interestingly, other regions such as bilateral striatum exhibited a similar pattern of responses.

More broadly, the findings of valence-sensitive responses are consistent with the bipolarity model of emotion (Barrett and Russell, 1999; Russell and Carroll, 1999), which argues that emotions are represented along a gradient from negative to positive with a neutral midpoint. According to this model, positive and negative information neutralize one another during their joint processing (Larsen and McGraw, 2014). The observed competitive interaction patterns in the precuenus and superior temporal gyrus are consistent with the prediction of bipolarity hypothesis. However, the absence of competitive interactions in the vmPFC and striatum indicates this model does not hold true for all valence-related regions. To note, in an olfactory fMRI study (Grabenhorst et al., 2007) that investigated perception of odor mixtures containing both pleasant and unpleasant components, the authors reported processing of pleasant and unpleasant components in separate brain regions, providing evidence for the bivalent model.

In regions sensitive to stimulus salience, using two competing models, this study investigated how overall intensity was reflected during joint processing of positive and negative stimuli. One model was based on the intensity of individual items (i.e., |Pleasant| + |Unpleasant|), whereas other model was based on the combined intensity of the valence of the stimuli (i.e., |Pleasant + Unpleasant|). We observed *cooperative* interaction patterns in multiple regions including the dorsal portions of the amygdala, anterior insula, lateral OFC and mid-cingulate cortex,

suggesting overall intensity was based on individual intensities of oppositely valenced stimuli. These results coincide with the findings of a decision-making fMRI study involving benefits and costs (Kahnt and Tobler, 2013). Here, a similar type of salience process (termed “elemental salience”) influenced choice-based decisions and was associated with activity in the right temporoparietal junction.

The amygdala has been frequently reported in both animal and human work studying the processing of emotional information. While earlier proposals linked amygdala exclusively to processing of aversive stimuli (Davis, 1992; LeDoux, 2000), recent frameworks suggest the amygdala is involved in detection and processing of motivationally significant stimuli to coordinate adaptive behavioral responses (Sander et al., 2003; Pessoa, 2010; Cunningham and Brosch, 2012). Our findings of cooperative interference effects in the presence of oppositely valenced stimuli are consistent with these frameworks and indicate intensity also drives amygdala activity during joint processing of positive and negative information.

The anterior insula and mid-cingulate cortex regions are considered key nodes of the salience network involved in detection and processing of salient stimuli in the environment (Uddin, 2015), and exhibit functional diversity by their participation in multiple task domains including interoceptive awareness, cognitive control and emotional processing (Anderson et al., 2013). The observed pattern of responses from these regions suggests overall salience during joint processing of high-arousing pleasant and unpleasant stimuli may strongly engage these regions. Furthermore, in regions such as bilateral amygdala, bilateral insula and mid-cingulate cortex, pleasant-plus-unpleasant stimuli elicited greater response compared to the average

response during valence matched emotional stimuli (i.e., “P-P” and “U-U”). This suggests that processing of two high-arousing stimuli of opposite valence may engage these regions more strongly compared to the stimuli of the same valence.

The majority of past work has focused on investigating how responses in individual brain regions are sensitive to valence and salience aspects of the emotional stimuli. Very little is known about how functional connectivity between brain regions is shaped by these valence and salience dimensions. Here, we investigated this by specifically focusing on the functional connectivity of the vmPFC with rest of the brain. Neuroanatomical work in animal models has demonstrated that vmPFC is densely connected with several cortical and sub-cortical regions suggesting this region potentially integrates information with rest of the brain (Cavada et al., 2000). In humans, Tobler and colleagues reported resting-state functional connectivity of the vmPFC/OFC with diverse set of regions including the striatum, anterior insula and portions of medial prefrontal cortex (Kahnt et al., 2012). Additionally, some studies have investigated functional interactions of the vmPFC during task conditions, but specifically focused on connectivity with the amygdala during regulation of emotional responses (Urry et al., 2006; Banks et al., 2007). Therefore little is known about how vmPFC integrates information with other brain regions during emotional perception.

The current study observed functional connectivity between the vmPFC and precentral gyrus that increased as a function of valence: the strength of functional interactions increased from unpleasant to pleasant with neutral in between. Even in the absence of any overt behavioral response, the observed functional coupling

between the vmPFC and precentral gyrus, a region typically associated with motor activity, is consistent with recent proposals of integration between emotion and action related processes in the brain (Blakemore and Vuilleumier, 2016; Hommel et al., 2017).

Interestingly, the vmPFC exhibited functional connectivity with a multitude of regions including the anterior insula, mid-cingulate cortex, supplementary motor area and inferior parietal sulcus based on the *saliency* of the stimuli where the strength of functional interactions was stronger during pleasant and unpleasant (relative to neutral) conditions. These findings are notable because although vmPFC is sensitive to valence in activation-based responses, our results suggest that it also integrates information with nodes of salience network and parietal attentional regions during the processing of both pleasant and unpleasant stimuli. Overall, these findings of vmPFC functional connectivity are consistent with recent frameworks that propose large-scale integration of information during emotional processing which probably underlies the wide spread impact of emotion on perception, motivation, cognition and action (Pessoa, 2017).

To conclude, this study investigated appetitive-aversive interactions during a passive emotional perception task. Using standard activation based analysis, evidence supporting both competitive and cooperative interactions during joint processing of pleasant and unpleasant stimuli was observed. Furthermore, connectivity analysis revealed distinct functional coupling patterns sensitive to valence and intensity aspects of the stimuli exhibited by the vmPFC. Taken together, these findings advance our current understanding of the brain mechanisms of appetitive-aversive

interactions and support the view of context dependent processing of emotional information.

Chapter 5 Conclusions and future directions

Although understanding brain mechanisms of appetitive-aversive interactions is relevant to our daily lives and has potential clinical relevance, our knowledge about these brain mechanisms is still rudimentary. To fill in some of the gaps in our knowledge base, we conducted two functional MRI studies that investigated appetitive-aversive interactions during perception and attention in healthy adult human brain.

Study 1

Cognitive control mechanisms which allow us to optimize information processing based on our internal goals or changing task demands are critical for our regular behaviors. In the past decade, a sizable number of neuroimaging studies investigated the influence of reward motivation on cognitive control mechanisms (Locke and Braver, 2008; Padmala and Pessoa, 2011; Etzel et al., 2016). These studies have revealed *selective* effects of reward on control processes suggesting that reward motivation sharpens or fine tunes executive functions leading to enhanced performance across a diverse set of tasks (Pessoa, 2013; Botvinick and Braver, 2015). The majority of the past work investigated the impact of reward on control mechanisms involving only neutral information. However, in many situations, we are exposed to aversive stimuli that interfere with task performance especially when not relevant to the task at hand (Pessoa, 2005; Vuilleumier, 2005). Our knowledge about how potential reward influences the processing of potent aversive distractors is

incomplete and the limited evidence thus far is clearly mixed (Kaltwasser et al., 2013; Wei et al., 2016).

To fill in this gap, in the first study of this dissertation work (Chapter 3), we investigated how reward expectancy influences control mechanisms in the context of aversive distractors. Specifically, we tested whether motivation manipulated via performance-based rewards mitigate the influence of potent aversive stimuli? Behaviorally, the prospect of reward reduced the deleterious impact of aversive distractors during a visual discrimination task. In terms of brain responses, interactions paralleling behavior were observed in multiple regions including the anterior insula and dorsal anterior cingulate cortex, but not in the amygdala. During reward cue processing, stronger responses were observed in subcortical regions important for reward processing, as well as fronto-parietal regions important for cognitive control. Notably, stronger reward-cue responses in the ventral striatum were associated with reduced behavioral interference in the presence of negative pictures during the subsequent task phase. Furthermore, during processing of reward (vs. no-reward) cues, the ventral striatum exhibited stronger functional connectivity with fronto-parietal regions important for attentional control. Taken together, our findings suggest that potential reward enhanced attentional control mechanisms enabled participants to reduce the deleterious impact of potent aversive images.

Although the interaction pattern observed between potential reward and aversive processing may seem consistent with opponency between appetitive-aversive motivational systems (Konorski, 1967; Dickinson and Dearing, 1979), in our task reward was task-relevant whereas aversive stimuli were task-irrelevant. So the

observed interaction pattern could simply reflect competition between task-relevant and task-irrelevant processes. Interestingly, other recent behavioral and ERP studies have reported that potential reward enhances the processing of negative stimuli when they were relevant to the task at hand (Wei and Kang, 2014; Wei et al., 2016). These findings suggest that task context might play an important role in determining the influence of reward motivation on aversive processing. Future work could investigate the role of task-context by directly comparing the influence of reward motivation on task-relevant and task-irrelevant aversive processing. In particular, it would be interesting to compare the responses in the amygdala during these task contexts given the important role of this region in emotional processing.

In the presence of potent distractors such as high-arousing aversive stimuli, behavioral interference costs could result from stronger initial attentional capture and/or slower disengagement from those stimuli. Some behavioral evidence suggests that specifically difficulties in disengagement from negative stimuli are more prominent in individuals with elevated levels of self-reported anxiety (Fox et al., 2001; Georgiou et al., 2005). Based on the absence of reward influence on the stronger amygdala responses to aversive items in our study, one could infer that reward expectancy might have influenced slower disengagement processes rather than the initial attentional capture. However, given the poor temporal resolution of the fMRI signal, this is purely speculative and our experimental manipulation was not designed to parse out the influence of reward expectancy on attentional capture vs. disengagement processes from task-irrelevant aversive stimuli. Future studies could

employ specific attentional manipulations that would allow teasing apart these influences of reward expectancy which would be of potential importance.

It is well known that both positive (i.e, gaining reward) and negative (i.e., avoiding punishment) reinforcement influence our behaviors. In our study, motivation was manipulated with only potential for reward. However, motivation to avoid punishments also leads to improvements in behavior across many tasks (Engelmann and Pessoa, 2007; Savine et al., 2010; Braem et al., 2013). Furthermore, some past work has suggested that reward vs. punishment motivation (in the context of neutral items) might influence behavior via different control mechanisms (Potts, 2011; Paschke et al., 2015). Future work could directly compare the influence of reward vs. punishment motivation on aversive distractor processing.

The majority of past studies have focused on investigating the interference effects of negative (relative to neutral) distractors during perceptual and attentional tasks. Some work reported that high-arousing positive stimuli also elicit similar interference effects suggesting that the salience of items plays a major role rather than valence (Schimmack, 2005; Codispoti et al., 2016) whereas others argue that interference from positive items is different from negative ones at least under certain task conditions (Gupta et al., 2016; Iordan and Dolcos, 2017). Future work could investigate how reward and punishment motivation influence processing of these positive distractor stimuli.

Finally, during processing of reward cues we observed enhanced functional connectivity between ventral striatum and fronto-parietal attentional regions suggesting that reward motivation enhanced top-down attentional control that might

help mitigate the influence of potent aversive distractors. By employing network-level analysis using graph-theory based methods, some recent fMRI studies of emotional and motivational processing have extended the idea of functional connectivity between two regions to integration of information between large-scale brain networks (Kinnison et al., 2012; McMenamin et al., 2014). Future work could investigate how these kinds of functional interactions between large-scale brain networks during reward processing influence behavior in the context of emotional distractors.

Study 2

During many situations, one might be exposed to positive and negative emotional information in an overlapping or simultaneous fashion. Hence understanding brain mechanisms during joint processing of positive and negative emotional stimuli is relevant to our daily lives. However most of the past brain imaging work focused on investigating the processing of positive and negative stimuli separately. In the second fMRI study of this dissertation work (Chapter 4), we investigated brain mechanisms underlying the joint processing of positive and negative emotional information during a passive viewing task. Specifically we focused on probing the pattern of appetitive-aversive interactions in brain regions that were sensitive to valence and salience aspects of the emotional stimuli.

In a subset of regions that were sensitive to stimulus valence, *competitive* interaction patterns were observed, such that responses during processing of pleasant-plus-unpleasant items were reduced relative to those during pleasant-plus-neutral items. These competitive interactions are consistent with the proposals of opponency

between appetitive and aversive motivational systems (Konorski, 1967; Dickinson and Dearing, 1979). Notably, in other valence-coding regions such as the ventro-medial prefrontal cortex and bilateral striatum no evidence for competitive interactions was detected. At least in the context of our task that involved pictures of erotica and young male adult population, it appears that antagonistic relationship between appetitive and aversive systems is not pervasive in the brain.

Conversely, in regions that were sensitive to salience, responses during processing of two salient stimuli of opposite valence were stronger relative to those during one salient-plus-neutral stimuli. This suggests that stimulus salience might lead to *cooperative* interaction pattern between oppositely valenced stimuli (Barberini et al., 2012). Overall, distinct patterns of appetitive-aversive interactions revealed contextual modulation of emotional processing in the human brain. In other words, our findings suggest that processing of emotional information is not absolute but is modulated in the context of other emotional items (Fujimura et al., 2013). This kind of contextual modulation of emotional processing happens in many real world settings. For instance, in some countries, cigarette packages contain an aversive picture with the hope that negative value from the picture reduces the positive value of smoking cigarettes.

In this study we chose to present positive and negative stimuli in a sequential fashion rather than presenting them simultaneously. This was done purposefully to control the locus of attention and is relevant to many real-life situations where positive and negative information are processed in a serial fashion. Moreover, some previous behavioral work has reported similar subjective reports of emotional

experience in both sequential/simultaneous cases (Schimmack and Colcombe, 2007). Nevertheless, future studies should compare and contrast the brain mechanisms of appetitive-aversive interactions when stimuli were processed sequentially versus simultaneously.

We used a passive viewing task to avoid potential contamination from motor-related processes on the brain responses (Hayes et al., 2014). So, it might be difficult to fully interpret the functional role of the observed brain activity. As traditionally appetitive and aversive stimuli are linked to opposing approach and avoidance type behaviors respectively (Lang and Bradley, 2013), future studies could investigate interactions between positive and negative emotional processing during tasks that involve an active behavioral component.

In this study, we used high-arousing mutilated and erotic images to manipulate negative and positive emotional processing. However, because of previously reported sex differences especially during processing of the erotic stimuli (Hamann et al., 2004; Sabatinelli et al., 2004; Rupp and Wallen, 2008), we only included male participants in this study. So the observed results may not be generalizable to the entire population. By employing appetitive and aversive conditioning procedures to imbue positive and negative value to otherwise neutral stimuli, future studies could investigate interactions during joint processing of positive and negative stimuli in participants of both genders.

Finally, the functional MRI technique employed here offers limited spatial resolution as typical BOLD response in each voxel represents pooled activity from several thousand neurons. We have attempted to mitigate this limitation to some

extent by collecting fMRI data at higher spatial resolution (1.5 mm isotropic) than typically employed (3 mm isotropic). This issue is particularly relevant while interpreting salience signals because of the possibility that positive and negative information could be processed by distinct but anatomically intermingled neuronal populations. As previously noted, this might be the case in the basolateral amygdala where it appears that there is no clear anatomical separation between positive and negative valence coding neuronal populations (Zhang et al., 2013). In this situation, one could (spuriously) interpret fMRI activity from this region as representing salience whereas single cell activity indicates separate coding of positive and negative valence. Interestingly, in addition to these valence coding cells, some neurons in the amygdala respond to both positive and negative information representing salience (Belova et al., 2007). Since fMRI signal pools activity from these divergent neuronal populations, our ability to fully elucidate the underlying brain mechanisms is limited. So to better characterize appetitive-aversive interactions at a finer spatial scale, parallel studies should be conducted in animal models which provide resolution at the level of individual neurons. Thus the combined knowledge from parallel human and animal work will provide a richer mechanistic understanding of the brain (Hayes et al., 2014).

To conclude, in this dissertation work, we have taken initial strides at investigating brain mechanisms underlying interactions between appetitive and aversive information processing during perception and attention. Our findings from the first study contribute to the understanding of how potential reward influences attentional control and reduces negative distractor processing in the human brain. The

findings of competitive and cooperative type interactions from the second study supported contextual modulation of emotional processing in the human brain.

Appendices

Appendix A: Sexual Attraction Scale

Sexual Attraction Scale

Select a number that describes your present sexual attraction.

1	2	3	4	5	6	7
Other Sex Only	Other Sex Mostly	Other Sex Somewhat More	Both Sexes Equally	Same Sex Somewhat More	Same Sex Mostly	Same Sex Only

*Participants who reported only 1 or 2 on this scale were eligible to participate in the study

Bibliography

Adolphs R (2002) Neural systems for recognizing emotion. Curr Opin Neurobiol 12:169-177.

Adolphs R, Tranel D (2000) Emotion recognition and the human amygdala. In: The Amygdala: A Functional Anlysis (Aggleton JP, ed), pp 587-630. New York: Oxford University Press.

Aharon I, Etcoff N, Ariely D, Chabris CF, O'Connor E, Breiter HC (2001) Beautiful faces have variable reward value: fMRI and behavioral evidence. Neuron 32:537-551.

Amemori K-i, Graybiel AM (2012) Localized microstimulation of primate pregenual cingulate cortex induces negative decision-making. Nat Neurosci 15:776-785.

Anderson AK, Christoff K, Stappen I, Panitz D, Ghahremani DG, Glover G, Gabrieli JD, Sobel N (2003) Dissociated neural representations of intensity and valence in human olfaction. Nat Neurosci 6:196-202.

Anderson ML, Kinnison J, Pessoa L (2013) Describing functional diversity of brain regions and brain networks. Neuroimage 73:50-58.

Avants BB, Tustison N, Song G (2009) Advanced normalization tools (ANTS). Insight J 2:1-35.

Banks SJ, Eddy KT, Angstadt M, Nathan PJ, Phan KL (2007) Amygdala-frontal connectivity during emotion regulation. Soc Cogn Affect Neurosci 2:303-312.

Barberini CL, Morrison SE, Saez A, Lau B, Salzman CD (2012) Complexity and competition in appetitive and aversive neural circuits. Front Neurosci 6.

Barrett LF, Russell JA (1999) The structure of current affect controversies and emerging consensus. Curr Dir Psychol Sci 8:10-14.

Baxter MG, Murray EA (2002) The amygdala and reward. Nat Rev Neurosci 3:563-573.

Becerra L, Breiter HC, Wise R, Gonzalez RG, Borsook D (2001) Reward circuitry activation by noxious thermal stimuli. Neuron 32:927-946.

Belova MA, Paton JJ, Morrison SE, Salzman CD (2007) Expectation modulates neural responses to pleasant and aversive stimuli in primate amygdala. Neuron 55:970-984.

Bissonette GB, Gentry RN, Padmala S, Pessoa L, Roesch MR (2014) Impact of appetitive and aversive outcomes on brain responses: Linking the animal and human literatures. Front Syst Neurosci 8:24.

Bissonette GB, Burton AC, Gentry RN, Goldstein BL, Hearn TN, Barnett BR, Kashtelyan V, Roesch MR (2013) Separate populations of neurons in ventral striatum encode value and motivation. PloS One 8:e64673.

Blakemore RL, Vuilleumier P (2016) An emotional call to action: Integrating affective neuroscience in models of motor control. Emotion Review:1754073916670020.

Boehler CN, Hopf JM, Stoppel CM, Krebs RM (2012) Motivating inhibition - reward prospect speeds up response cancellation. Cognition 125:498-503.

Bogdan R, Pizzagalli DA (2006) Acute stress reduces reward responsiveness: implications for depression. Biol Psychiatry 60:1147-1154.

Botvinick M, Braver T (2015) Motivation and cognitive control: from behavior to neural mechanism. Psychology 66:83.

Bradley MM, Codispoti M, Cuthbert BN, Lang PJ (2001) Emotion and motivation I: defensive and appetitive reactions in picture processing. Emotion 1:276-298.

Braem S, Duthoo W, Notebaert W (2013) Punishment sensitivity predicts the impact of punishment on cognitive control. PloS One 8:e74106.

Braem S, Verguts T, Roggeman C, Notebaert W (2012) Reward modulates adaptations to conflict. Cognition 125:324-332.

Brischoux F, Chakraborty S, Brierley DI, Ungless MA (2009) Phasic excitation of dopamine neurons in ventral VTA by noxious stimuli. Proceedings of the National Academy of Sciences 106:4894.

Bromberg-Martin ES, Matsumoto M, Hikosaka O (2010) Dopamine in motivational control: rewarding, aversive, and alerting. Neuron 68:815-834.

Bullmore E, Sporns O (2009) Complex brain networks: graph theoretical analysis of structural and functional systems. Nat Rev Neurosci 10:186-198.

Burgos-Robles A, Kimchi EY, Izadmehr EM, Porzenheim MJ, Ramos-Guasp WA, Nieh EH, Felix-Ortiz AC, Namburi P, Leppla CA, Presbrey KN (2017) Amygdala inputs to prefrontal cortex guide behavior amid conflicting cues of reward and punishment. Nature 201:7.

Cacioppo JT, Gardner WL, Berntson GG (1999) The affect system has parallel and integrative processing components: Form follows function. J Pers Soc Psychol 76:839.

Calkins AW, Rogers AH, Campbell AA, Simon NM (2015) Comorbidity of anxiety and depression. Anxiety Disorders:299.

Carter RMK, MacInnes JJ, Huettel SA, Adcock RA (2009) Activation in the VTA and nucleus accumbens increases in anticipation of both gains and losses. Frontiers in behavioral neuroscience 3.

Cavada C, Compañy T, Tejedor J, Cruz-Rizzolo RJ, Reinoso-Suárez F (2000) The anatomical connections of the macaque monkey orbitofrontal cortex. A review. Cereb cortex 10:220-242.

Chiew KS, Braver TS (2013) Temporal dynamics of motivation-cognitive control interactions revealed by high-resolution pupillometry. Front Psychol 4:15.

Choi JM, Padmala S, Pessoa L (2012) Impact of state anxiety on the interaction between threat monitoring and cognition. Neuroimage 59:1912-1923.

Choi JM, Padmala S, Spechler P, Pessoa L (2014) Pervasive competition between threat and reward in the brain. Soc Cogn Affect Neurosci 9:737-750.

Cisler JM, Bush K, Steele JS (2014) A comparison of statistical methods for detecting context-modulated functional connectivity in fMRI. Neuroimage 84:1042-1052.

Clithero JA, Rangel A (2014) Informatic parcellation of the network involved in the computation of subjective value. Soc Cogn Affect Neurosci 9:1289-1302.

Codispoti M, De Cesarei A, Biondi S, Ferrari V (2016) The fate of unattended stimuli and emotional habituation: Behavioral interference and cortical changes. Cogn Affect Behav Neurosci 16:1063-1073.

Cohen JY, Amoroso MW, Uchida N (2015) Serotonergic neurons signal reward and punishment on multiple timescales. eLife 4:e06346.

Cohen M (1997) Parametric analysis of fMRI data using linear systems methods. Neuroimage 6:93-103.

Cooper JC, Knutson B (2008) Valence and salience contribute to nucleus accumbens activation. Neuroimage 39:538-547.

Cox RW (1996) AFNI: Software for analysis and visualization of functional magnetic resonance neuroimages. Computers and Biomedical Research 29:162-173.

Cox RW, Chen G, Glen DR, Reynolds RC, Taylor PA (2017) FMRI Clustering in AFNI: False-Positive Rates Redux. Brain Connect 7:152-171.

Craig AD (2009) How do you feel--now? The anterior insula and human awareness. Nat Rev Neurosci 10:59-70.

Cunningham WA, Brosch T (2012) Motivational salience: Amygdala tuning from traits, needs, values, and goals. Curr Dir Psychol Sci 21:54-59.

Davis M (1992) The role of the amygdala in fear and anxiety. Annu Rev Neurosci 15:353-375.

Daw ND, Kakade S, Dayan P (2002) Opponent interactions between serotonin and dopamine. Neural Netw 15:603-616.

Delgado MR (2007) Reward Related Responses in the Human Striatum. Annals of the New York Academy of Sciences 1104:70-88.

Delgado MR, Li J, Schiller D, Phelps EA (2008) The role of the striatum in aversive learning and aversive prediction errors. Philosophical Transactions of the Royal Society B: Biological Sciences 363:3787-3800.

Dickinson A, Pearce JM (1977) Inhibitory interactions between appetitive and aversive stimuli. Psychol Bull 84:690.

Dickinson A, Dearing MF (1979) Appetitive-aversive interactions and inhibitory processes. In: Mechanisms of Learning and Motivation (Dickinson A, Boakes RA, eds), pp 203–231. Hillsdale, NJ: Erlbaum.

Dillon DG, Rosso IM, Pechtel P, Killgore WD, Rauch SL, Pizzagalli DA (2014) Peril and pleasure: an rdoc-inspired examination of threat responses and reward processing in anxiety and depression. Depress Anxiety 31:233-249.

Eklund A, Nichols TE, Knutsson H (2016) Cluster failure: Why fMRI inferences for spatial extent have inflated false-positive rates. Proceedings of the National Academy of Sciences:201602413.

Engelmann JB, Pessoa L (2007) Motivation sharpens exogenous spatial attention. Emotion 7:668-674.

Engelmann JB, Damaraju EC, Padmala S, Pessoa L (2009) Combined effects of attention and motivation on visual task performance: Transient and sustained motivational effects. Front Hum Neurosci 3:doi:10.3389/neuro.3309.3004.2009.

Engelmann JB, Meyer F, Fehr E, Ruff CC (2015) Anticipatory anxiety disrupts neural valuation during risky choice. J Neurosci 35:3085-3099.

Erthal FS, de Oliveira L, Mocaiber I, Pereira MG, Machado-Pinheiro W, Volchan E, Pessoa L (2005) Load-dependent modulation of affective picture processing. Cogn Affect Behav Neurosci 5:388-395.

Etkin A, Egner T, Kalisch R (2011) Emotional processing in anterior cingulate and medial prefrontal cortex. Trends Cogn Sci 15:85-93.

Etkin A, Buchel C, Gross JJ (2015) The neural bases of emotion regulation. Nat Rev Neurosci 16:693-700.

Etzel JA, Cole MW, Zacks JM, Kay KN, Braver TS (2016) Reward Motivation Enhances Task Coding in Frontoparietal Cortex. Cereb cortex 26:1647-1659.

Everitt BJ, Cardinal RN, Parkinson JA, Robbins TW (2003) Appetitive behavior: impact of amygdala-dependent mechanisms of emotional learning. Annals of the New York Academy of Sciences 985:233-250.

Feinberg DA, Moeller S, Smith SM, Auerbach E, Ramanna S, Glasser MF, Miller KL, Ugurbil K, Yacoub E (2010) Multiplexed echo planar imaging for sub-second whole brain FMRI and fast diffusion imaging. PloS One 5:e15710.

Fiorillo CD (2013) Two dimensions of value: dopamine neurons represent reward but not aversiveness. Science 341:546-549.

Fox E, Russo R, Bowles R, Dutton K (2001) Do threatening stimuli draw or hold visual attention in subclinical anxiety? Journal of Experimental Psychology: General 130:681-700.

Friston KJ, Penny WD, Glaser DE (2005) Conjunction revisited. Neuroimage 25:661-667.

Friston KJ, Buechel C, Fink GR, Morris J, Rolls E, Dolan RJ (1997) Psychophysiological and modulatory interactions in neuroimaging. Neuroimage 6:218-229.

Fujimura T, Katahira K, Okanoya K (2013) Contextual modulation of physiological and psychological responses triggered by emotional stimuli. Front Psychol 4.

Georgiou GA, Bleakley C, Hayward J, Russo R, Dutton K, Eltiti S, Fox E (2005) Focusing on fear: Attentional disengagement from emotional faces. Vis Cogn 12:145-158.

Gorman JM (1996) Comorbid depression and anxiety spectrum disorders. Depress Anxiety 4:160-168.

Grabenhorst F, Rolls ET, Margot C, da Silva MA, Velazco MI (2007) How pleasant and unpleasant stimuli combine in different brain regions: odor mixtures. J Neurosci 27:13532-13540.

Greve DN, Fischl B (2009) Accurate and robust brain image alignment using boundary-based registration. Neuroimage 48:63-72.

Gupta R, Hur YJ, Lavie N (2016) Distracted by pleasure: Effects of positive versus negative valence on emotional capture under load. Emotion 16:328-337.

Haber SN, Knutson B (2010) The reward circuit: linking primate anatomy and human imaging. Neuropsychopharmacology 35:4-26.

Hadj-Bouziane F, Liu N, Bell AH, Gothard KM, Luh W-M, Tootell RB, Murray EA, Ungerleider LG (2012) Amygdala lesions disrupt modulation of functional MRI activity evoked by facial expression in the monkey inferior temporal cortex. Proceedings of the National Academy of Sciences 109:E3640-E3648.

Hamann S (2012) Mapping discrete and dimensional emotions onto the brain: controversies and consensus. Trends Cogn Sci 16:458-466.

Hamann S, Herman RA, Nolan CL, Wallen K (2004) Men and women differ in amygdala response to visual sexual stimuli. Nat Neurosci 7:411-416.

Harsay HA, Cohen MX, Oosterhof NN, Forstmann BU, Mars RB, Ridderinkhof KR (2011) Functional connectivity of the striatum links motivation to action control in humans. J Neurosci 31:10701-10711.

Hayes DJ, Duncan NW, Xu J, Northoff G (2014) A comparison of neural responses to appetitive and aversive stimuli in humans and other mammals. Neurosci Biobehav Rev 45:350-368.

Hommel B, Moors A, Sander D, Deonna J (2017) Emotion meets action: towards an integration of research and theory. Emotion Review:1754073916689379.

Hu K, Padmala S, Pessoa L (2013) Interactions between reward and threat during visual processing. Neuropsychologia 51:1763-1772.

Hubner R, Schlosser J (2010) Monetary reward increases attentional effort in the flanker task. Psychonomic Bulletin & Review 17:821-826.

Iglesias JE, Liu C-Y, Thompson PM, Tu Z (2011) Robust brain extraction across datasets and comparison with publicly available methods. IEEE Trans Med Imaging 30:1617-1634.

Iordan AD, Dolcos F (2017) Brain Activity and Network Interactions Linked to Valence-Related Differences in the Impact of Emotional Distraction. Cereb cortex 27:731-749.

Ishai A, Pessoa L, Bikle PC, Ungerleider LG (2004) Repetition suppression of faces is modulated by emotion. Proc Natl Acad Sci USA 101:9827-9832.

Jennings JH, Sparta DR, Stamatakis AM, Ung RL, Pleil KE, Kash TL, Stuber GD (2013) Distinct extended amygdala circuits for divergent motivational states. Nature 496:224-228.

Jensen J, McIntosh AR, Crawley AP, Mikulis DJ, Remington G, Kapur S (2003) Direct activation of the ventral striatum in anticipation of aversive stimuli. Neuron 40:1251-1257.

Jensen J, Smith AJ, Willeit M, Crawley AP, Mikulis DJ, Vitcu I, Kapur S (2007) Separate brain regions code for salience vs. valence during reward prediction in humans. Hum Brain Mapp 28:294-302.

Jin J, Zelano C, Gottfried JA, Mohanty A (2015) Human Amygdala Represents the Complete Spectrum of Subjective Valence. J Neurosci 35:15145-15156.

Kahnt T, Tobler PN (2013) Salience signals in the right temporoparietal junction facilitate value-based decisions. J Neurosci 33:863-869.

Kahnt T, Chang LJ, Park SQ, Heinzle J, Haynes J-D (2012) Connectivity-based parcellation of the human orbitofrontal cortex. J Neurosci 32:6240-6250.

Kaltwasser L, Ries S, Sommer W, Knight R, Willems RM (2013) Independence of valence and reward in emotional word processing: electrophysiological evidence. Front Psychol 4:168.

Kang D, Liu Y, Miskovic V, Keil A, Ding M (2016) Large-scale functional brain connectivity during emotional engagement as revealed by beta-series correlation analysis. Psychophysiology 53:1627-1638.

Kensinger EA, Schacter DL (2006) Processing emotional pictures and words: effects of valence and arousal. Cogn Affect Behav Neurosci 6:110-126.

Kim J, Shinkareva SV, Wedell DH (2017) Representations of modality-general valence for videos and music derived from fMRI data. Neuroimage 148:42-54.

Kim J, Pignatelli M, Xu S, Itohara S, Tonegawa S (2016) Antagonistic negative and positive neurons of the basolateral amygdala. Nat Neurosci 19:1636-1646.

Kinnison J, Padmala S, Choi JM, Pessoa L (2012) Network analysis reveals increased integration during emotional and motivational processing. J Neurosci 32:8361-8372.

Knutson B, Adams CM, Fong GW, Hommer D (2001) Anticipation of increasing monetary reward selectively recruits nucleus accumbens. J Neurosci 21:RC159.

Konorski J (1967) Intergrative Activity of the Brain: An Interdisciplinary Approach. Chicago:: University of Chicago Press.

Kranz GS, Kasper S, Lanzenberger R (2010) Reward and the serotonergic system. Neuroscience 166:1023-1035.

Krebs RM, Boehler CN, Roberts KC, Song AW, Woldorff MG (2012) The involvement of the dopaminergic midbrain and cortico-striatal-thalamic circuits in the integration of reward prospect and attentional task demands. Cereb cortex 22:607-615.

Kumar P, Berghorst LH, Nickerson LD, Dutra SJ, Goer F, Greve D, Pizzagalli DA (2014) Differential effects of acute stress on anticipatory and consummatory phases of reward processing. Neuroscience.

LaBar KS, Gatenby JC, Gore JC, LeDoux JE, Phelps EA (1998) Human amygdala activation during conditioned fear acquisition and extinction: a mixed-trial fMRI study. Neuron 20:937-945.

Lang P, Bradley M, Cuthbert B (1997a) Motivated attention: affect, activation, and action. In: Attention and Orienting: Sensory and Motivational Processes (Lang P, Simons R, Balaban M, eds). Hillsdale, NJ: Erlbaum Associates.

Lang PJ, Bradley MM (2013) Appetitive and defensive motivation: Goal-directed or goal-determined? Emotion Review 5:230-234.

Lang PJ, Bradley MM, Cuthbert BN (1990) Emotion, attention, and the startle reflex. Psychol Rev 97:377-395.

Lang PJ, Bradley MM, Cuthbert B (1997b) International affective picture system (IAPS): Instruction Manual and Affective ratings. In: NIMH Center for the Study of Emotion and Attention.

Lang PJ, Bradley MM, Cuthbert B (2005) International affective picture system (IAPS): Instruction Manual and Affective ratings. In: NIMH Center for the Study of Emotion and Attention.

Larsen JT, McGraw AP (2014) The case for mixed emotions. Social and Personality Psychology Compass 8:263-274.

Larsen JT, McGraw AP, Cacioppo JT (2001) Can people feel happy and sad at the same time? J Pers Soc Psychol 81:684-696.

LeDoux JE (2000) Emotion circuits in the brain. Annu Rev Neurosci 23:155-184.

Leknes S, Tracey I (2008) A common neurobiology for pain and pleasure. Nat Rev Neurosci 9:314-320.

Levita L, Hare TA, Voss HU, Glover G, Ballon DJ, Casey BJ (2009) The bivalent side of the nucleus accumbens. Neuroimage 44:1178-1187.

Lindquist KA, Satpute AB, Wager TD, Weber J, Barrett LF (2015) The brain basis of positive and negative affect: evidence from a meta-analysis of the human neuroimaging literature. Cereb cortex:bhv001.

Litt A, Plassmann H, Shiv B, Rangel A (2010) Dissociating Valuation and Saliency Signals during Decision-Making. Cereb cortex 21:95-102.

Liu X, Hairston J, Schrier M, Fan J (2011) Common and distinct networks underlying reward valence and processing stages: a meta-analysis of functional neuroimaging studies. Neuroscience and Biobehavioral Reviews 35:1219-1236.

Locke HS, Braver TS (2008) Motivational influences on cognitive control: behavior, brain activation, and individual differences. Cogn Affect Behav Neurosci 8:99-112.

Loftus GR, Masson ME (1994) Using confidence intervals in within-subject designs. Psychonomic Bulletin & Review 1:476-490.

Matsumoto H, Tian J, Uchida N, Watabe-Uchida M (2016) Midbrain dopamine neurons signal aversion in a reward-context-dependent manner. eLife 5:e17328.

Matsumoto M, Hikosaka O (2009) Two types of dopamine neuron distinctly convey positive and negative motivational signals. Nature 459:837-841.

McGinty VB, Hayden BY, Heilbronner SR, Dumont EC, Graves SM, Mirrione MM, du Hoffmann J, Sartor GC, España RA, Millan EZ, DiFeliceantonio AG,

Marchant NJ, Napier TC, Root DH, Borgland SL, Treadway MT, Floresco SB, McGinty JF, Haber S (2011) Emerging, reemerging, and forgotten brain areas of the reward circuit: Notes from the 2010 Motivational Neural Networks conference. Behav Brain Res 225:348-357.

McMenamin BW, Langeslag SJ, Sirbu M, Padmala S, Pessoa L (2014) Network organization unfolds over time during periods of anxious anticipation. J Neurosci 34:11261-11273.

Mitchell DG, Nakic M, Fridberg D, Kamel N, Pine DS, Blair RJ (2007) The impact of processing load on emotion. Neuroimage 34:1299-1309.

Mizuhiki T, Richmond BJ, Shidara M (2012) Encoding of reward expectation by monkey anterior insular neurons. J Nuerophysiol 107:2996-3007.

Mocaiber I, Sanchez TA, Pereira MG, Erthal FS, Joffily M, Araujo DB, Volchan E, de Oliveira L (2011) Antecedent descriptions change brain reactivity to emotional stimuli: a functional magnetic resonance imaging study of an extrinsic and incidental reappraisal strategy. Neuroscience 193:241-248.

Morrens J (2014) Dopamine neurons coding prediction errors in reward space, but not in aversive space: a matter of location? J Neurophysiol 112:1021-1024.

Morrison SE, Salzman CD (2009) The Convergence of Information about Rewarding and Aversive Stimuli in Single Neurons. J Neurosci 29:11471-11483.

Mumford JA, Poline J-B, Poldrack RA (2015) Orthogonalization of Regressors in fMRI Models. PloS One 10:e0126255.

Mumford JA, Turner BO, Ashby FG, Poldrack RA (2012) Deconvolving BOLD activation in event-related designs for multivoxel pattern classification analyses. Neuroimage 59:2636-2643.

Namburi P, Beyeler A, Yorozu S, Calhoon GG, Halbert SA, Wichmann R, Holden SS, Mertens KL, Anahtar M, Felix-Ortiz AC, Wickersham IR, Gray JM, Tye KM (2015) A circuit mechanism for differentiating positive and negative associations. Nature 520:675-678.

Narumoto J, Okada T, Sadato N, Fukui K, Yonekura Y (2001) Attention to emotion modulates fMRI activity in human right superior temporal sulcus. Cognitive Brain Research 12:225-231.

Nasser HM, McNally GP (2012) Appetitive–aversive interactions in Pavlovian fear conditioning. Behav Neurosci 126:404.

Nasser HM, McNally GP (2013) Neural correlates of appetitive–aversive interactions in Pavlovian fear conditioning. Learn Mem 20:220-228.

Nichols T, Brett M, Andersson J, Wager T, Poline J-B (2005) Valid conjunction inference with the minimum statistic. Neuroimage 25:653-660.

Ochsner KN, Knierim K, Ludlow DH, Hanelin J, Ramachandran T, Glover G, Mackey SC (2004) Reflecting upon feelings: an fMRI study of neural systems supporting the attribution of emotion to self and other. J Cogn Neurosci 16:1746-1772.

Ossewaarde L, Qin S, Van Marle HJF, van Wingen GA, Fernández G, Hermans EJ (2011) Stress-induced reduction in reward-related prefrontal cortex function. Neuroimage 55:345-352.

Padmala S, Pessoa L (2011) Reward Reduces Conflict by Enhancing Attentional Control and Biasing Visual Cortical Processing. J Cogn Neurosci 23:3419-3432.

Padmala S, Pessoa L (2014) Motivation versus aversive processing during perception. Emotion 14:450-454.

Palminteri S, Lebreton M, Worbe Y, Grabli D, Hartmann A, Pessiglione M (2009) Pharmacological modulation of subliminal learning in Parkinson's and Tourette's syndromes. Proceedings of the National Academy of Sciences 106:19179-19184.

Park SQ, Kahnt T, Rieskamp J, Heekeren HR (2011) Neurobiology of value integration: when value impacts valuation. J Neurosci 31:9307-9314.

Paschke LM, Walter H, Steimke R, Ludwig VU, Gaschler R, Schubert T, Stelzel C (2015) Motivation by potential gains and losses affects control processes via different mechanisms in the attentional network. Neuroimage 111:549-561.

Paton JJ, Belova MA, Morrison SE, Salzman CD (2006) The primate amygdala represents the positive and negative value of visual stimuli during learning. Nature 439:865-870.

Pessoa L (2002) Neural processing of emotional faces requires attention. Proceedings of the National Academy of Sciences 99:11458-11463.

Pessoa L (2005) To what extent are emotional visual stimuli processed without attention and awareness? Curr Opin Neurobiol 15:188-196.

Pessoa L (2010) Emotion and cognition and the amygdala: from "what is it?" to "what's to be done?". Neuropsychologia 48:3416-3429.

Pessoa L (2013) The Cognitive-Emotional Brain: From Interactions to Integration. Cambridge: MIT Press.

Pessoa L (2017) A network model of the emotional brain. Trends Cogn Sci.

Pezze MA, Feldon J (2004) Mesolimbic dopaminergic pathways in fear conditioning. Prog Neurobiol 74:301-320.

Phillips ML, Drevets WC, Rauch SL, Lane R (2003) Neurobiology of emotion perception I: the neural basis of normal emotion perception. Biol Psychiatry 54:504-514.

Pizzagalli DA (2014) Depression, stress, and anhedonia: toward a synthesis and integrated model. Annu Rev Clin Psychol 10:393-423.

Porcelli AJ, Lewis AH, Delgado MR (2012) Acute stress influences neural circuits of reward processing. Front Neurosci 6.

Potts GF (2011) Impact of reward and punishment motivation on behavior monitoring as indexed by the error-related negativity. Int J Psychophysiol 81:324-331.

Rissman J, Gazzaley A, D'Esposito M (2004) Measuring functional connectivity during distinct stages of a cognitive task. Neuroimage 23:752-763.

Robinson OJ, Overstreet C, Charney DR, Vytal K, Grillon C (2013) Stress increases aversive prediction error signal in the ventral striatum. Proc Natl Acad Sci U S A 110:4129-4133.

Roesch MR (2004) Neuronal Activity Related to Reward Value and Motivation in Primate Frontal Cortex. Science 304:307-310.

Rolls ET (1972) Activation of amygdaloid neurones in reward, eating and drinking elicited by electrical stimulation of the brain. Brain Res Rev 45:365-381.

Rothkirch M, Schmack K, Schlagenhauf F, Sterzer P (2012) Implicit motivational value and salience are processed in distinct areas of orbitofrontal cortex. Neuroimage 62:1717-1725.

Rousselet GA, Pernet CR (2012) Improving standards in brain-behavior correlation analyses. Front Hum Neurosci 6:119.

Ruge H, Goschke T, Braver TS (2009) Separating event-related BOLD components within trials: the partial-trial design revisited. Neuroimage 47:501-513.

Rupp HA, Wallen K (2008) Sex differences in response to visual sexual stimuli: A review. Arch Sex Behav 37:206-218.

Russell JA, Carroll JM (1999) On the bipolarity of positive and negative affect. Psychol Bull 125:3.

Russell JA, Barrett LF (1999) Core affect, prototypical emotional episodes, and other things called emotion: dissecting the elephant. J Pers Soc Psychol 76:805.

Sabatinelli D, Flaisch T, Bradley MM, Fitzsimmons JR, Lang PJ (2004) Affective picture perception: gender differences in visual cortex? Neuroreport 15:1109-1112.

Sabatinelli D, Bradley MM, Lang PJ, Costa VD, Versace F (2007) Pleasure rather than salience activates human nucleus accumbens and medial prefrontal cortex. J Neurophysiol 98:1374-1379.

Sabatinelli D, Fortune EE, Li Q, Siddiqui A, Krafft C, Oliver WT, Beck S, Jeffries J (2011) Emotional perception: meta-analyses of face and natural scene processing. Neuroimage 54:2524-2533.

Salamone JD (1994) The involvement of nucleus accumbens dopamine in appetitive and aversive motivation. Behav Brain Res 61:117-133.

Salamone John D, Correa M (2012) The Mysterious Motivational Functions of Mesolimbic Dopamine. Neuron 76:470-485.

Salamone JD, Correa M, Farrar AM, Nunes EJ, Pardo M (2009) Dopamine, behavioral economics, and effort. Frontiers in Behavioral Neuroscience 3:13.

Sander D, Grafman J, Zalla T (2003) The human amygdala: an evolved system for relevance detection. Reviews in the Neurosciences 14:303-316.

Sarinopoulos I, Grupe DW, Mackiewicz KL, Herrington JD, Lor M, Steege EE, Nitschke JB (2010) Uncertainty during anticipation modulates neural responses to aversion in human insula and amygdala. Cereb cortex 20:929-940.

Sarter M, Gehring WJ, Kozak R (2006) More attention must be paid: the neurobiology of attentional effort. Brain Res Rev 51:145-160.

Savine AC, Beck SM, Edwards BG, Chiew KS, Braver TS (2010) Enhancement of cognitive control by approach and avoidance motivational states. Cognition & Emotion 24:338-356.

Schimmack U (2005) Attentional interference effects of emotional pictures: threat, negativity, or arousal? Emotion 5:55-66.

Schimmack U, Colcombe S (2007) Eliciting mixed feelings with the paired-picture paradigm: A tribute to Kellogg (1915). Cogn Emot 21:1546-1553.

Schultz W (2000) Multiple reward signals in the brain. Nat Rev Neurosci 1:199-207.

Schultz W, Dayan P, Montague PR (1997) A neural substrate of prediction and reward. Science 275:1593-1599.

Schupp H, Cuthbert B, Bradley M, Hillman C, Hamm A, Lang P (2004) Brain processes in emotional perception: Motivated attention. Cogn Emot 18:593-611.

Serences JT (2004) A comparison of methods for characterizing the event-related BOLD timeseries in rapid fMRI. Neuroimage 21:1690-1700.

Seymour B, Daw ND, Roiser JP, Dayan P, Dolan R (2012) Serotonin selectively modulates reward value in human decision-making. J Neurosci 32:5833-5842.

Shabel SJ, Janak PH (2009) Substantial similarity in amygdala neuronal activity during conditioned appetitive and aversive emotional arousal. Proceedings of the National Academy of Sciences 106:15031-15036.

Shattuck DW, Leahy RM (2002) BrainSuite: an automated cortical surface identification tool. Medical image analysis 6:129-142.

Siegel JS, Power JD, Dubis JW, Vogel AC, Church JA, Schlaggar BL, Petersen SE (2014) Statistical improvements in functional magnetic resonance imaging analyses produced by censoring high-motion data points. Hum Brain Mapp 35:1981-1996.

Small DM, Gregory MD, Mak YE, Gitelman D, Mesulam MM, Parrish T (2003) Dissociation of neural representation of intensity and affective valuation in human gustation. Neuron 39:701-711.

Smith SM, Jenkinson M, Woolrich MW, Beckmann CF, Behrens TE, Johansen-Berg H, Bannister PR, De Luca M, Drobnjak I, Flitney DE, Niazy RK, Saunders J,

Vickers J, Zhang Y, De Stefano N, Brady JM, Matthews PM (2004) Advances in functional and structural MR image analysis and implementation as FSL. Neuroimage 23 Suppl 1:S208-219.

Strait CE, Sleezer BJ, Hayden BY (2015) Signatures of value comparison in ventral striatum neurons. PLoS Biol 13:e1002173.

Talmi D, Dayan P, Kiebel SJ, Frith CD, Dolan RJ (2009) How humans integrate the prospects of pain and reward during choice. J Neurosci 29:14617-14626.

Thierry A, Tassin J, Blanc G, Glowinski J (1976) Selective activation of the mesocortical DA system by stress. Nature.

Tricomi EM, Delgado MR, Fiez JA (2004) Modulation of caudate activity by action contingency. Neuron 41:281-292.

Turk-Browne NB (2013) Functional interactions as big data in the human brain. Science 342:580-584.

Uddin LQ (2015) Salience processing and insular cortical function and dysfunction. Nat Rev Neurosci 16:55-61.

Ulrich-Lai YM, Christiansen AM, Ostrander MM, Jones AA, Jones KR, Choi DC, Krause EG, Evanson NK, Furay AR, Davis JF, Solomon MB, de Kloet AD, Tamashiro KL, Sakai RR, Seeley RJ, Woods SC, Herman JP (2010) Pleasurable behaviors reduce stress via brain reward pathways. Proc Natl Acad Sci U S A 107:20529-20534.

Urry HL, van Reekum CM, Johnstone T, Kalin NH, Thurow ME, Schaefer HS, Jackson CA, Frye CJ, Greischar LL, Alexander AL, Davidson RJ (2006) Amygdala and ventromedial prefrontal cortex are inversely coupled during

regulation of negative affect and predict the diurnal pattern of cortisol secretion among older adults. J Neurosci 26:4415-4425.

Vogt J, De Houwer J, Crombez G, Van Damme S (2013) Competing for attentional priority: temporary goals versus threats. Emotion 13:587-598.

Vromen JM, Lipp OV, Remington RW (2015) The spider does not always win the fight for attention: Disengagement from threat is modulated by goal set. Cogn Emot 29:1185-1196.

Vuilleumier P (2005) How brains beware: neural mechanisms of emotional attention. Trends Cogn Sci 9:585-594.

Vuilleumier P, Richardson MP, Armony JL, Driver J, Dolan RJ (2004) Distant influences of amygdala lesion on visual cortical activation during emotional face processing. Nat Neurosci 7:1271-1278.

Watanabe N, Sakagami M, Haruno M (2013) Reward Prediction Error Signal Enhanced by Striatum-Amygdala Interaction Explains the Acceleration of Probabilistic Reward Learning by Emotion. J Neurosci 33:4487-4493.

Wei P, Kang G (2014) Task relevance regulates the interaction between reward expectation and emotion. Exp Brain Res 232:1783-1791.

Wei P, Wang D, Ji L (2016) Reward expectation regulates brain responses to task-relevant and task-irrelevant emotional words: ERP evidence. Soc Cogn Affect Neurosci 11:191-203.

Wilcox R (2015) Inferences about the skipped correlation coefficient: Dealing with heteroscedasticity and non-normality. J Mod App Stat Meth 14:4.

Wilcox RR (2012) Introduction to robust estimation and hypothesis testing: Academic Press.

Winston JS, Gottfried JA, Kilner JM, Dolan RJ (2005) Integrated neural representations of odor intensity and affective valence in human amygdala. J Neurosci 25:8903-8907.

Wittmann BC, Schiltz K, Boehler CN, Düzel E (2008) Mesolimbic interaction of emotional valence and reward improves memory formation. Neuropsychologia 46:1000-1008.

Woo CW, Krishnan A, Wager TD (2014a) Cluster-extent based thresholding in fMRI analyses: Pitfalls and recommendations. Neuroimage.

Woo CW, Krishnan A, Wager TD (2014b) Cluster-extent based thresholding in fMRI analyses: pitfalls and recommendations. Neuroimage 91:412-419.

Wright P, He G, Shapira NA, Goodman WK, Liu Y (2004) Disgust and the insula: fMRI responses to pictures of mutilation and contamination. Neuroreport 15:2347-2351.

Yokoyama T, Padmala S, Pessoa L (2015) Reward learning and negative emotion during rapid attentional competition. Front Psychol 6:269.

Zhang W, Schneider DM, Belova MA, Morrison SE, Paton JJ, Salzman CD (2013) Functional circuits and anatomical distribution of response properties in the primate amygdala. J Neurosci 33:722-733.

Zweifel LS, Fadok JP, Argilli E, Garelick MG, Jones GL, Dickerson TM, Allen JM, Mizumori SJ, Bonci A, Palmiter RD (2011) Activation of dopamine neurons

is critical for aversive conditioning and prevention of generalized anxiety. Nat Neurosci 14:620-626.